MODELLING, SIMULATION AND ROBUST CONTROL OF A BENSON BOILER DURING HOT STARTUP

By

Dunn Mukosa

BScEng (Electrical)

Submitted in fulfillment of the academic requirements for the degree of Masters of Science in Engineering, in the Department of Electrical, Electronic and Computer Engineering, University of KwaZulu Natal, Durban, South Africa.

August 2005

I hereby declare that all the material incorporated into this thesis is my own original and unaided work except where specific reference is made by name or by reference. From the knowledge of the author, the work contained in this thesis has not been submitted for a degree at any other university.

Signed: _____

D Mukosa

As the candidate's supervisor I have/have not approved this thesis/dissertation for submission

Signed:..... Name:..... Date:.....

ACKNOWLEDGEMENTS

The work in this thesis was performed under the careful supervision of Professor E Boje of the Department of Electrical, Electronic and computer Engineering, University of KwaZulu Natal. Many of the ideas in this thesis originate from discussion with my supervisor.

I wish to thank Professor E Boje for the advice, support and friendly working environment he provided me. My thanks extend to Mrs. Bennett, the staff of the school of Electrical, Electronic and Computer engineering, and fellow postgraduates for providing a pleasant and stimulating working environment.

In additional, I would like to thank the following people:

My family and Towa for the support and encouragement they have given me.

The financial support of the Natural Resource Foundation (NRF) and the University of KwaZulu Natal.

God for making everything possible.

ABSTRACT

Large boilers have typically been designed for continuous operation from 60-100% load. With restructuring of electrical supply and in some cases because of local fuel supply constraints, some of these boilers are run for only two shifts per day and this entails warm start ups. A reasonable objective is to bring the plant online as quickly as possible within the equipments constraint and without risk of tripping major plant equipment such as feed pumps and circulation pumps.

The project required the development of a model accurate enough to represent the boiler thermal dynamics. The thesis compares the simulated model results with the measured results from a Benson boiler from Majuba power station. The developed model is then used to investigate gain scheduled and robust control approaches to the design of the control system for collector vessel level and evaporator flow rate. Once the control problems are clearly understood, an investigation into fast start up is undertaken.

The subject of the start up of Benson boilers has limited open literature. This is because flexibility in plant operation has only recently become an important issues with electricity utilities. The limited research in the field of robust control of start up of Benson boiler has made the extensive work done by both Eitelberg and Boje [2001,2002,2004] state of the art. Most of the research done in this thesis follows from the work done by Eitelberg and Boje.

SYMBOLS

symbol	SI	Description
A, A_{cv}	m^2	Inner pipe cross section area and collector vessel cross section area.
c_s	J/(kgk)	Specific heat capacity of steel
d_z d_i	m	Length of spatially divided block and inner diameter of a tube
g	m/s^2	Gravity constant
G_{circ} and G_{feed}	-	Circulation and Feed valve controller
h, h_g, h_l, h_{fg}	J/kg	Specific enthalpy of fluid, saturation enthalpy of steam and water phase, and enthalpy of vaporization
l_{cv}	m	Level of water in the collecting vessel
K_l and K_{cv}		Collector vessel gain controller and Collector vessel gain
l and l_{ref}	m	Length of tube and collector vessel set point
l_{cv}	m	Collecting vessel level
$L_{feed}, L_{circ}, L_{evap}$	-	Open loop transfer of feed, circulation and evaporator respectively.
$L_{circcontrol}$, $L_{levelcontrol}$		Closed loop transfer of circulation loop and Feed loop

$\dot{m}, \dot{m}_{evap}, \dot{m}_{water\_s}$, $\dot{m}_{water\_m}, \dot{m}_{circ}, \dot{m}_{collector}, \dot{m}_{eco}$	kg/s	Mass flow rate of the fluid, mass flow rate from the evaporator, simulated and measured mass flow rate entering the collector vessel, total circulating mass flow rate , simplified mass flow rate entering collector vessel and mass flow into the economiser
m_{vessel} and m_s	kg	Mass in the collector vessel and of steel
N_{evap}		Transfer function from the Economiser input and evaporator mass flow rate output
P	Pa	Operation pressure
P_{circ} and P_{feed}	-	Circulation and feed valve transfer function
$\dot{q}_A, \dot{q}_{heat}, \dot{q}_{water}$	W	Heat flux added to the fluid, heat added to the tube and heat added to the fluid
$\dot{q}$	W/m^2	Heat flux into the fluid
q_{heat}, q_{water}	J	Heat energy added to the tube wall and heat added to the fluid
q_{coef}	W/m^2K	Heat flux coefficient
$T, T_s T_w$	K	Fluid temperature, saturation temperature and wall temperature
U	m	Inside tube parameter

vs	m/s	Velocity of fluid
v, v_s	m^3	Volume of the fluid in a block and volume of a steel block
V_m	m/s	Mean fluid velocity
x, x_{do}	-	$x = \frac{h - h_l}{h_g - h_l}$ Steam quality & steam quality at dryout
ρ, ρ_s	kg / m^3	Density of fluid and density of steel
λ	W/(K m)	Thermal conductivity
ξ	-	Friction factor of steel pipe
ΔKe	J	Change in kinetic energy
ΔPe	J	Change in potential energy
Φ	kg/m^2s	Mass flow velocity
τ_o	N/m^2	Friction coefficient
Δh	J/kg	Change of specific enthalpy

ABBREVIATIONS

Abbreviations	SI	Description
DNB	-	Departure from Nucleate boiling
Eqn	-	Abbreviation of equation
had85	Kg/s	Drain flow rate in Benson mode
MCR	%	Maximum continuous rating
Nu	-	Nusselt number
OTSG	-	Once through steam generator
PI	-	Proportional Integrator controller
Pr	-	Prandtl number
Re	-	Reynolds number
S/H	-	Super Heater

CONTENTS

List of Figures

Chapter 1

BENSON BOILER START-UP ROBUST CONTROL

1.1 Introduction

In the last 30 to 40 years a lot of effort and time has been put in developing mathematical models of a Benson boiler. A Benson boiler is a once-through steam generator (OTSG). The models have been developed from first principles in order to analyze and understand the dynamics of a OTSG (see Lausterer, Franke and Eitelberg (1980), Adams and J.Adams, D.R Clark, J.R Louis, and J.P Spanbauer (1965) and Borsi (1974)). Models developed from first principles are a good stepping stone for:

- Simulating the operation condition for better understanding of the feed water and circulation behavior of the Benson boiler
- Development of more efficient cold/hot startup procedures.

Benson boilers are used thermal power plants for electricity generation. They are designed to operate between 50 -100% of Maximum Continuous Rating (MCR) and the cold/hot start up process takes about 5 hours.

There is an increase in demand for plant operational flexibility, which in allows the profitability of power generation to be optimised. This can be achieved by implementing a daily two shift system for each boiler. The demand for flexibility presents the following control problem:-

- Abrupt change in density as water is converted to steam at lower pressure
- Plant uncertainty at different load demands.
- High cost of de-ionised water and fuel oil due to long inefficient start-ups.
- Instability in the collecting vessel. The collecting vessel has a 7.5 second capacity at minimum evaporator flow.
- Steam generated in wrong places in the boiler tubes results in 10-15 minute thermal oscillation and mass flow being higher than usual during warm start up.

This thesis concentrates on the simulation and control analysis of the hot startup of a Benson boiler, by developing a simple Matlab model which captures the relevant boiler dynamics. The most important simulation and control problems are:

- Stiffness of State Differential Equation due by close thermal coupling between fluids and wall.
- The oscillation in the evaporator and collecting vessel section of the boiler which is caused by some gain-changing non linear system components.

1.2 Thesis Overview

Chapter 2

The first step in the project was to understand the boiler operation. Chapter 2 of the thesis gives a brief overview of the boiler operation conditions. Most of the referenced literature in chapter 2 is from L & C SteinMüller (1999), which is not in the public domain. The chapter describes the water circulation through the economiser, evaporator and the collecting vessel. After understanding the operation of the boiler, the next step was developing a Benson boiler model.

Chapter 3

The chapter describes the boiler model development. The boiler model follows from work done by Lausterer, Franke and Eitelberg (1980). Assuming a known pressure and input specific enthalpy, the simplification done in this thesis gives only the energy equation (state equation). The other thermodynamic quantities can be derived from the known pressure and calculated specific enthalpy.

The chapter then proves (using Incropera and Dewitt, 2001) that the flow in the boiler is fully developed and turbulent. Using Butterworth and Hewitts (1977), dryout occurs at (x_{do}= 0.97) high steam quality and is therefore omitted in the two phase flow heatflux correlation. This implies only one equation is used to describe nucleate and subcooled boiling. The Nusselt number is described by Dumont and Heyen (2001). Since quite a number of two phase heatflux correlations have been derived, the chapter explains why Jens and Lottes (1951) heatflux correlation is used in this thesis, based on Butterworth and Hewitt (1977), Collier (1981), and Lausterer, Franke and Eitelberg (1980). Due to the limitation of the operation conditions of the two phase flow correlation, the model is not very accurate. Due to stiffness of the simulation, the implicit integration method given by Bulrisch and Stoer (1980) is used to solve the stiff equations.

Chapter 4

Once the model is derived, the next step in the project was obtaining a simulation model in Matlab/Simulink environment. The program structure used in this thesis is from Maffezzoni, Magnani and Marcocci (1983). Each section of the boiler (economiser, helical and vertical tubes) has its own code, defining its parameters and state equations. The code of each section was based on the working code from Eitelberg and Boje (2004). During the simulation, the heat up-take of each section of the boiler was obtained from Eitelberg and Boje (2001). In order to reduce the stiffness of the model, a unique method from Eitelberg and Boje (2003) is used. The method allows progressive development of nucleate and subcooled boiling, avoiding discontinuity. The technique makes use of linear interpolation, although the transition from single to two phase flow is not linear. The feed pump PI controller is designed using the control tool box in Matlab, and the model is simulated. The Simulation results are compared to measured results at Eskom's Majuba Power Station, Unit 6.

.

Chapter 5

Chapter 5 describes the simulated results. The simulated and measured quantities that are compared are the flow rates and the output specific enthalpy. A hot start up of the boiler is modelled, by keeping the initial temperature at about 280 °C and initial pressure at about 4.5 MPa. The results show a circulation pump tripping during start up, resulting in an increase in boiler temperature. The circulation commences 20 minutes after the pump trips. This reduces the fluid temperature in the boiler.

An oscillation is observed in the simulation results, which is not seen in the set of measured results. Using a simplified control loop diagram from Eitelberg and Boje (2001), the source of the oscillation is found to either be the valve lag or the bandwidth (gain) of the circulation loop. The boiler model represents most of the boiler dynamics, including the 10-15 minute thermal oscillation explained by Maffezzoni and Ferrarini (1989) and the oscillation caused by blow down interlocking at a collecting vessel level of about 4 m. The modeling of the single phase is more accurate than the two phase flow. This is because of the approximation of the two phase flow and the simplification done to reduce stiffness.

Chapter 6

The chapter describes the control analysis of the boiler. The boilers control problems and the performance specifications of the required controller are defined. The PI controller is designed using quantitative feed back theory (QFT). The first step in the control analysis is obtaining a linear model of the plant. The plant is linearised using the Taylor series to give a transfer function model of the form $P(s) = \underline{C}(\underline{I}s - \underline{A})^{-1}\underline{B} + \underline{D}$, as explained by Ogata (1997). The model is not linearised above 50% MCR, since steam is generated in the evaporator and the gain in the circulation loop is zero. Once the linear model is obtained, Bulirsch and Stoer (1979) is used to prove that the system is stiff.

Once the plant is linearised, the mass flow rate transfer through the economiser to evaporator water mass flow rate is defined as N_{evap}. $N_{evap} \approx \dot{m}_{evap}(1-x)$ because the frequency responses for N_{evap} at different MCR below 0.1 rad/s are the same and do not depend on input specific enthalpy. Simplifying the control loop structure of the boiler given by Eitelberg and Boje (2001), the positive feedback around the evaporator is found to be unstable at the corner frequency of the feed and circulation loop. The instability results in limit cycling control loops around some gain changing non-linear system components. Assuming the feed control loop tuned to its maximum bandwidth, the circulation loop is tuned to give a stable and more robust response. A PI controller is designed from low frequency to high frequency using quantitative feedback theory. Due to plant uncertainty at different loads during start up, a gain scheduled PI controller is implemented. Using Parseval's theorem (typically used to show power transfer from input to output of a system), it is shown that the greater the circulation bandwidth, the less the oscillation in the collecting level. Once the controller is designed, the operability of the boiler with the PI level controller is studied.

Chapter 7

Chapter 7 describes the operability of the boiler with the PI circulation controller. The boiler model is run with different collecting level set points. The levels are set to 2, 4 and 6 metres. The boiler is then run with a constant blow down flow at a level set point of 2 metres. The purpose of operating the boiler with a constant blow down is to reduce the evaporator input specific enthalpy, as more blow down means less circulation and hence more cold feed water. Constant blow down also results in less blow down interlock activation.

When the level set point is set at 6 metres, there is a lot of blow down interlock since the collecting vessel can easily fill up. The results show a circulation flow oscillation with a frequency equal to the frequency of the closing and opening of the blow down valves. The model running at 2 and 4 metres gives similar results. At set points of 2 and 4 metres, there is very little blow down intervention. This is because at these set point levels, the PI controller has enough time to regulate the level, before the level becomes too high, preventing any blow down intervention.

To reduce the risk of the collecting vessel filling up, while reducing the thermal oscillation by increasing cold feed water, the model is run with a constant blow down, with a level set point of 2 metres. Since the initial specific enthalpy of the model cannot be changed as measured values are used, the simulation demonstrates the difference in the feed water when the boiler has a constant blow down and a variable blow down. This method seems to be the best start up procedure of the boiler, although the start up would take longer. The start up would take longer because more cold water is pumped into the economiser. The controller would prevent any pump from tripping, while making the start up more reliable and robust. The model is then run without gain scheduling. The results show that the boiler response is slower as the collecting vessel easily fills up. Hence maximum bandwidth is required for more reliable operation.

.

Conclusion

From the results obtained in the control analysis, the author concluded that the controller and operation philosophy would help make the start up procedure more robust by preventing pump trips and reduce instability in collecting vessel level and evaporator floe. The results of the control analysis and simulation show that gain scheduling is required for maximum bandwidth at different loads during start up. The start up procedure proposed in the thesis would help reduce the 10-15 minute thermal oscillation, as more cold water is fed into the economiser during hot start up.
Further studies could include measuring the cost effectiveness of the designed controller, redesigning the collecting vessel for hot start up operation and changing the boiler hot start up procedure.

There are three appendices which contain material which is important to the work, but which might have impaired the continuity of the text. The appendices will be referred to as they are required for extra details.

Chapter 2

GENERAL DESCRIPTION OF A BENSON BOILER

2.1 Introduction

In order to develop a Benson boiler model, the boiler setup and operation have to be understood. The description of the specific boiler used in this study is from L & C SteinMüller (1999). In simple terms, a OSTG is combination of parallel continuous tubes connected by headers resulting in a common inlet for feed water and outlet for steam, as shown in Figure 2.1.

Benson boiler technology employs a once-through water/steam circuit with the water proceeding through the economizer, evaporator, and superheater surfaces without recirculation through any subsystem during normal operation. The boiler is equipped with a circulation system to stabilize operation during the start up and shut down phases and at low loads (below 45 % MCR). The circulation system ensures adequate cooling of the economiser and evaporator systems in that load range, by allowing a minimum flow greater than the evaporation rate.

The combustion air system provides and controls the correct amount of hot air at the optimum temperature to enable complete combustion of pulverized fuel (PF) to take place in the furnace. The amount of air that the combustion air system puts into the boiler must be balanced with the amount of gas that the flue gas system draws out, so that the correct pressure is maintained in the furnace. This pressure is slightly lower than atmospheric pressure so that flue gas will not leak out of the furnace. Secondary air provides the main combustion air and its inlet velocity at the burners contributes directly to the removal of the flue gas from the area of combustion. This increases the rate of heat input through the convection portion of the boiler. Coal is fed to the mills by chain scraper variable volumetric coal feeders. Fuel oil is provided to the oil burner via a fuel oil plant. Oil is circulated through the system to the boiler via the fuel oil pumping plant. Circulation of the oil is maintained to keep the fuel oil in a fluid state so that it flows easily. The boiler and turbine are controlled by the unit co-ordinator. Any variation in the turbine demands causes the unit co-ordinator to send a signal to the boiler master controller, which adjusts the feed water/fuel and fuel/air ratios to suit the new conditions.
The Benson boiler is made up of three broad sections:-

i) The fuel supply which provides the primary source of energy.
ii) S/H and the circulation tubes.
iii) Finally the fluid water/steam inside the tubes.

The chapter focuses on creating a better understanding of the steam generation in a Benson boiler. No super heating or reheating is considered in this thesis.

The Benson boiler analyzed in this thesis has a around 600 kg/s steam flow capacity at maximum continuous rating (around 720 MW = MCR). The boiler is equipped with a circulation system to meet minimum flow for cooling evaporator and economizer during

the start up and shutdown phases and at low loads (below 45 % MCR). The circulation system ensures adequate cooling of the economiser and evaporator systems in the low load range. The main water/steam circuits consist of the high pressure (HP) section which includes the economiser, evaporator, separating vessel, collecting vessel, superheaters, and HP relief station.

Water flows from the circulating pump delivery line (upstream of circulation flow control valve) via the leak off valve to the suction line from the. The leak-off valve is open when the pump is not operative and closed through an interlocking system during recirculation. To avoid the water level in the rising while the circulating pump is on hot standby (boiler in Benson mode), an automatic drain line at the drain nozzle of the bleeds off excess water to S/H1 via an attemperator.

The feed-water is preheated in the high pressure (HP) heaters before entering the economiser. From the economizer the water enters the evaporator, where all parallel tubes pass through the heating zone. The evaporation point occurs in the upper region of the evaporator.

Figure 2.1 shows the feed and circulation loop of the boiler. The re-circulation flow appears as a disturbance in the feed water loop. As seen in figure 2.1, feed water passes through economiser into hopper tubes. From the upper tubes the water flows through the helical tubes and vertical tubes into separation vessel. From the separating vessel the water flows to the collecting vessel. The circulation pump pumps the water from the collecting vessel back to the economiser. The circulation system allows the minimum circulation flow required to cool the economiser and evaporator during a hot start-up and other low-load operation, when the evaporation rate is below this minimum flow.

Once steam forms, the separating vessels separate generated steam from water. The generated steam passes through the superheaters to the high pressure turbine. From the high pressure turbine the steam is reheated and passed to intermediate and low pressure turbine.

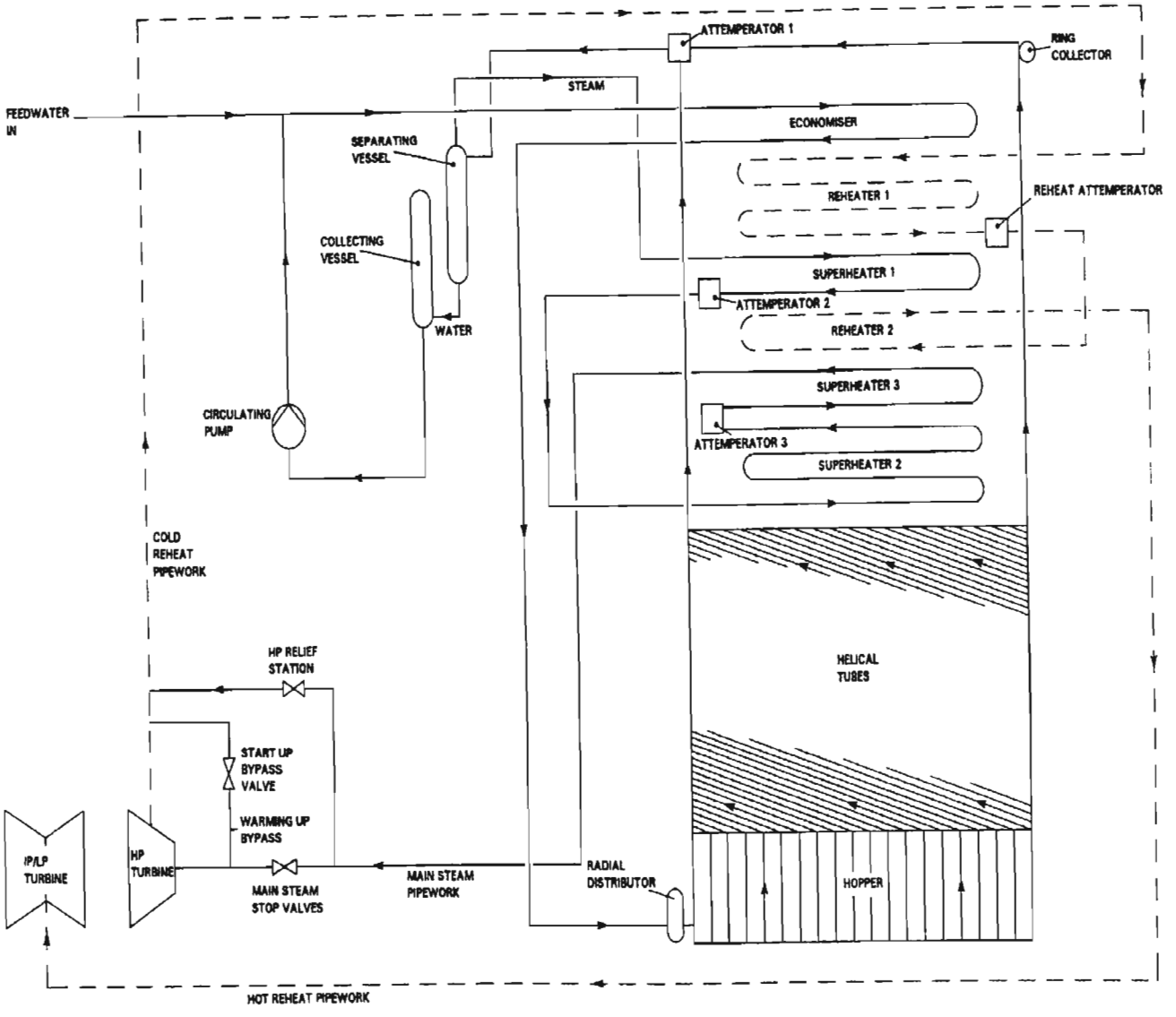

Figure 2.1: Simplified structure of a Benson boiler [copied from L & C SteinMüller (1999)]

2.2 Economiser

The economiser is located at the top of the boiler after the super heaters and re-heaters, in the low-temperature flue gas zone. The feed water temperature is raised from approximately 250 °C to approximately 280 °C in the economiser. The economiser tube bundle comprises of parallel finned tubes. The finning of the tubes increases the heat exchange surface, improving heat absorption.

Convection is the main form of heat transfer from the flue gases to the tubes, while heat is transferred from tube to the water by conduction and convection. The water flows from top to bottom through the economiser, i.e. counter to the flue gas stream, which improves heat exchange.

There is no control on the economiser. Any change in process conditions in the economiser, such as feed water flow, is as a result of an increase or decrease in steam demand

2.3 Evaporator

Water from the economiser flows into the bottom of the evaporator, where it is heated up to form steam. This steam is passed on to the superheater. The evaporator system can be split into five sections, all having different parameters and operation conditions

The following main components make up the evaporator (figure 2.1):

- the hopper tubes
- the helical wall tubes
- the vertical wall tubes
- the separating vessels
- the collecting vessel

Water from the economiser flows into the hopper tubes. The hopper tubes are located at the bottom of the boiler and consist of parallel vertically arranged finned tubes. The water flows from the hopper tubes into the helical tubes.

The helical tubes form the walls of the combustion chamber and are an important part of the heat-absorbing section (about 48 % of total heat uptake) of the boiler. These tubes are designed to absorb radiant heat. .

The helical tubes are parallel finned and are designed to improve water/steam flow pattern and increase heat absorption surface compared to vertical tubes. The helical tubes are angled at about 15° at beginning, and at 17° at the top end. This change in angle is for flow stability of the water/steam (proprietary information, L & C SteinMüller (1999)). If the flow stability of the water/steam is not maintained, departure from nucleate boiling (DNB) can occur. DNB dramatically reduces the cooling effect of the water/steam on the tubes, which can result in an increase in tube metal temperature and eventually in tube failure.

Water/steam from the helical tubes is taken to the vertical tubes (sling tubes and wall tubes). The inside sling tubes support the tube banks of the economiser, superheaters and reheaters. The heat is transferred by conduction and convection through the sling tubes.

The water/steam enters the separation vessel tangentially, which provides the mixture with a swirl. The cyclonic action separates the water from the steam. The steam leaves the separating vessels through connecting pipes and continues to Superheater 1 (S/H1).The water flows out of each separating vessel through pipes, which continue to the . The four separating vessels are located on the front wall of the boiler. Water/steam from the ring collecting passes through connecting pipes to the separating vessels. When the boiler is operating in Benson mode, the steam flows through the separating vessels,

which act as mixing vessels, minimising any temperature gradients in the steam (this ensures a good temperature balance, which is important for the flow circuits in the superheaters and reheaters). When the boiler is on re-circulation, however, the separating vessels, in conjunction with the downstream, operate in a similar way to a boiler drum. .

Water from the separating vessels enters the. A proportional controller controls the collecting vessel level, while maintain the minimum flow in the economiser. Once the level is the collecting vessel becomes high (above 64 %, figure 2.2), the blow down valves open to prevent water flowing back to the separating vessels and carrying over into the S/H. When the collecting vessel level is too low (below 10%, figure 2.2), the re-circulation is stopped to prevent the pump from tripping.

From the collecting vessel, the water is re-circulated to the evaporator. The recirculation flow is regulated by the water level in the. The water level control logic is shown below derived from experimental data.

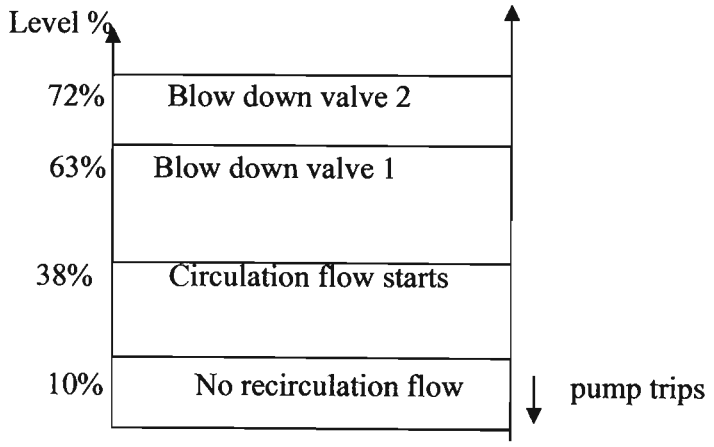

Figure 2.2: Control logic of the collecting vessel depends on the fluid level in the collecting vessel

2.4 Superheaters

The saturated steam generated in the evaporator passes from the separating vessels into the superheaters. There are three superheater banks, all of which are of horizontal construction and four-flow circuit design. The tube banks are supported by inside sling tubes.

Super heater 1 (S/H1) is a convection-type superheater and is situated below the economiser at the top of the boiler. The superheater system converts saturated steam from the evaporator into superheated steam suitable for use in the HP turbine. The steam is cycled counter to the gas flow (i.e. from top to bottom, figure 2.3), from S/H1 to S/H2. The steam is taken by unfired connecting pipes outside the boiler front wall to attemperator. Here the steam temperature is controlled to a set value. The steam from attemperator is taken through connecting pipes to the Superheater 2 (S/H2). Superheater 2 (S/H2) is the lowest heating surface, directly above the combustion chamber, and is a

radiant-type superheater. Superheater 3 (S/H3) is located directly above S/H2 i.e. not counter flow. Steam from the S/H2 outlet enters attemperator 3, where the temperature is adjusted to ensure that the S/H3 outlet temperature will be within regulated range. The physical arrangement of the super heaters is shown in figure 2.3.

Since the project is on circulation flow control, the superheaters are not described in detail.

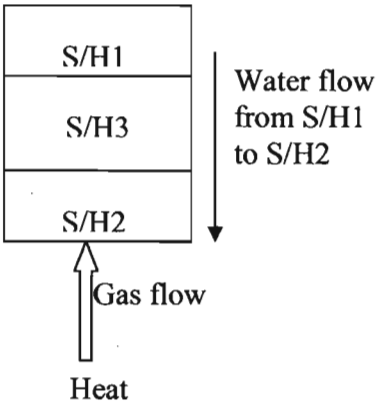

Figure 2.3: Physical arrangement of the superheaters

Chapter 3

MODELLING

3.1 Introduction

The first step in developing the Benson boiler model is understanding the dynamics of the boiler. This is achieved by first defining the state equation of the model from first principles. Conserved quantities are the mass, momentum and energy, as given by Lausterer, Franke and Eitelberg, (1980)

$$\frac{\partial \dot{m}}{\partial t} = -A\frac{\partial p}{\partial z} - \tau_0 u - A\rho g \sin\varphi - \frac{1}{A}\frac{\partial}{\partial z}\left(\frac{\dot{m}^2}{\rho}\right) \tag{3.1}$$

$$\frac{\partial p}{\partial t} = -\frac{1}{A}\frac{\partial \dot{m}}{\partial z} \tag{3.2}$$

$$\frac{\partial h}{\partial t} = \frac{\dot{m}}{\rho A}\left[\frac{1}{\rho}\frac{\partial p}{\partial z} - \frac{\partial h}{\partial z} + \frac{\tau_0 u}{\rho A}\right] + \frac{\dot{q}u}{\rho A} + \frac{1}{\rho}\frac{\partial p}{\partial t} \tag{3.3}$$

Symbols	*SI Units*	*Descriptions*	*Symbols*	*SI Units*	*Descriptions*
A	m	inner tube cross section area	$\dot{q}$	W/m^2	heat flux
dz	m	length of spatially divided block	t	sec	Time
φ	degrees	angle between z-axis and horizontal	u	m	inner tube wall parameter
h	J/kg	specific enthalpy	z∈[0,∞]	m	space coordinate
g	m/s^2	gravity constant	ρ	kg/m^3	Density
$\dot{m}$	kg/s	fluid mass flow	τ_0	N/m^2	friction coefficient

Table 3.1: Shows symbols and units used in this chapter

In this thesis the nonlinear partial differential equations are simplified to retain only the necessary thermal and hydrostatic dynamics. Only the water/steam flow sections of the boiler, which are relevant to start-up behaviour, are considered in the thesis. The sections include the economiser and evaporator (helical and vertical tubes).

Discretising the Boiler in the spatial direction converts the nonlinear partial differential equations 3.1 to 3.3 into a nonlinear ordinary differential equations. The heat flux correlations depend on whether the flow is single or two phase. The correlations used in this project are all empirical correlations.

3.2 State Equations and Variables

Spatially discretising the boiler tubes gives simple lumped models. A single tube is modeled assuming equal behavior per tube and taking into account that the tubes are a combination of parallel tubes connected together using fins. The modeling was done assuming a known pressure, p (z, t) and input specific enthalpy, h (0, t) from high pressure heater outlet temperature. Figure 3.1 shows a small block of a tube. The whole boiler is divided into small blocks, and the length of each block depends on the section of the boiler where the block is located. There is a trade off between the numerical stiffness and resolution, hence the more accurate the model, the stiffer the simulation.

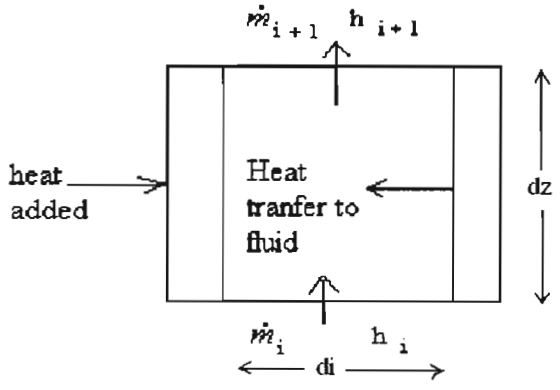

Figure 3.1: Small spatial block of tube

If the boiler pressures and specific enthalpies are known, all other thermodynamic properties such as density and temperature can be calculated. Assuming a known pressure and using eqn (3.3) to find specific enthalpy, eqn (3.1) and eqn (3.2) are eliminated. The mass flow rate is found algebraically and the density is a function of the specific enthalpy and pressure.

As seen from the spatial block fig 3.1, the state variable of the block is the specific enthalpy (h). The other thermodynamic variables such as temperature and density are functions of pressure and specific enthalpy, and are calculated using steam tables. Since the specific enthalpy is a state variable, the energy conservation equation is the state differential equation.

The energy conservation equations:

Energy balance in the small block

$$\frac{\partial h}{\partial t} = \frac{\dot{m}}{\rho A}\left[\frac{1}{\rho}\frac{\partial p}{\partial z} - \frac{\partial h}{\partial z} + \frac{\tau_0 u}{\rho A}\right] + \frac{\dot{q} u}{\rho A} + \frac{1}{\rho}\frac{\partial p}{\partial t} \qquad \text{(Eqn 3.3)}$$

Typical steady state values for evaporator are (calculation in Appendix B),

$$\frac{\tau_0 u}{\rho A} \approx 176 J/(kg/m),\ \frac{\partial h}{\partial z} \approx 7800 J/(kg/m) \text{ and } \frac{1}{\rho}\frac{\partial p}{\partial z} \approx 10.5 J/(kg/m) \quad (3.4)$$

From eqn (3.4), it's observed that,

$$\frac{\partial h}{\partial z} >> \frac{\tau_0 u}{\rho A} + \frac{1}{\rho}\frac{\partial p}{\partial z} \quad (3.5)$$

The numerical values of the friction and hydrostatic terms (Appendix B) in the boiler at operation pressure of about 10MPa are negligible as their contribution is very small. Pressure waves occur in local areas, but take a couple of seconds to move across the boiler and so are omitted in the time scale of interest. Boiler design ensures pressure oscillations are well damped. Hence eqn (3.3) simplifies (3.6),

$$\frac{\partial h}{\partial t} = \frac{\dot{m}}{\rho A}\left[-\frac{\partial h}{\partial z}\right] + \frac{\dot{q}u}{\rho A} + \frac{1}{\rho}\frac{\partial p}{\partial t} \quad (3.6)$$

The boiler data gives the pressure drop across each section of the boiler. A linear interpolation is used to calculate the pressure drop across each spatial block. From this data linear pressure drop is assumed since there is a very small pressure drop across the vertical section of the boiler. A pressure drop of about 0.06 MPa at an operation pressure of 10 MPa is observed from measured data. This means that the total drop across the vertical section of the boilers is the sum of drops in each spatial block. Almost all of the pressure drop is hydrostatic.

Spatially discretising by dividing each pipe is into n blocks and assigning the length of each block to be dz gives,

$$\text{Length of a Tube, L} = \Sigma_{k=1}^{n} dz_k \quad (3.7)$$

Spatial discretization of eqn (3.6) using a forward difference equation gives,

$$\frac{\partial h}{\partial z} \approx \frac{h(t, z+dz) - h(t,z)}{dz} \quad (3.8)$$

Simplifying gives the following ordinary nonlinear differential equation:

$$\frac{dh}{dt} = \frac{1}{\rho A dz}\left[-\dot{m}\left(h(t,z+dz) - h(t,z)\right) + \dot{q}udz + Adz\frac{dp}{dt}\right]$$

$$\Rightarrow \frac{dh}{dt} = \frac{1}{\rho A dz}\left[-\dot{m}\left(h(t,z+dz) - h(t,z)\right) + \dot{q}_A + v\frac{dp}{dt}\right] \quad (3.9)$$

Equation (3.9) is the nonlinear state equation used to simulate for the boiler.

Mass balance inside a small block

For a small block (figure 3.1), rate of change of mass in the block is equal to the difference in rate of mass into the block and the rate of mass out of the block. This means the mass flow rate through each block can be calculated as follows;

$$\frac{dm}{dt} = \dot{m}_{in} - \dot{m}_{out} \tag{3.10}$$

$$\Rightarrow \dot{m}_{out} = \dot{m}_{in} - \frac{dm}{dt}$$

Now the volume of the small block remains constant, only the density of the fluid varies with time as heat is added, or pressure is changed.

$$\dot{m}_{out} = \dot{m}_{in} - v\frac{d\rho}{dt} \tag{3.11}$$

The density of the fluid is a function of both specific enthalpy and pressure, this implies that,

$$\frac{d\rho(h,p)}{dt} = \frac{\partial\rho}{\partial p}\frac{dp}{dt} + \frac{\partial\rho}{\partial h}\frac{dh}{dt} \tag{3.12}$$

$$\Rightarrow \dot{m}_{out} = \dot{m}_{in} - v\left(\frac{\partial\rho}{\partial p}\frac{dp}{dt} + \frac{\partial\rho}{\partial h}\frac{dh}{dt}\right) \tag{3.13}$$

$\frac{dp}{dt}$ is required only for simplification purposes, obtained by numerical differentiation of p (z, t).

Energy balance within a control volume of a tube wall

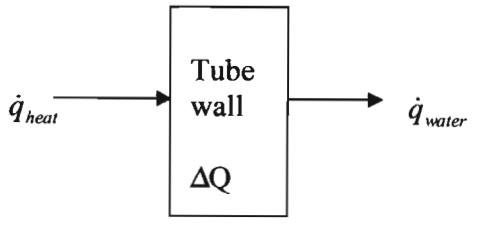

Figure 3.2: Energy balance in a tube wall of the boiler

Applying the first law of thermodynamics (rate at which energy enters a control volume plus rate at which energy is generated in the control volume, minus the rate of energy

leaving the control volume is equal to the increase in stored energy in the control volume.) to figure 3.2 gives energy balance equation 3.14.

$$\Delta q = \dot{q}_{heat} - \dot{q}_{water} \Rightarrow m_s c_s \frac{dT_w}{dt} = \dot{q}_{heat} - \dot{q}_{water}$$
$$\Rightarrow \frac{dT_w}{dt} = \frac{\dot{q}_{heat} - \dot{q}_{water}}{\rho_s v_s c_s} \quad (3.14)$$

The solution for the state equations requires proper definition of initial and boundary condition.

Initial condition

$$\dot{m}(0,0) = \dot{m}_0(z) \qquad 0 \leq z \leq L \qquad (3.15)$$

$$h(z,0) = h_0(z) \qquad 0 \leq z \leq L \qquad (3.16)$$

Boundary conditions

$$\dot{m}(0,t) = \dot{m}_{in}(t) \qquad t > 0 \qquad (3.17)$$

$$h(0,t) = h_{in}(t) \qquad t > 0 \qquad (3.18)$$

$$p(0,t) = p_{in}(t) \qquad t > 0 \qquad (3.19)$$

Eqn (3.15) to (3.19) constitute a two point boundary condition, explained by Lausterer, Franke and Eitelberg (1980).

3.3 Heat Flux Correlations

The heat transfer regime on interest includes both single and two phase flow and so requires two correlations, one for each type of flow. The Reynolds number (Re) is typically of the order of 2×10^5 (Appendix A), implying that the flow is turbulent, since Re>>2300 as explained by Incropera and Dewitt (2001). The flow is considered to be fully developed through the whole length of the boiler. Because is turbulent, the velocity profile is flatter due to mixing in the radial direction, and this means that the velocity is constant across the diameter of the tube.

The post dryout phenomena in figure 3.3 occurs at $x_{do} < x < 1$, and $x_{do} \approx 0.9734$ (see Butterworth and Hewitt, 1977 and Appendix B), which is a very high steam quality. During subcooled boiling, the wall temperature settles to a nearly constant temperature (Butterworth and Hewitt, 1977) and the temperature difference between fluid and tube wall is very small. This means that the heat added to the tube is transferred to the fluid. This results in $x_{do} \approx 0.97$. As a result, 3% of evaporation is dryout, hence dryout is omitted, resulting in one correlation for two phase flow. The post dryout phenomena is ignored for this specific investigation, because the interest is not on the dryout phenomena. For modelling, which requires dryout analysis, the subcooled and nucleate boiling phenomena can be separated from dryout and post dryout phenomena in the two phase turbulent flow.

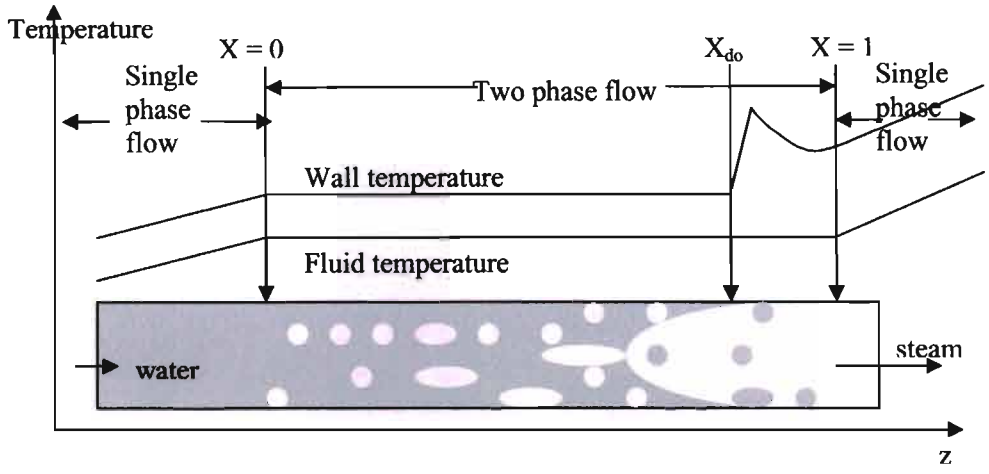

Figure 3.3: Simplified phenomena of turbulent flow in the heated pipe, Lausterer, Franke and Eitelberg, (1980)

3.3.1 Single phase

For the single phase, both the steam and water turbulent flow have the same correlation (see Incropera and Dewitt, 2001).

Reynolds number

$$\mathrm{Re} = \frac{\rho V_m d_i}{\mu} \tag{3.20}$$

Mass flow, $\dot{m} = \rho V_m A$ (3.21)

⇨ replacing (3.21) into (3.20)

$$\mathrm{Re} = \frac{4\dot{m}}{\mu \cdot \pi \cdot d_i} \tag{3.22}$$

The Nusselt number for fully developed (hydrodynamics and thermal) turbulent flow in a smooth tube is given by Dumont and Heyen (2001) and Incropera and Dewitt (2001).

$$Nu = \frac{\xi/8(\mathrm{Re}-1000)\,\mathrm{Pr}}{1+1.27(\xi/8)^{1/2}(\mathrm{Pr}^{2/3}-1)} \tag{3.23}$$

The correlation is valid for $0.5 < \mathrm{Pr} < 2000$ and $10^4 < \mathrm{Re} < 5\times10^5$

(Typical boiler $\mathrm{Re} \approx 1.5\times10^5$)

Newton law of cooling for tube wall:

$$\dot{q} = q_{coef}(T_w - T) \tag{3.24}$$

For fully developed internal flow

$$Nu = \frac{q_{coef} d_i}{\lambda} \Rightarrow q_{coef} = \frac{Nu\lambda}{d_i} \tag{3.25}$$

Replacing (3.24) into (3.25)

$$\Rightarrow \dot{q} = \frac{Nu\lambda(T_W - T)}{d_i} \ (\mathrm{W/m^2}) \tag{3.26}$$

Equation (3.26) is the heatflux for single phase turbulent water or steam flow.

3.3.2 Two phase

Investigator(year)	correlations
Mcadams et al. (1949)	$T_w - T_s = \frac{\dot{q}^{1/3.86}}{2.267}$,0.21 ≤p ≤0.63 MPa $\dot{q}$ (W/m^2), T_w and T_s (° C)
Jens-Lottes. (1951)	$T_w - T_s = \frac{0.79\,\dot{q}^{0.25}}{\exp^{p/6.2}}$, 0.7 ≤p ≤ 17.2 MPa $\dot{q}$ (W/m^2), T_w and T_s (° C)
Thoms(1965)	$T_w - T_s = \frac{0.22\,\dot{q}^{0.5}}{\exp^{p/8.6}}$,5.17 ≤p ≤13.79 MPa $\dot{q}$ (W/m^2), T_w and T_s (° C)

Table3.1: Two phase correlations, copied from Collier (1981)

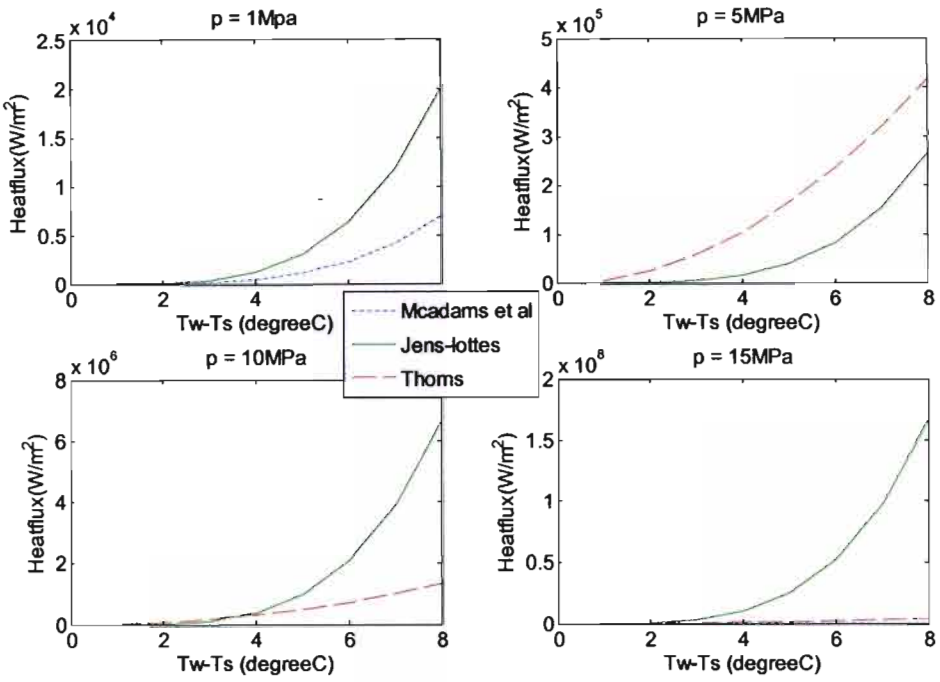

Figure 3.4: The diagram above shows the responses of the heatflux correlations at four different pressure values. The change in wall temperature is plotted against the saturation temperature.

Table 3.1 shows that Jens and Lottes heat flux correlation is valid for a much wider range of pressure as compared to the other two correlations. Mcadams et al (1949), and Jens and Lottes (1951) give more comparable results at pressure of 1 MPa. Thom (1965), and Jens and Lottes give more comparable results at a pressure of 5 and 10 MPa

Butterworth and Hewitt (1977) and Collier (1981) use the last two equations in table 1 for two phase forced convection heat flux.

Jens and Lottes heat flux correlation is used for subcooled and nucleate boiling because it covers a wider operation pressure than the other two (start up pressure changes from 3 MPa to 9 MPa) and as seen from figure 3.4, is more responsive to a change in wall temperature, and is used in the original boiler model of Lausterer, Franke and Eitelberg (1980).

The correlation is not entirely accurate as it evidently does not have similar responses to the other two correlations. This means the simulation of the two phase dynamics are approximated.

$$\dot{q} = \left(\frac{e^{p/6.2}(T_w - T_s)}{0.79} \right)^4 \text{(W/m}^2\text{)} \qquad (3.27)$$

3.4 Numerical Solution of the Model Equation

The model equations require an efficient numerical solution. The widely differing time scales of the rate of heat flux results in a stiff system (described in section 6.3, after linearization of the simulation model). The system stiffness occurs when the fluid flow changes from single to two phase flow or from two phase flow to single phase flow. Stiffness is also caused by heat transfer from tube walls to fluid.

Letting x be the state vector, then

$$\underline{\dot{x}} = \underline{f}(x, t)$$

Solving the stiff system requires an implicit numerical method. Using the implicit Euler method given by Bulirsch and Stoer (1980) the solution is given by,

$$\underline{x}_{i+1} = \underline{x}_i + \Delta t\, \underline{f}(\underline{x}_{i+1}, t_{i+1}) \qquad (3.28)$$

and $\underline{x}_i = \underline{x}(t_i)$

Chapter 4

SIMULATION

4.1 Introduction

The simulation is performed in the Simulink environment. The function containing the source code is called from Simulink and the numerical solutions of the state equations are obtained using an implicit integration method in simulink.
The equations solved here are eqn (3.9) and eqn (3.14),

$$\frac{dh}{dt} = \frac{1}{\rho A dz}\left[\dot{m}\left(h(t,z+dz)-h(t,z)\right)+\dot{q}_A+v\frac{dp}{dt}\right]$$

$$\frac{dT_W}{dt} = \frac{\dot{q}_{heat} - \dot{q}_A}{\rho_S v_S c_S}$$

The mass flow rate is calculated algebraically using eqn (3.11)

$$\dot{m}_{out} = \dot{m}_{in} - v\left(\frac{\partial\rho}{\partial p}\frac{dp}{dt}+\frac{\partial\rho}{\partial h}\frac{dh}{dt}\right)$$

Look up steam tables are used to obtain all the thermodynamic variables, which are functions of both pressure and specific enthalpy. The required gradients are obtained using look up tables whose data is derived numerically offline from steam tables.

The model consists of subsystems which are integrated together in the master program, similar to the method used by Maffezzoni, Magnani and Marcocci (1983). Each section of the boiler, economiser, helical and vertical tubes have their own M-file (modules) describing their physical properties and state differential equation. This means that each section of the boiler can be modeled independently from the other sections

An M-file contains the measured data and look up tables from the boiler at Majuba Power Station which are used to define the initial condition. The master program reads the initial and boundary conditions. Then it sequentially calls the M-files of each section as shown in figure 4.1.

The state differential equations of each section are solved in Simulink. This is achieved by making the master program (differential equation) a Matlab M-file function. The outputs of the M-function are the numerical values of the state derivatives.

4.2 The Program Structure of a Single Step

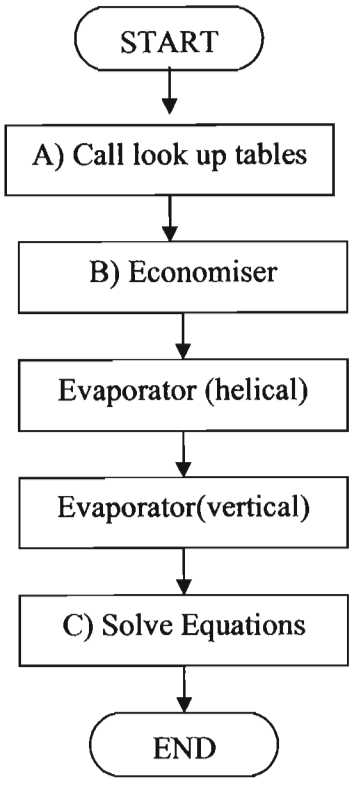

Figure 4.1: Structure of the master program.

Modular decomposition of the whole boiler means that care has to be taken in formulating the input/output variables of the individual modules. This means specifying the boundary condition of the respective differential condition. Each section of the boiler is spatially discretized into small blocks. The differential equations of each block are solved simultaneously, taking care of the input and output variables of each block. The input and output variables of each block are selected so as to allow coupling with adjacent blocks. The spatial discretization is shown in figure 4.3.

.

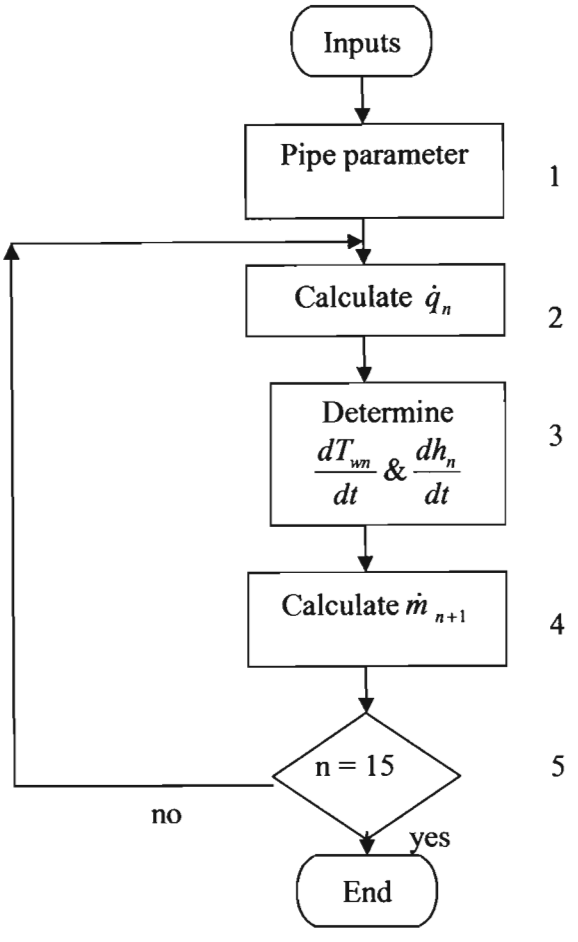

Figure 4.2: Program structure of a lumped element

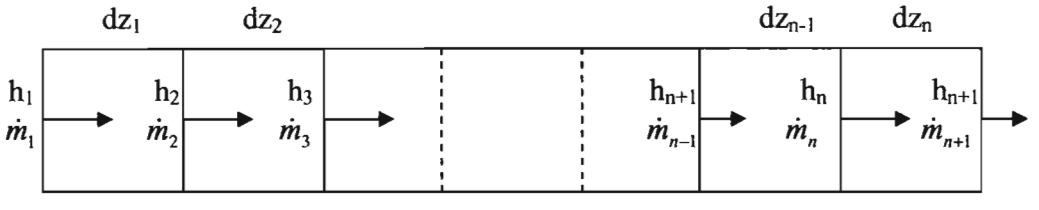

Figure 4.3: Inputs to each block are outputs from previous block

4.3 The Program Code

The program code is given in **Appendix C**. The algorithm of the code and model was developed with help from already working code from Eitelberg and Boje (2004)

Part A

Level A of figure 4.1 shows the initialisation stage of the master program (Benson_model). The first stage of the code defines the global variables. Most of the global variables are defined in the Matlab command window by running a separate M-file called *"start up"*. The code in the M-file *start up* calls the steam tables and reads model inputs from measured thermodynamic properties of a boiler at Majuba Power Station. The code uses steam tables to generate lookup tables of thermodynamic properties.

The boiler M-function (Benson_model) starts by reading the input from simulink and then defining initial and boundary conditions. The function then calls each section of the boiler in the order shown in figure 4.2. The Sections which are not required for a specific analysis can be omitted. When simulating a specific section of the boiler, care has to be taken when defining the initial and boundary conditions

Part B

Each boiler section in figure 4.1 is expanded to give figure 4.2. The M-file code starts by defining the global variables. The parameters of that section of the boiler are then defined. The heat uptake value of each section is not a linear function of the load demand, and is given by Eitelberg and Boje (2001).

Heat added To Economiser = Load Demand x 0.145
Heat added To Evaporator (Helical) = Load Demand x 1.050
Heat added To Evaporator (Vertical) = Load Demand x 0.105 (4.1)

From equation 4.1, it can be observed that the economiser and evaporator heat uptake is greater than 100% MCR (heat uptake in economiser plus evaporator is approximately = 130% of MCR). This is because the boiler is about 30% efficient.

The steam temperature and density of each small block is calculated. The heat flux of the block is calculated by first deciding whether the flow is single or two phase flow.

$h_l < h < h_g$, two phase flow (4.2)

$h < h_l$ or $h_g < h$, single phase flow (4.3)

For those blocks which have transition from single to two phase flow, the heat flux calculation depended on the water/steam fraction. A method from Eitelberg and Boje (2003) is used to calculate the heat flux. The method finds the boundary between single and two phase flow and allows for progressive development of nucleate and subcooled boiling. The method avoids introduction of discontinuity which complicates the solution of the dynamic equations describing the boiler. The discontinuity can be seen in figure 4.4.

- The method assumes that the water to water/steam boundary starts when the specific enthalpy of water is 10000 J/kg less than the saturation enthalpy of water. The boundary extends until the specific enthalpy of water/steam mixture is 10000J/kg more than the saturation enthalpy of water.
- The method also assumes that the water/steam to steam boundary ends when the specific enthalpy of water/steam mixture is 10000 J/kg less than the saturation enthalpy of steam. The boundary extends until the specific enthalpy of steam is 10000J/kg more than the saturation enthalpy of steam.

This technique helps reducing the step change in heat flux and hence reduces the stiffness of the differential equation. For values below 10000 J/kg a "minimum step size" error is generated during simulation as a large heat flux step change occurs between adjacent lumped blocks (see figure 4.4).

At 10 MPa the latent heat of evaporation (h_{fg}) is about 1.5 MJ/kg. This implies that 10KJ/kg is small relative to specific enthalpy difference between single-phase and two-phase. The method makes use of linear interpolation, although the transition from one phase to another is not linear. But the method is very simple and works well with the simulation. Heat flux is given by,

$$\dot{q} = \text{Eqn (3.26)} \times \text{sp} + \text{Eqn (3.27)} \times \text{tp} \tag{4.4}$$

For block with fluid transition between water and water/steam mixture,

$$\text{Where, sp} = \frac{h_l + |h - h_l| - h}{2|h - h_l|} \tag{4.5}$$

$$\text{tp} = 1 - \text{sp} \tag{4.6}$$

For block with fluid transition between steam and water/steam mixture,

$$\text{tp} = \frac{h_g + |h - h_g| - h}{2|h - h_g|} \tag{4.7}$$

$$\text{sp} = 1 - \textit{two-phase} \tag{4.8}$$

then Eq. (4.7) and Eq. (4.8) are replaced in Eq. (4.4)

The coefficient increases rapidly from single phase to two phases resulting in a rapid increase of heatflux. The rapid change requires small step sizes to solve the differential equations. The coefficient reduces when steam is formed, resulting in smaller heatflux and hence a reduction in the rate of change of specific enthalpy.

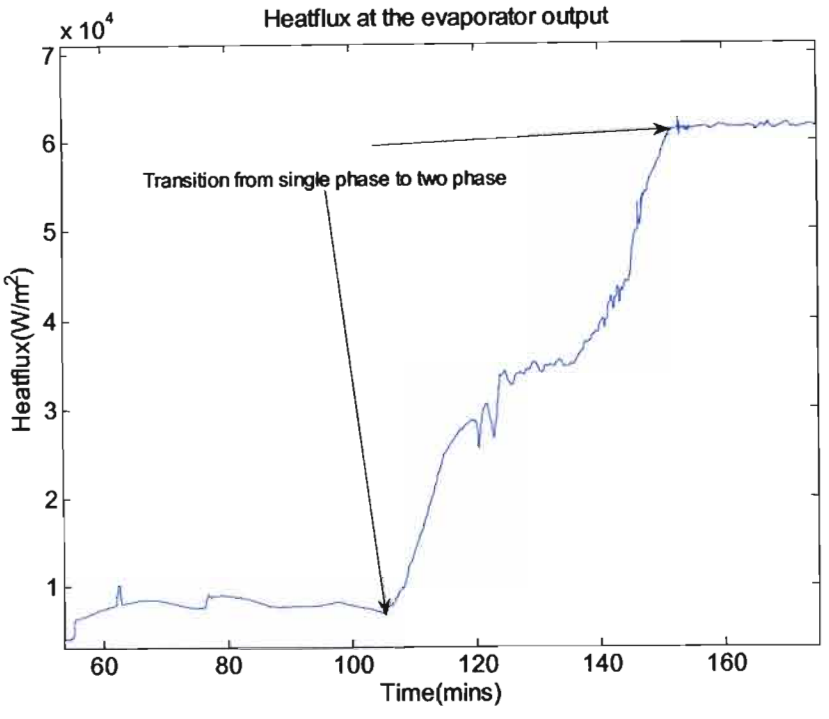

Figure 4.4: Simulated heatflux at the evaporator output from Majuba Unit 6, heatflux transition from single to two phase flow is smooth.

Once the heatflux is calculated, dh/dt is calculated using eqn (3.9) and the mass flow rate is calculated using eqn (3.13)

Part C

Level C in figure 4.1 represents the simulink environment where the differential equations are solved. The inputs of the boiler M-function shown in figure 4.6 includes:

- Measured load demand which is the input power to the boiler.
- Measured evaporator input mass flow rate. Initially the whole boiler is assumed to have the same flow rate.
- Measured economiser pressure.
- Measured evaporator input temperature which is used to calculate the initial specific enthalpy of the boiler. Initially the economiser and evaporator are assumed to have a constant specific enthalpy. This simplifies the start up simulation. This is necessary because most thermodynamic properties of each lumped block are not known during start up and can only be approximated. But due to evaporation taking place in both the economiser and evaporator at start up this makes the approximation extremely complicated.

The results of the simulation are the specific enthalpy, mass flow rates and the steam qualities of the lumped elements. The simulation is run for 350 minutes and uses implicit

integration method, ode15s (stiff), to solve the nonlinear differential equations. The outputs of the simulation are stored in the Matlab command window.

4.4 Simulink Model of a Benson Boiler

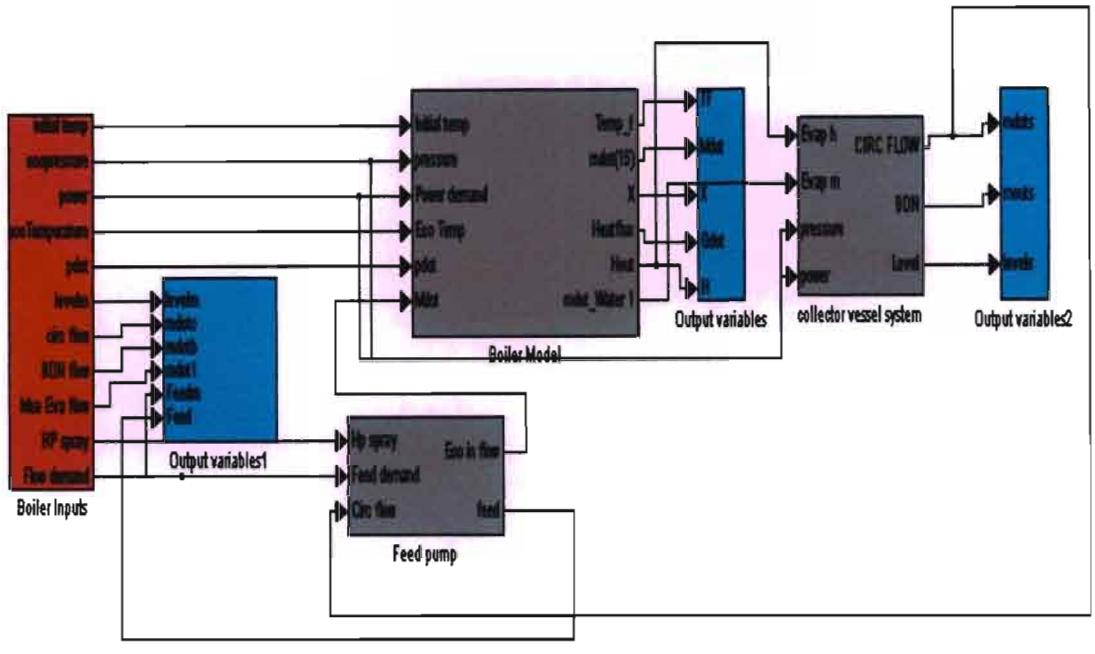

Figure 4.5: The simulink boiler model

Figure 4.5 shows the entire circulation system of the model. The inputs in figure 4.6 are connected into the tube section (figure 4.7), where the specific enthalpy and mass flow rate of each section of the boiler is calculated. The fraction of water at the evaporator output, flows into the collecting vessel (figure 4.8). The circulation flow from the collecting vessel is then added to the feed flow before the economiser input which can be seen in figure 4.13.

4.4.1 Tube section

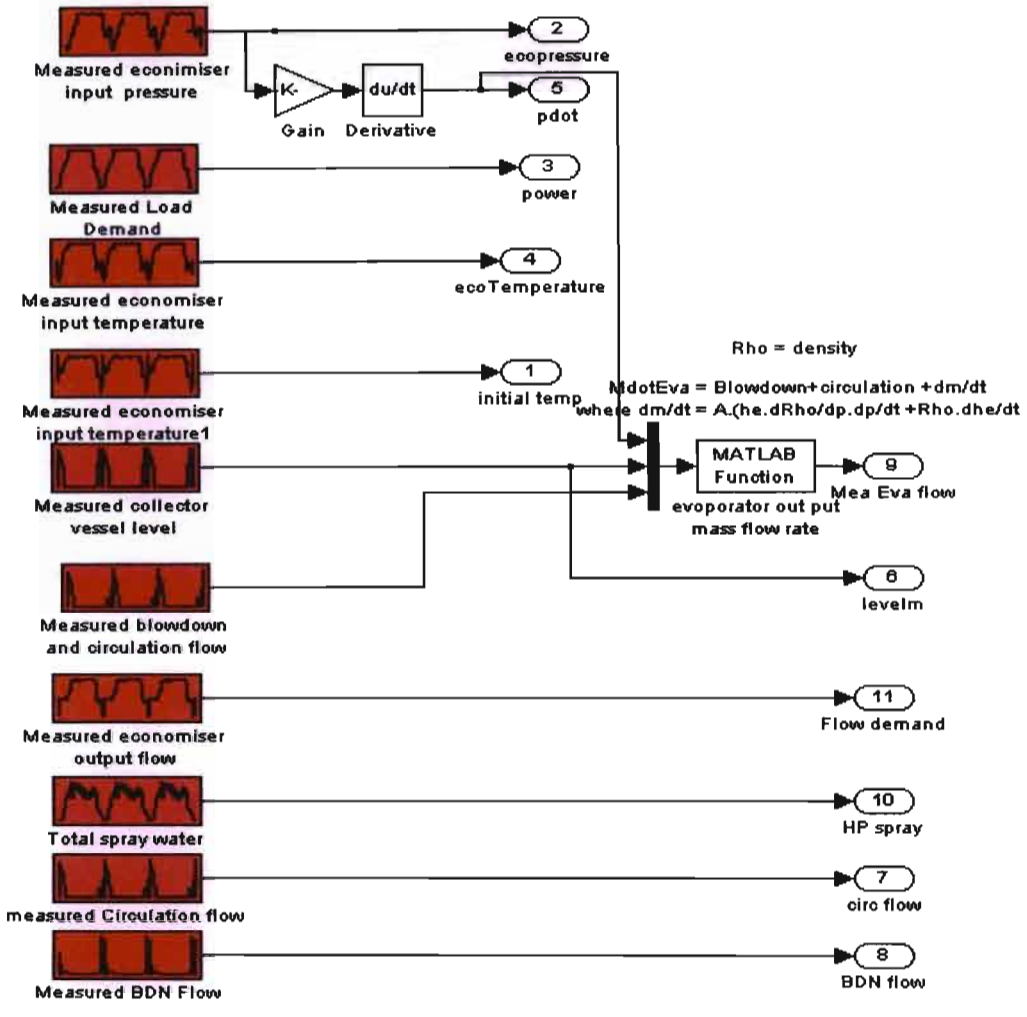

Figure 4.6: Simulink boiler model Inputs

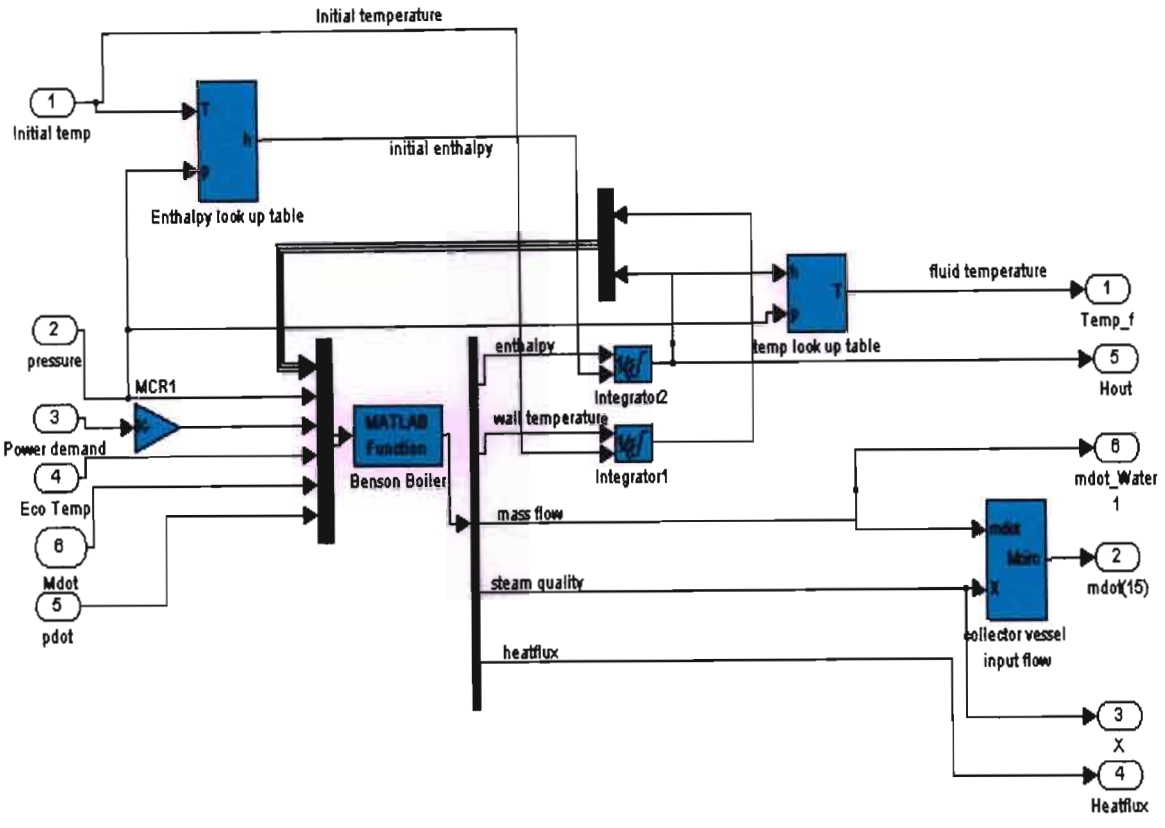

Figure 4.7: Boiler Tube System

4.4.2 Collecting vessel

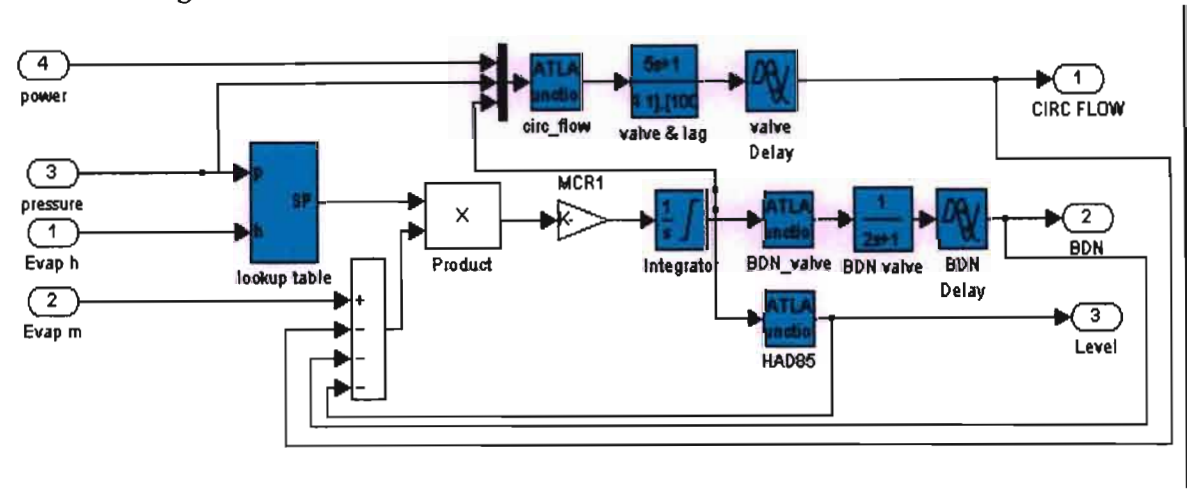

Figure 4.8: Boiler Model Subsystem

The circulation flow function (circ_flow) in figure 4.8 contains linear equations which relate the measured circulation flow to the measured collecting vessel level. The function represents the proportional controller of the circulation flow.

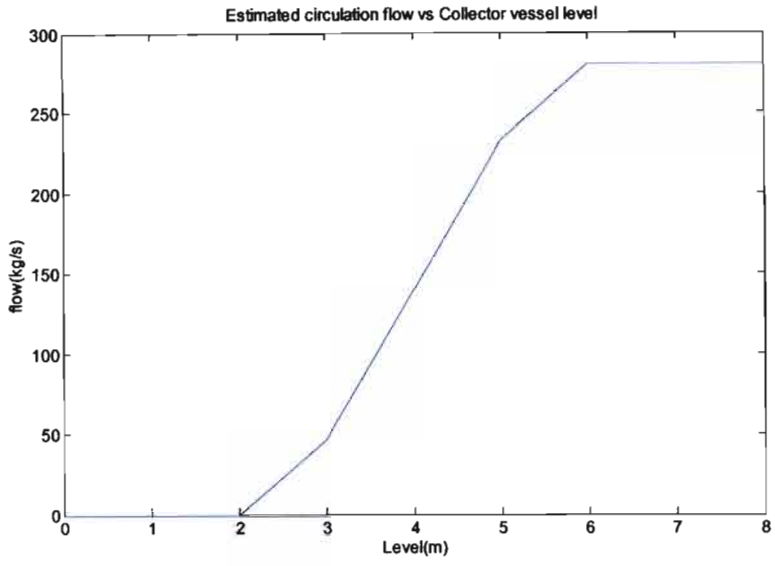

Figure 4.9 : Estimated circulation flow relationship with collecting vessel level of Majuba Unit 6 (proportional gain).

The derived linear relation is:

$$Circulationflow = \frac{280-0}{5.5-2.5}(level-2.5) \qquad (4.9)$$

The code of the function (circ_flow) also implements the logic which governs the circulation pump and is given in the Appendix C. The derived circulation model is then run with the measured collecting vessel level as input and the result obtained is compared to the measured circulation.

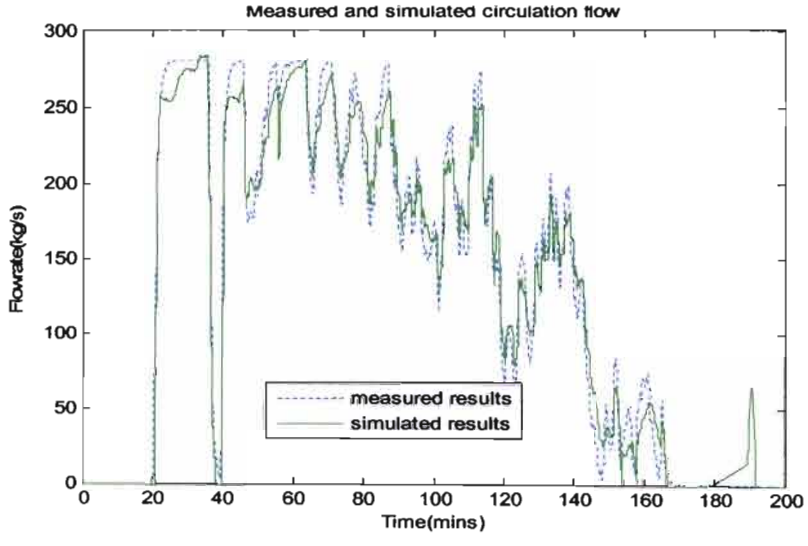

Figure 4.10: Measured and simulated circulation flow of Majuba Unit 6

The same method is applied to the blow down valve function (BDN_valve) in figure 4.8. A linear equation which relates the blow down valve flow to the collecting vessel level is obtained.

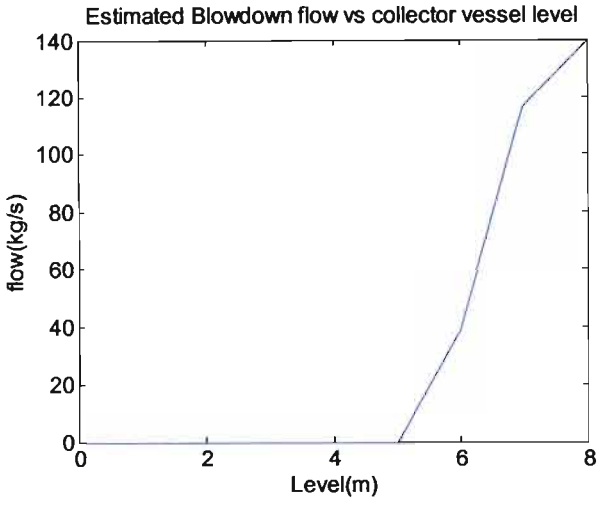

Figure 4.11: Estimated blow down flow with collecting vessel level of Majuba Unit 6

$$Blowdownflow = \frac{135-0}{7.3-5.5}(level-5.5) \qquad (4.10)$$

The code in this function (BDN_valve) is given in the Appendix C. The model of the blow down valve model is then run with the measured collecting vessel level as input and the results obtained compared to the measured blow down flow.

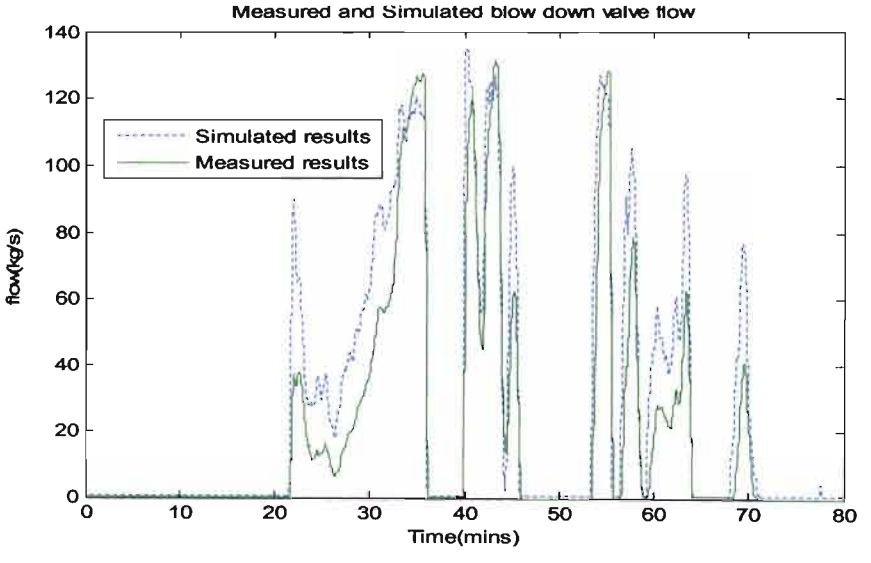

Figure 4.12: Measured and simulated Blow down valve flow of Majuba Unit 6

Had85 in figure 4.8 is a drain to attemperator number 3, and water normally flows from the collecting vessel when the circulation pump is on hot standby. The had85 function is a look-up table which relates the drain flow to the collecting vessel level.

4.4.3 Feed pump section

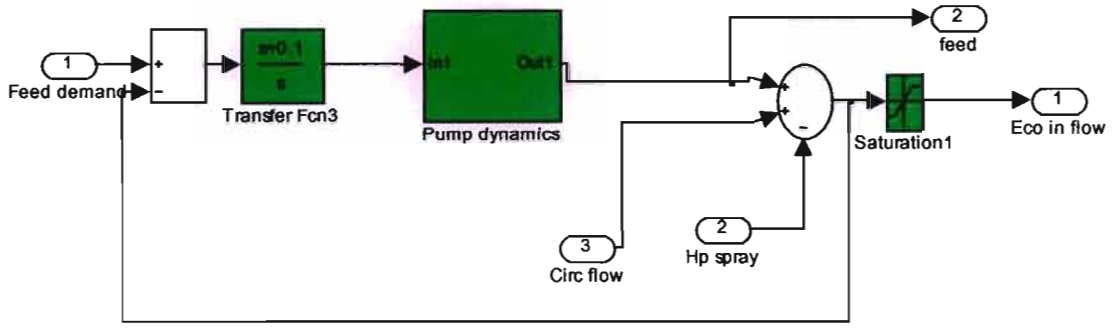

Figure 4.13: Boiler Model Feed Water Subsystem

The PI control of the feed pump in figure 4.13 is designed to meet the time response of the pump. The root locus and the step response of the controller are shown below.

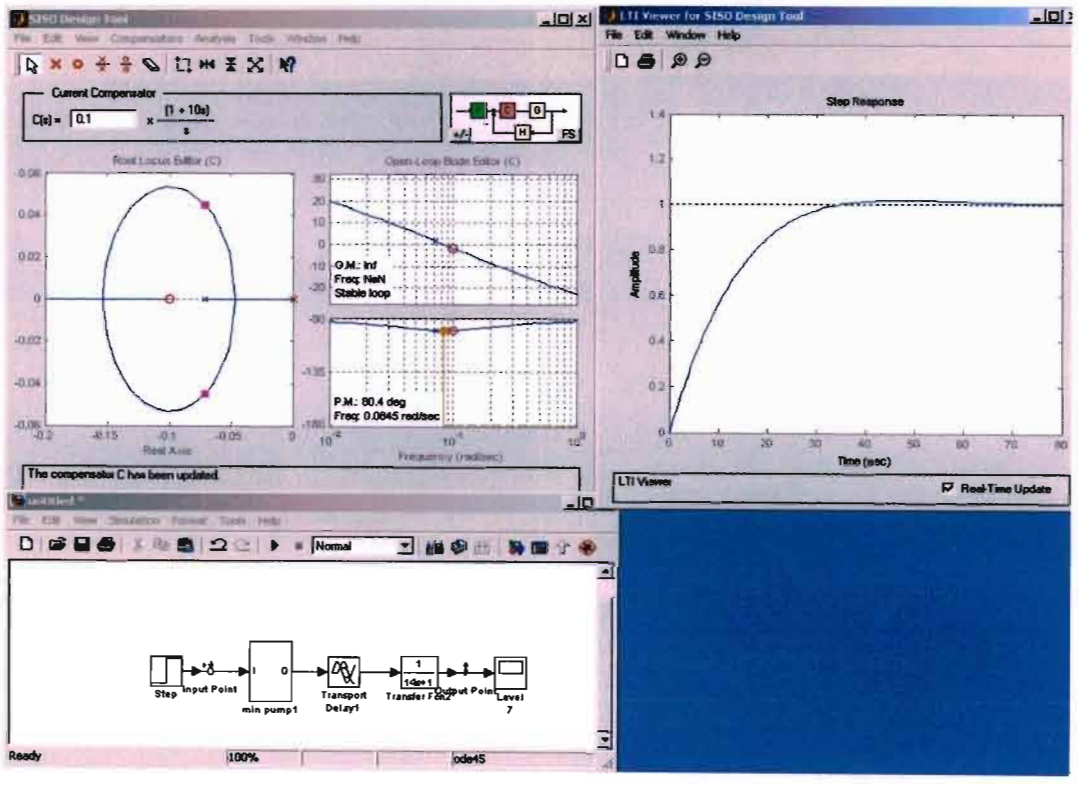

Figure 4.14: The root locus and the stability margins for the feed pump designed PI controller.

The pump block in figure 4.15 represents the feed pump trip characteristic. The block contains a relay which switches the pump on when the flow command is more than 40 kg/s and trips the pump if the command flow is less than 30 kg/s.

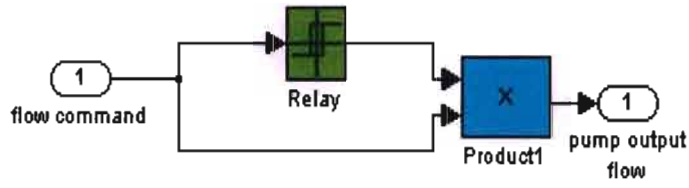

Figure 4.15: Pump trip logic, Eitelberg and Boje (2003)

Chapter 5

SIMULATION RESULTS AND DISCUSSION

5.1 Introduction

The simulation results are compared to the measured boiler results at Majuba Power Station Unit 6. Most of the thermodynamic properties are functions of pressure and specific enthalpy, and the pressure is known for the duration of the simulation. The measured evaporator output flow $\dot{m}_{water\_m}$ is compared to the simulated evaporator output flow $\dot{m}_{water\_s}$. Since the boiler specific enthalpy was not measured, it could not be compared to the simulated specific enthalpy.

1) $\dot{m}_{water\_s}$ is calculated as shown below:

$$\dot{m}_{water\_s} = \dot{m}_{evap} - \dot{m}_{steam} \tag{5.1}$$

$$\dot{m}_{steam} = x \times \dot{m}_{evap} \tag{5.2}$$

Replacing eqn (5.1) into eqn(5.2)

$$\dot{m}_{water\_s} = \dot{m}_{evap}(1-x) \quad \underline{(kg/s)} \tag{5.3}$$

2) $\dot{m}_{water\_m}$ is calculated as shown below:

from the collecting vessel we have,

$\dot{m}_{circ} = Cirpumpflow + Blowdownvalveflow$, l_{cv} is collecting vessel level

$$\dot{m}_{water\_m} = \frac{dm_{vessel}}{dt} + \dot{m}_{circ}$$

$$\Rightarrow \dot{m}_{water\_m} = A_{cv}\frac{d\rho(t)l_{cv}(t)}{dt} + \dot{m}_{circ}$$

$$were, \frac{d\rho(t)l_{cv}(t)}{dt} = l_{cv}(t)\frac{d\rho(t)}{dt} + \rho(t)\frac{dl_{cv}(t)}{dt} \tag{5.4}$$

and

$$\frac{d\rho}{dt} = \frac{\partial\rho}{\partial p}\frac{\partial p}{\partial t} + \frac{\partial p}{\partial h}\frac{\partial h}{\partial t}$$

From the simulation model, $\dot{m}_{water\_s}$ is calculated using eqn (5.3), with the steam fraction and the mass flow rate of each block being outputs of the boiler function (Benson_model).

The circulation pump and the blow down valves flow are obtained from the measured boiler data. The blow down valves flow is approximated as 1 kg/s = 1 %. Since the valve opening is not linear, the values obtained are not that accurate. The initial conditions of the specific enthalpy and wall temperature state variable in the model (see figure 4.7) are obtained from the economiser input specific enthalpy and input temperature respectively.

The time vector used in the simulation is obtained from the measured boiler data.

5.2 Initial Condition

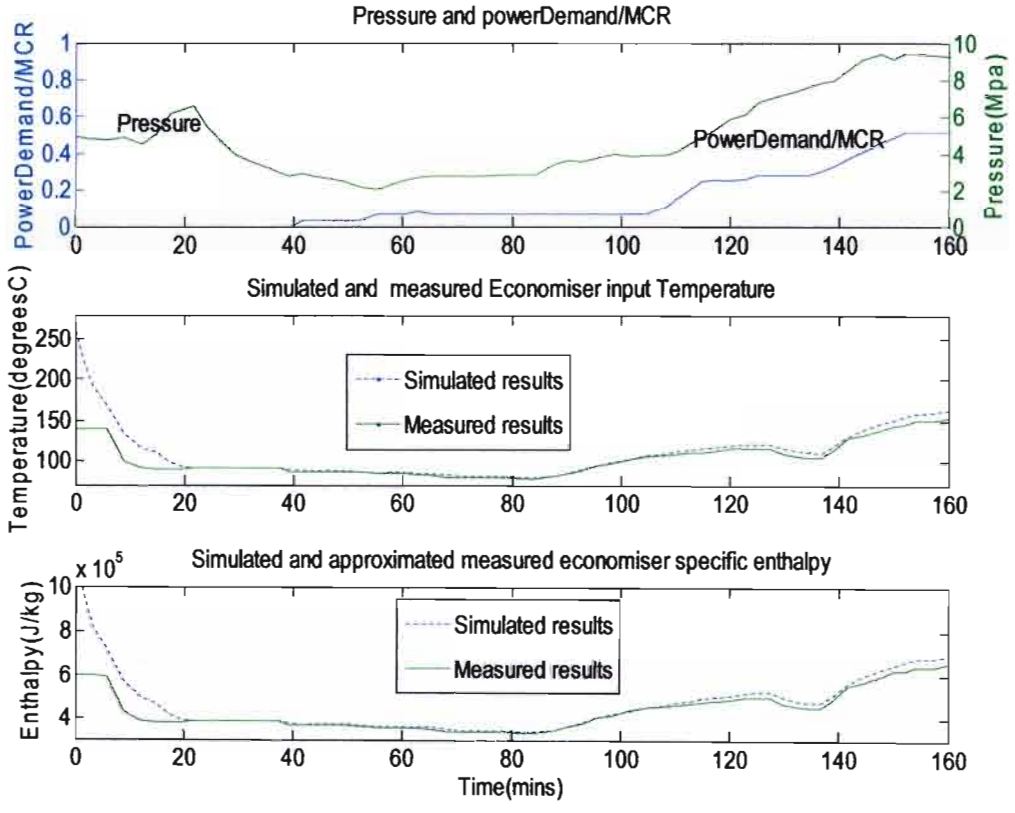

Figure 5.1: Simulated and Measured initial conditions during Start Up, Majuba Unit 6. Measured enthalpy approximated from measured initial temperature.

Figure 5.1 shows a hot start up simulation. Initially the pressure is about 4.5 MPa and the initial specific enthalpy is more than 2000 kJ/kg. The low pressure and high specific enthalpy result in boiling occurring in the economiser and evaporator. The initial specific enthalpy and the temperature are high, but cold feed and re-circulated water are injected

into the economiser when the boiler is operating below 55% MCR. This results in a drop in water temperature in the economiser and evaporator during start up. After 35 minutes the flow rate drops to almost zero, (see figure 5.2) due to the tripping of the circulation pump. This results in a sudden increase in specific enthalpy and temperature as there is no mass flow to carry the added energy away. After 40 minutes, cold feed water is pumped into the economiser and there is a sudden drop in temperature. After 100 minutes the pressure and the specific enthalpy start increasing, resulting in an increase in temperature, see figure 5.1.

5.3 Evaporator Start Up Simulation Results

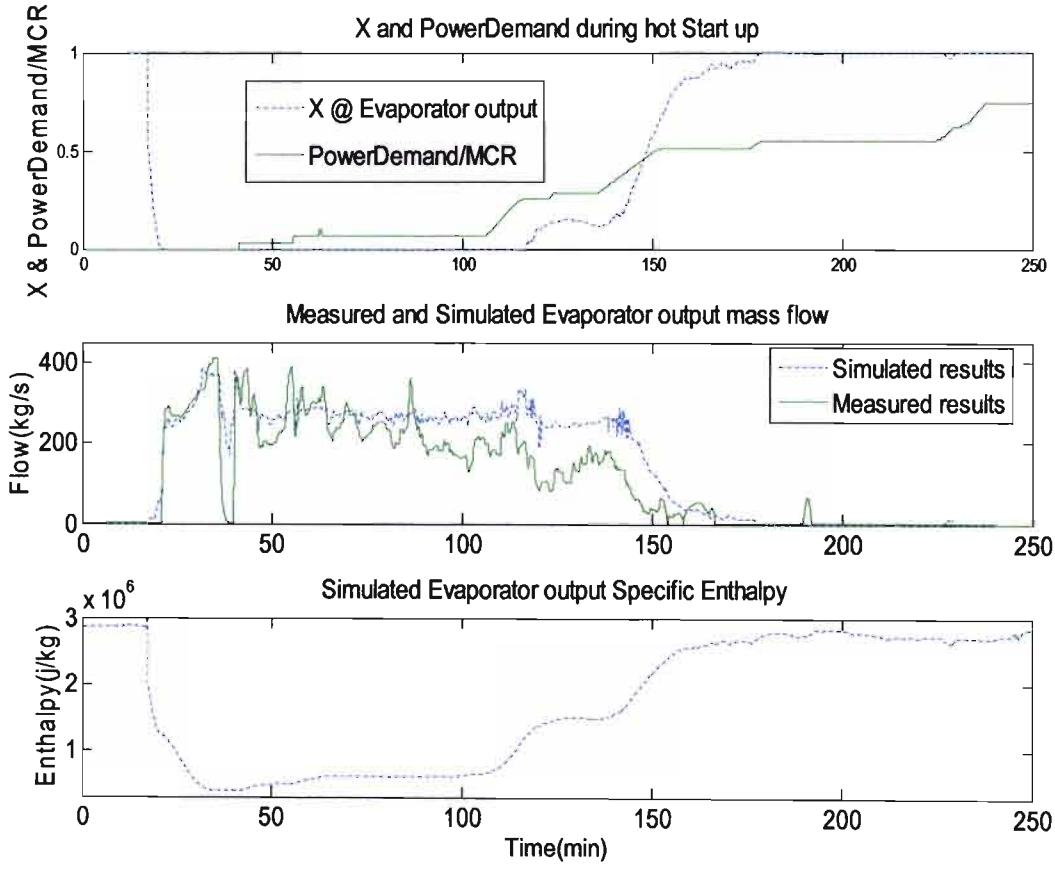

Figure 5.2: Boiler Model Start Up Response, Majuba Unit 6

Figure 5.2 shows the duration of the start up. Since it is a hot start up and the initial pressure is low, the boiler initially has a high steam fraction. This results in low circulation mass flow rate. After about 25 minutes the mass flow rate pumped into the economiser is increased which results in a sharp decrease in specific enthalpy and steam fraction. The simulation shows that once the boiler is operating above 60% MCR, the steam fraction increases to 1.

During the simulation, the first 50 minutes of the simulation can be seen to track the measured results. The simulation of the single phase for both water and steam flow was accurately modelled as seen in figure 5.2, between 0 to 25 minutes and 170 to 250 minutes respectively. When two phase flow occurs, the simulation results do not match the measured results accurately as seen in mass flow rate in figure 5.2. The reason could be due to the fact that two phase flow is calculated using an approximated correlations by Jens and Lottes (1951), eqn (3.27). It is also important to note that the boiler takes about 5.5 hrs to reach MCR.

5.4 Collecting Vessel Start Up Results.

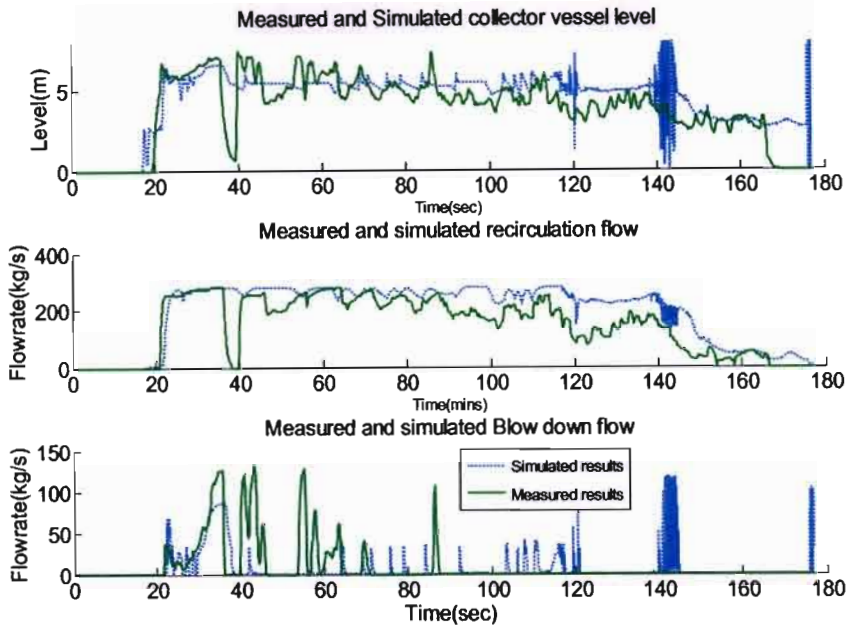

Figure 5.3 : Circulation flow, blow down valve flow and collecting vessel level simulation of Majuba Unit 6

Figure 5.3 shows the simulation results compared to the measured results. As seen from figure 5.3, the hot start up of the boiler was modelled accurately enough to show the necessary dynamics required for control analysis. The 10-15 min oscillations which could be caused by blow down interlock are clearly seen in the simulation results. The oscillation observed at 140 minutes is zoomed in to give figure 5.4. Figure 5.4 shows a consistent oscillation from 140 to 145 minutes. The oscillation seems to begin in the collecting vessel circuit since the simulated mass evaporator flow rate does not oscillate as much as the simulated collecting level and blow down mass flow rate. An FFT of the simulated circulation flow rate is taken to give figure 5.5

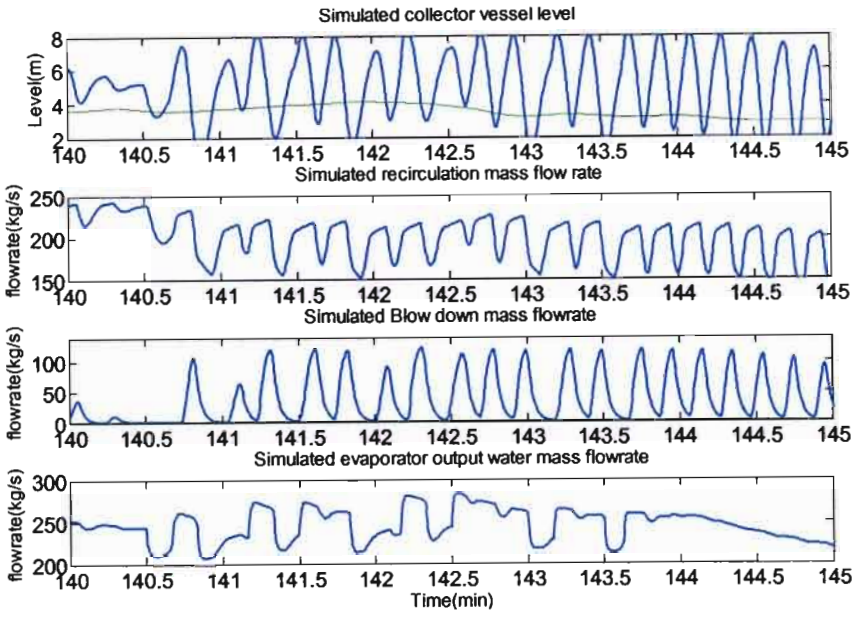

Figure 5.4: Zoomed figure 5.3 between 140-145 minutes. The instability is shown in this region., is not observed in the measured data

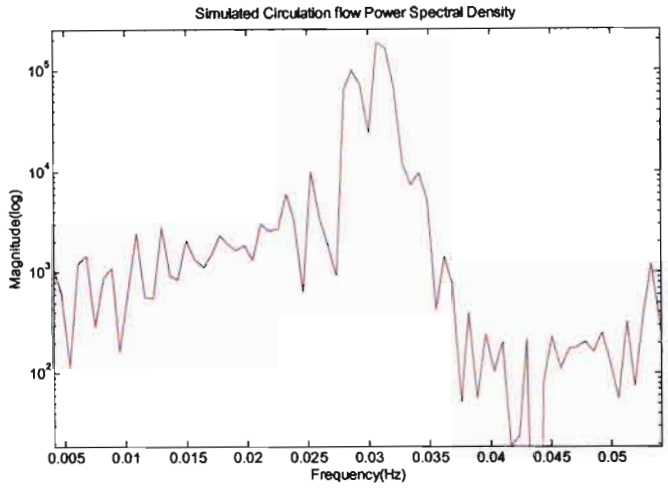

Figure 5.5: FFT analysis (sampling rate of 1 Hz) of collecting vessel level showing frequency (≈ 0.03 Hz) of oscillation. Since the oscillation is erratic, the power spectrum analysis has two distinctive peaks between 0.027 Hz and 0.031 Hz.

In order to determine the source of the oscillation, the mass flow rate and density through the boiler are analysed. The oscillation could be caused by abrupt change in density as water is converted into steam, as explained by Maffezzoni and Ferrarini (1989). The other source of the oscillation could be due to instability in the collection vessel, with additional gain caused by blow down.

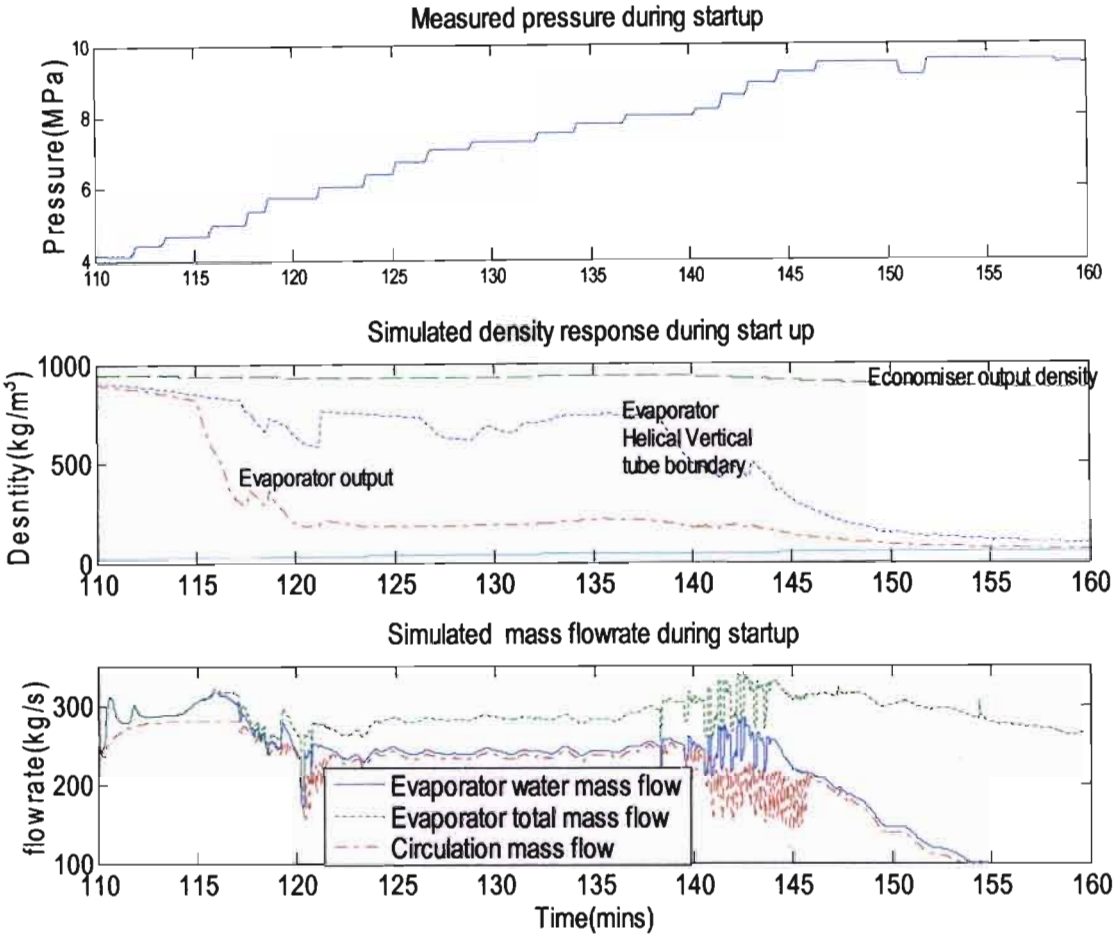

Figure 5.6: Density and Evaporator Mass Flow Rate

Figure 5.6 shows that steam starts forming after about 115 minutes and no oscillation is observed. This means that the abrupt change in the density is not the cause of the oscillation. As observed in figure 5.4, the circulation mass flow rate oscillates longer than the mass flow from the evaporator, also seen in figure 5.6. This means the source of the oscillation is in the collecting vessel circulation circuit.

At steady state there is no mass or energy accumulation in the evaporator and the gain of the boiler tube section is $N_{evap} = 1 - x$, described by Eitelberg and Boje (2001). Due to axial x- gradient in 2 phase region, the dynamic gain of the evaporator is much more complex because of mass accumulation and non linear transient mechanisms. To keep the problem simple, N_{evap} is used since it is not expected to differ dramatically from 1-x under most operation conditions (see Eitelberg and Boje, 2001). To find the effect of circulation mass flow rate on the evaporator mass flow rate, we only consider the circulation loop and ignore the feed loop.

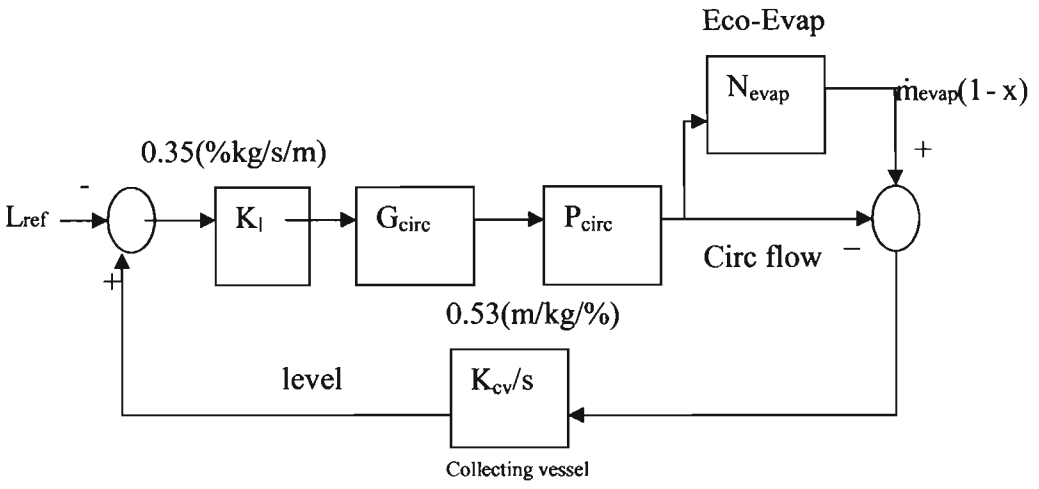

Figure 5.7: Simplified control loop representing the economiser and evaporator as N_{evap} (Eitelberg and Boje,2004).

G_{circ} denotes the controller in the circulation loop
P_{circ} absorbs the loop and valve characteristic of the circulation loop

Assuming an average density of water of about 700kg/m^3 at 10 MPa , the collecting vessel level gain is approximately

$$K_{cv} = \frac{100}{0.268 \times 700} = 0.5 \text{ (m/ kg/\%)} \qquad (5.5)$$

$$\text{Letting } L = \frac{K_I \times K_{circ} \times G_{circ} \times P_{circ} \times (1 - N_{evap})}{s} \qquad (5.6)$$

$$\text{then} \quad T_{Fcirc/Fevap} = \frac{L}{1+L} \qquad (5.7)$$

The Nichols plot of $T_{Fcirc/Fevap}$ is shown in figure 5.8.

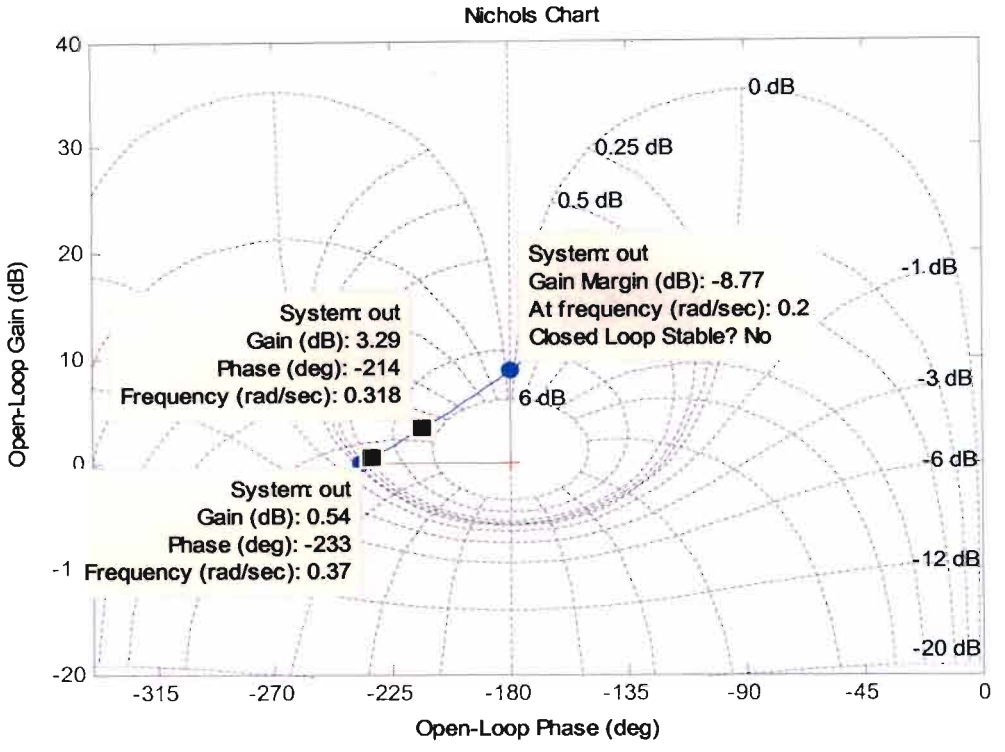

Figure 5.8: Nichols Chart of L with N_{evap} = 0, hence x= 1, Implying Steam generation

Figure 5.8 shows the closed loop system is unstable at a frequency of about 0.20 rads/sec. It implies that at a frequency of approximately 0.20 rads/sec, the system goes into a limit cycle and oscillates at frequency of approximately 3.2 mHz. The frequency is similar to the frequency observed in the FFT energy spectrum of the simulated circulation flow. From the observation it can be concluded that the oscillation seen in figure 5.3 could be caused by valve delay resulting in a lot of lag at low frequency or the bandwidth in the circulation loop.

5.5 Evaporator Shut down Simulation Results

The shut down process in figure 5.9 shows the same trend, were the simulation of the two phase flow is not that accurate as the simulation of the single phase flow. The start up and shut down results models the boiler in single phase flow more accurately than in two phase flow. The shut down simulation shows that once the boiler is operating below 50% MCR, the steam quality drops to about zero.

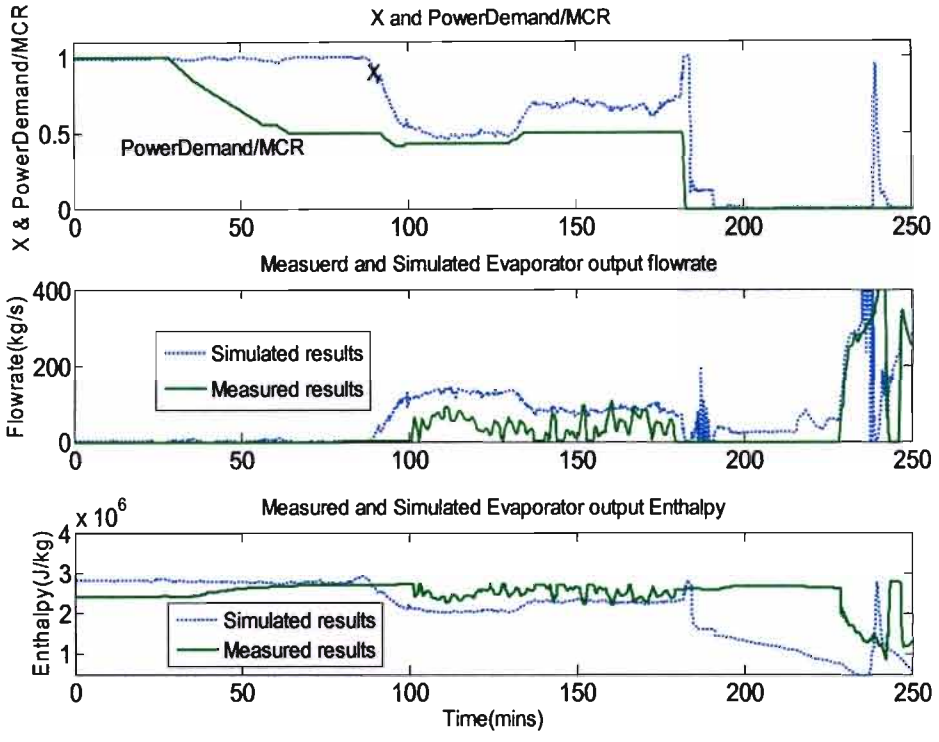

Figure 5.9: Simulink Model response during shutdown of Majuba Unit 6

5.6 Effect of Blow Down Flow on Evaporator Mass Flow.

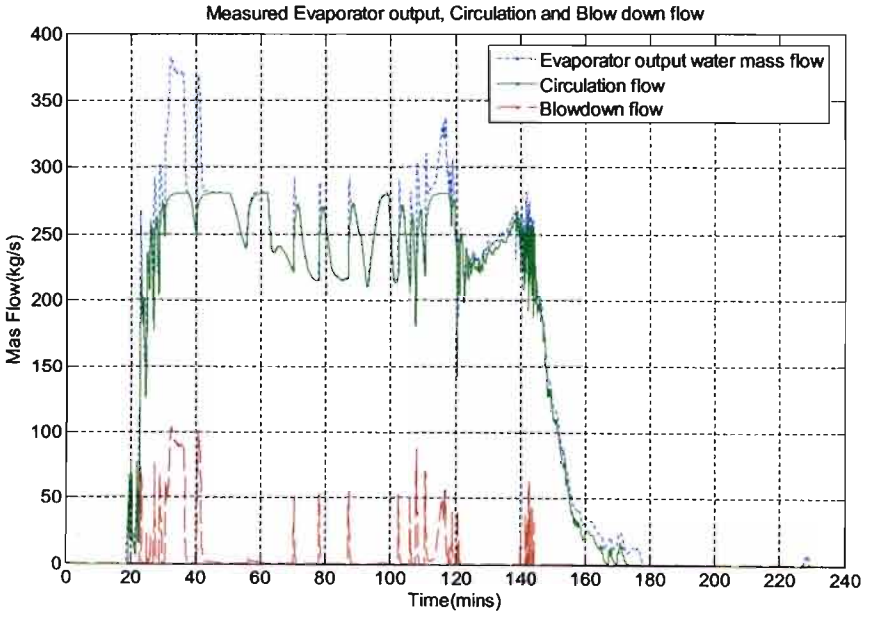

Figure 5.10: The effect of the Blow down flow on the evaporator flow during start up.

A limit cycle with a lower frequency than that observed in figure 5.3 is generated in the circulation loop around the boiler. A closer look at the simulated evaporator output flow shows an oscillation with a period of about 10 – 15 minutes. The blow down valves plays a role in the generation of the limit cycle. This is observed in figure 5.10. When the blow down valves open the drain the collecting vessel, resulting in a drop in the water level and circulation flow. The blow down valves opening depends on the level in the collecting vessel, and when the level is higher than 5 metres, the blow down valves open. When the collecting vessel level is below 4.5 metres, the blow down valves close. The draining of the collecting vessel results in the oscillation, considering also that the collecting vessel has a filling up capacity of approximately 7.44 seconds (Appendix B) at minimum evaporator flow.

The oscillation observed in figure 5.10 occurs during hot start up as evaporation takes place at different points in the economiser and the evaporator (see Maffezzoni and Ferrarini, 1989). This results in a water plug, as the steam formed in the lower section of the boiler pushes the water in the upper section of the boiler, resulting in an increase in mass flow rate. The increase in mass flow rate results in an increase in the collectinvessel level. The blow down valves open to prevent the collectin vessel from filling. This results in less circulation and more cold feed water.

5.7 Simulation Conclusion

The aim of developing the model was to capture the start up and shut down of the boiler with sufficient accuracy for circulation control design and analysis. The model did not accurately simulate the two phase flow, but that is not the subject being analysed in this thesis. Apart from the little lag in the model, the goals of the boiler model development have been achieved.

As seen from the simulation results, the boiler takes 5 hours to reach MCR. Due to low pressure and returned heat at start up, boiling occurs in different parts of the boiler resulting in a 10- 15 minute oscillation in the boiler, with blow down interlock assisting with oscillation by increasing the circulation loop gain. The effect of blow down interlock and level control are corner stones of the control problem.

In order to implement a two shifts a day scheme, the start up process and shut down process time should be reduced to the thermal rate limit of the thick walled equipment without risking tripping major plant equipment such as the feed pump and circulation pump. The ability to bring the plant online quickly would for example improve flexibility in plant operation and reduce the cost fuel oil and de-ionised water of the power plant during start up.

Chapter 6

CONTROL ANALYSIS

6.1 Introduction

During start up and shut down, Benson boilers operate in recirculation mode. This provides enough cooling to protect the evaporator from radiant heat. The separation vessels protect the superheaters from rapid cooling that would be caused by water carry over. Since the collecting vessel has a fill up capacity of about 7.5 seconds (with minimum evaporator flow), water carry over into the superheater in pre-Benson mode is possible if the circulation loop is not fast enough. The blow down interlock in the circulation loop contributes to the fluctuation in the mass flow rate. When the blow down valves open, the collecting vessel level collapses, resulting in less recirculation flow and hence more feed flow. In pre-Benson mode, cold feed water passes through the economiser and evaporator into the collecting vessel. The collecting vessel fills up, and once the level is too high the blow down valves open and the cycle repeats its self resulting in the 10-15 minute oscillation observed in the simulated and measured results. The oscillation stops when the boiler is operating in Benson mode, as all of the water fed into the economiser is converted into steam.

This section of the thesis looks into the problem generated by recirculation. A control analysis and design study is done to provide a more efficient and robust start up.

The control analysis involves the loop by loop analysis approach for multivariable feedback control design of the boiler. Linear models of the economiser and evaporator section of the boiler at different load demands are obtained. The linearization is done for loads below 50% MCR, because above 50% MCR the boiler is operating in Benson mode. Once the linear models are obtained, quantitative feed back theory is applied to solve the control problem.

6.2 Linearization of Nonlinear Benson Model

Since interest is in the circulation loop, which provides the evaporator mass flow during start-up, the model is linearised from the economiser input mass flow rate to the evaporator output mass flow rate.

When the boiler is operating in Benson mode, all the water flowing into the economiser is delivered by the feed pump. The amount of water fed into the economiser depends on the electricity demand and re-circulation flow in the pre-Benson mode. As a primary effect the circulation water flow appears as a disturbance in the feed water control loop. A simple control loop diagram from Eitelberg and Boje (2001) is used for the loop by loop multivariable control, figure 6.1.

The dynamics of the system is determined by the state differential equation, eqn (3.9)

$$\frac{dh}{dt} = \frac{1}{\rho A dz}\left[-\dot{m}(h(t,z+dz)-h(t,z))+\dot{q}_A+v\frac{dp}{dt}\right] \quad (6.1)$$

From 6.1, $\dot{h}$ can be rewritten in the form,

$$\dot{h} = f(h(z,t),h(z-1,t),\dot{q}(z,t),\dot{m}(t,z),\dot{p}(t,z)) \quad (6.2)$$

Equation 6.2 shows that $\dot{h}$ is a function of input specific enthalpy, mass flow rate, pressure and heatflux.

The output equation is given by

$$\dot{m}_{collector} = \dot{m}_{evap}\,(1 - x) \quad (6.3)$$

From eqn (6.3), $\dot{m}_{collector}$ can be written as,

$\dot{m}_{collector}$ = g ($\dot{m}_{evap}$, h_{15}), assuming the boiler is divided into 15 lumped blocks, the evaporator output specific enthalpy is h_{15}, and $\dot{m}_{evap}$ is algebraically determined from mass flow at the economiser input, eqn (3.13). For each lump element, $\dot{m}_{out}$ is a function of $\dot{m}_{in}$ and h_{out}

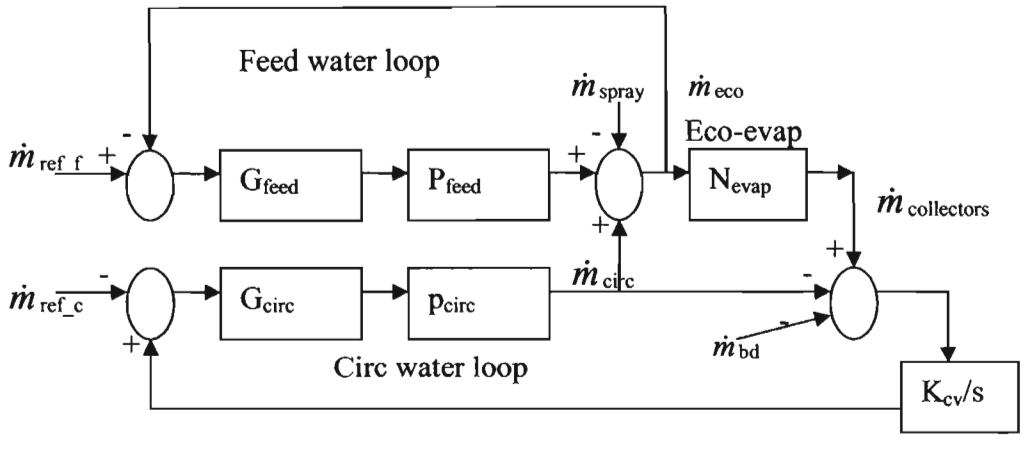

Figure 6.1: simplified water circulation, N_{evap} (see section 5.4) combines the economiser and the evaporator, Eitelberg and Boje (2001). The feed pump and valve dynamics have been absorbed into P_{feed} and the circulation valve and loop characteristic have been absorbed in P_{circ}. G_{circ} and G_{feed} represent the control regulating the collecting vessel level and feed water respectively.

Inputs to each lumped elements are the pressure, input specific enthalpy, heat added and input mass flow rate, as shown in figure 3.1.

Equation (6.1) and (6.2) are linearised about h_{0i}, h_{0i-1}, $\dot{m}_{0i}$, $\dot{q}_{0ij}$, $\dot{p}_{oi}$, $\dot{m}_{evaps}$, at steady state, where i represents each lumped element and j represent the different heat added to each lumped element.

The linearised equations give the state space model in the form given below (also see Ogata, 1997).

$$\Delta\dot{\underline{X}} = \underline{A}\Delta\underline{X} + \underline{B}\Delta\underline{U} \tag{6.4}$$

$$\Delta\underline{Y} = \underline{C}\Delta\underline{X} + \underline{D}\Delta\underline{U} \tag{6.5}$$

Using first order Taylor series to linearise eqn (6.1) and eqn (6.3), we obtain

$$a_i = \left.\frac{df}{dh}\right|_{u0i,xi0}, \; b_i = \left.\frac{df}{dh_{in}}\right|_{u0i,xi0}, \; c_i = \left.\frac{df}{dm}\right|_{u0i,xi0}, \; d_i = \left.\frac{df}{dp}\right|_{u0i,xi0}$$

$$e_{ij} = \left.\frac{df}{d\dot{q}_{ij}}\right|_{u0i,xi0}, \; r = \left.\frac{dg}{dh}\right|_{u0i,xi0} \; w = \left.\frac{dg}{d\dot{m}}\right|_{u0i,xi0} \tag{6.6}$$

Having 15 lumped elements gives a state matrix A shown below

$$\underline{A} = \begin{pmatrix} a_1 & 0 & 0 & \cdots & 0 & 0 & 0 \\ b_2 & a_2 & 0 & \cdots & 0 & 0 & 0 \\ 0 & b_3 & a_3 & \cdots & 0 & 0 & 0 \\ \vdots & & & \ddots & & & \vdots \\ \vdots & & & & \ddots & & \vdots \\ 0 & 0 & 0 & \cdots & b_{14} & a_{14} & 0 \\ 0 & 0 & 0 & \cdots & 0 & b_{15} & a_{15} \end{pmatrix}$$

For a specific lumped element, $\dot{h}$ is a function of the input and specific enthalpy of the lumped element. The lumped element will only be affected by specific enthalpy of adjacent lumped elements at its input. This means the other lumped element contribution will be zero as shown by the state matrix A, resulting in a diagonal matrix (A = Jacobian of enthalpy)

$$\underline{B} = \begin{pmatrix} b_1 & c_1 & d_1 & e_{1,1} & 0 & \cdots & 0 & 0 \\ 0 & c_2 & d_2 & 0 & e_{2,2} & & 0 & 0 \\ \vdots & \vdots & \vdots & & & \ddots & \vdots & \vdots \\ 0 & c_{14} & d_{14} & 0 & 0 & \cdots & e_{14,14} & 0 \\ 0 & c_{15} & d_{15} & 0 & 0 & \cdots & 0 & e_{15,15} \end{pmatrix} \qquad \underline{u} = \begin{bmatrix} h_{in} \\ \dot{m}_{in} \\ p \\ \dot{q}_1 \\ . \\ . \\ \dot{q}_{15} \end{bmatrix}$$

The matrix B contains the Jacobian of the input vectors.

Heatflux from the flame into a specific lumped element only depends on the heat added on that lumped element. The contribution from other lumped elements will be zero as shown in the input matrix B

The output matrix ,C, and direct transmission matrix, D, are shown below.

$\underline{C}$ = [0,0,0,0,0,0,0,0,0,0,0,0,0,0,r]

The model output ($\dot{m}_{evaps}$) only depends on the evaporator output specific enthalpy (r is Jacobian of evaporator specific enthalpy)

$\underline{D}$ = [0,w,0,0,0,0,0,0,0,0,0,0,0,0,0,0,0]

The model output ($\dot{m}_{evaps}$) only depends on the evaporator output mass flow rate. (w is Jacobian of output evaporator specific enthalpy)

N_{evap} is then given by $\underline{C}$ (Is-$\underline{A}$)$^{-1}$ $\underline{B}$ + $\underline{D}$

$\dot{m}_{eco}$ is the input, implying N_{evap}(s) is the transfer function from economiser input mass flow rate to the evaporator output mass flow rate.

From the results obtained in the simulation, it shows that above 55% MCR there is no circulation flow since all the water in the evaporator is converted into steam. So the gain of N_{evap} will be zero. Hence the model is linearised from 10% MCR to 50% MCR, in. An example of the linearised model at 50% MCR is given in Appendix B

The interesting thing to note about N_{evap} at high frequency is that the system will have a gain of about 0.2628. This shows that about 75% of water fed into the economiser is converted into steam at 50% MCR.

For N_{evap} at 50% MCR (from Appendix B), a step change input mass flow would result in an output of
1.028e-7/6.656e-8 = 1.544. (6.7)

Equation 6.7 shows that a step change of 1 kg/s at the economiser input results in the short term evaporator output mass flow increasing by 1.54 kg/s. The mass flow increase is due to the fact that the water fed into the economiser gains energy as it flows through the economiser and evaporator. The density is inversely proportional to the specific enthalpy. This means as the fluid enthalpy increases, the fluid volume increases, resulting in an increase in mass flow in the boiler tubes.

The developed linear model at 50% MCR is tested by adding a negative step of 1kg /s at 1000 seconds and then adding a positive step of 1 kg/s at 3000 seconds. The results obtained are compared to the nonlinear model response (figure 6.2). The economiser input mass flow rate is 284.27 kg/s and the stead state output mass flow rate at the evaporator output is about 284.27 * 0.2628 kg/s ≈ 74.71 kg/s (from eqn(6.7)). A negative step change of 1 kg/s at the input results in output of

$$74.71 - 1.544 \times 1 \approx 73.16 kg/s \qquad (6.8)$$

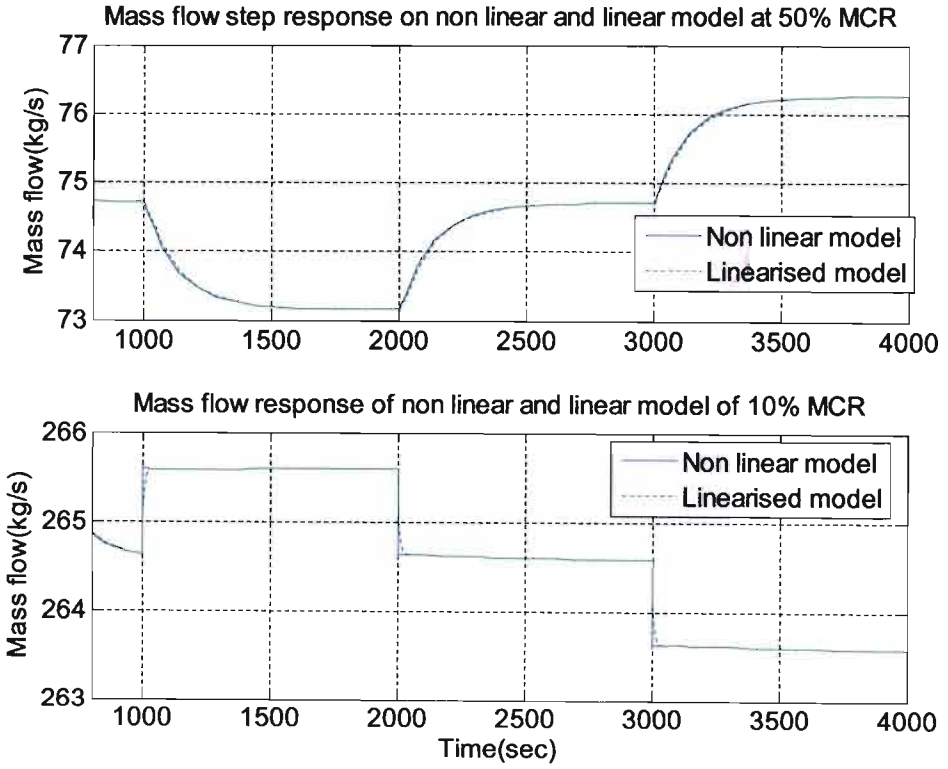

Figure 6.2: Step response of linear and non linear model of Benson boiler

6.3 Stiffness of the Simulation.

Bulirsch and Stoer (1979) explains that Stiffness occurs in a system where there are two or more very different time scales of the independent variable on which the dependent variables are changing. If the explicit Euler method is used to find a solution of a stiff differential equation and letting the eigenvalues of the differential equation be λ_i, i

$=\{1,2,3.....n\}$,the step size for the integration has to be less than $\frac{2}{|\lambda_{max}|}$ for the simulation to be stable (see Bulirsch and Stoer, 1979).

Finding the eigenvalues of the linearised state matrix A, we get

λ_i {A} = [-49.23, -28.82, -20.60, -16.08, -13.04, -0.57, -0.37, -0.22, -0.09,-0.03, -0.04, -0.04, -0.04, -0.04,-0.04]

Maximum simulation step size required = $\frac{2}{|-49|} = 0.0408\text{sec}$ for simulation to be stable.

If we used the smallest eigenvalue, we get a step size $= \frac{2}{|-0.03|} = 66.67\text{sec}$. The difference in magnitude of eigenvalues shows the difference in time step required for Euler integration method, and using the definition given by Bulirsch and Stoer (1979) proves the system is very stiff. A step size of 41 milliseconds means a simulation of 5 hours would require about 440000 simulation steps.

6.4 Frequency Analysis of Linearised Model

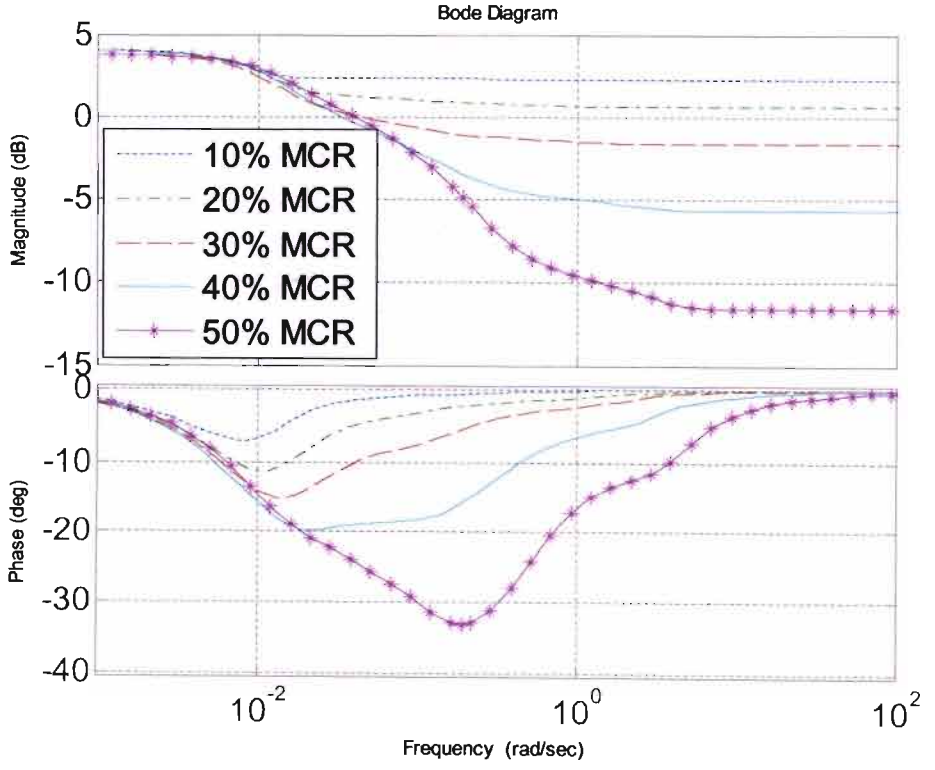

Figure 6.3: Frequency response of the linearised transfer through the economiser and evaporator (N_{evap}).

The frequency response of the linearised model is similar to the frequency response obtained by Eitelberg and Boje (2004). For frequencies below 0.1 rad/s the transfer function for the different heat rates give identical responses. This implies that the transfer through the evaporator, $N_{evap}(s)$, does not depend much on the specific enthalpy at the economiser input. This is significant because the fluid flow control can be expected to have significant higher bandwidth at a relatively high frequency of 0.1 rads/s, as observed by Eitelberg and Boje (2004). This implies for relatively high frequency the control system structure in figure 6.1 with, $N_{evap} = \dot{m}_{evap}(1- x)$ is valid.

For the analysis of the control system in figure 6.1, we simplify it by introducing two 'local' loops transfer function (see Eitelberg and Boje, 2004). Letting L_{feed} denote the feed water loop transfer function around the feed water pump when the circulation water is open:

$$L_{feed} = G_{feed}(s)P_{feed}(s) \tag{6.9}$$

Using the $G_{feed} = 0.1\times\left(\frac{s+0.1}{s}\right)$, designed in chapter 4

$P_{feed} = \frac{1}{s+1/14}e^{-4s}$, from Eitelberg and Boje (2001)

$$L_{feed} = 0.1\times\left(\frac{s+0.1}{s}\right)\frac{1}{s+1/14}e^{-4s} = 0.1\times\frac{(s+0.1)}{s^2+s/14}e^{-4s} \tag{6.10}$$

Letting L_{circ} denote the artificial circulation water loop transfer function around the when no water comes out of the evaporator:

$$L_{circ} = G_{circ}(s)P_{circ}(s)K_{cv}/s \tag{6.11}$$

Using the $G_{circ} = \frac{25s+1}{50s+1}$, from Eitelberg and Boje(2001)

$P_{circ} = \frac{1}{4s+1}e^{-4s}$, from Eitelberg and Boje(2001)

$$L_{circ} = \frac{25s+1}{50s+1}\frac{1}{4s+1}\frac{0.0053}{s}e^{-4s} = \frac{0.0053(25s+1)}{200s^3+54s^2+s}e^{-4s} \tag{6.12}$$

K_{cv}/s represents the transfer function of the collecting vessel from flow to level. Reducing the loop around the circulation loops, figure. 6.1 simplifies to figure 6.4.

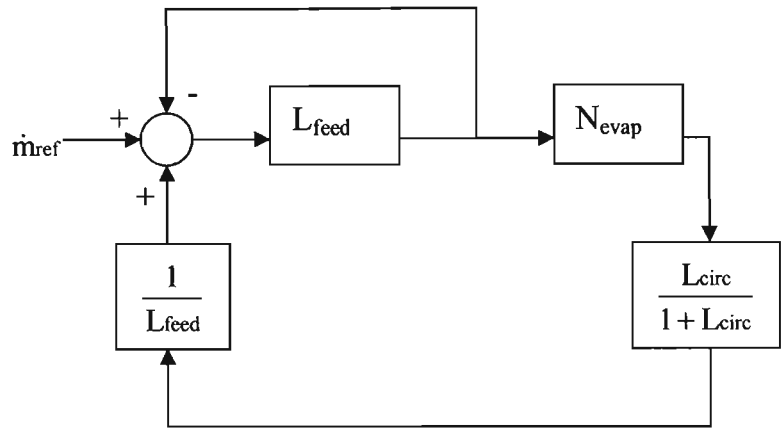

Figure 6.4: Reducing the circulation control loop in figure 6.1 gives a simplified control loop showing the positive feed back around the evaporator loop

Letting L_{evap} denote the positive feedback transfer function around the evaporator, and reducing the feed water control loop, Fig. 6.4 simplifies to Fig. 6.5.

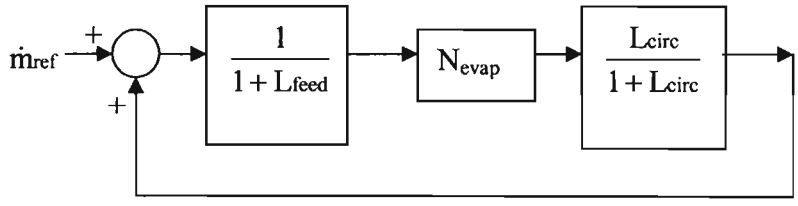

Figure 6.5: Simplified control loop of Fig. 6.4

From figure 6.5 it can be seen that

$$L_{evap} = -N_{evap}\frac{1}{1+L_{feed}}\frac{L_{circ}}{1+L_{circ}} \qquad (6.13)$$

L_{evap} derived by block diagram reduction is the same as the simplified L_{evap} found by Eitelberg and Boje (2004)

$\frac{1}{1+L_{feed}}$ has a high pass frequency character beyond the loop gain cross-over frequency, and the frequency character of $\frac{L_{circ}}{1+L_{circ}}$ is a low pass below the circulation loop gain cross-over frequency, as shown in Fig. 6.6

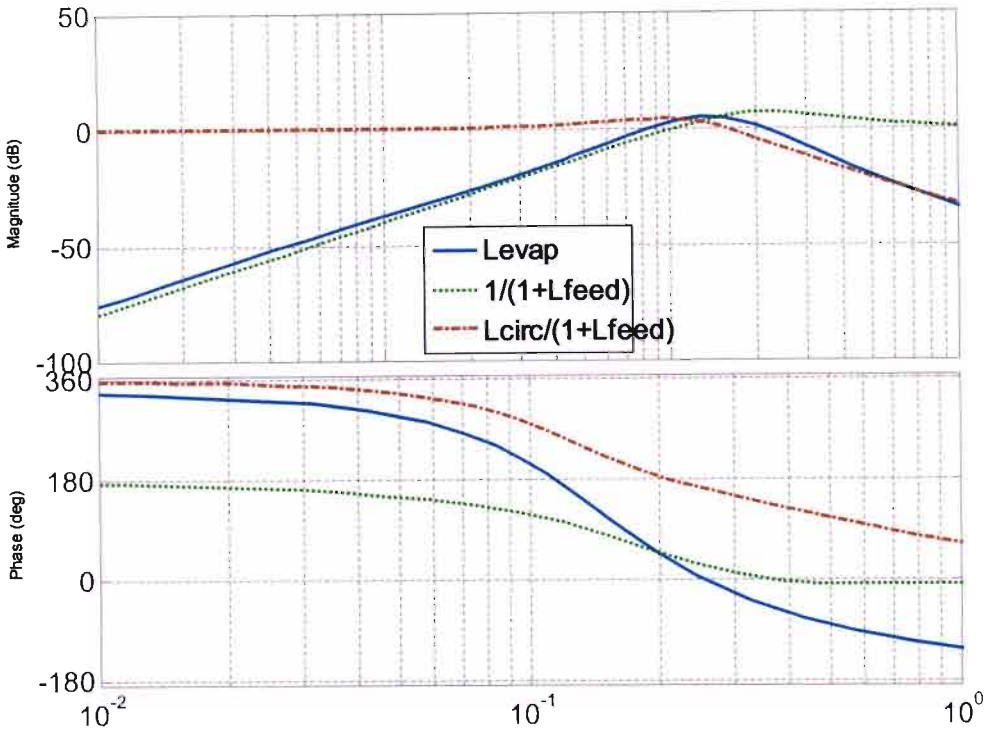

Figure 6.6: The Frequency response of the 1/ (1 + L_{circ}), L_{feed}/ (1 + L_{feed}) and L_{evap} with plant at 30% MCR

Figure 6.6 shows that the feed control loop term has a high pass effect and the circulation control loop has a low pass effect on L_{evap}. At the circulation and feed control loop corner frequency it is observed that

$$\left|\frac{1}{1+\mathrm{Lfeed}}\frac{L_{circ}}{1+L_{circ}}\right|>1 \qquad (6.14)$$

From figure 6.3 it observed that at the corner frequency of both L_{feed}/(1 + L_{feed}) and 1/(1+L_{circ}), N_{evap} can either be greater or smaller than unity, depending on the load demand(| N_{evap} | = [-3, …,3] dB at 0.1 rads/s). There is a possibility of $|L_{evap}|>1$, since Lfeed/ (1 + L_{feed}) and 1/ (1+L_{circ}) have a magnitude greater than unity. In this condition the system is likely to be unstable in the small signal sense. The frequency value of the limit cycle is observed at the point where $|L_{evap}|>1$. The frequency response of L_{evap} is show in figure 6.7.

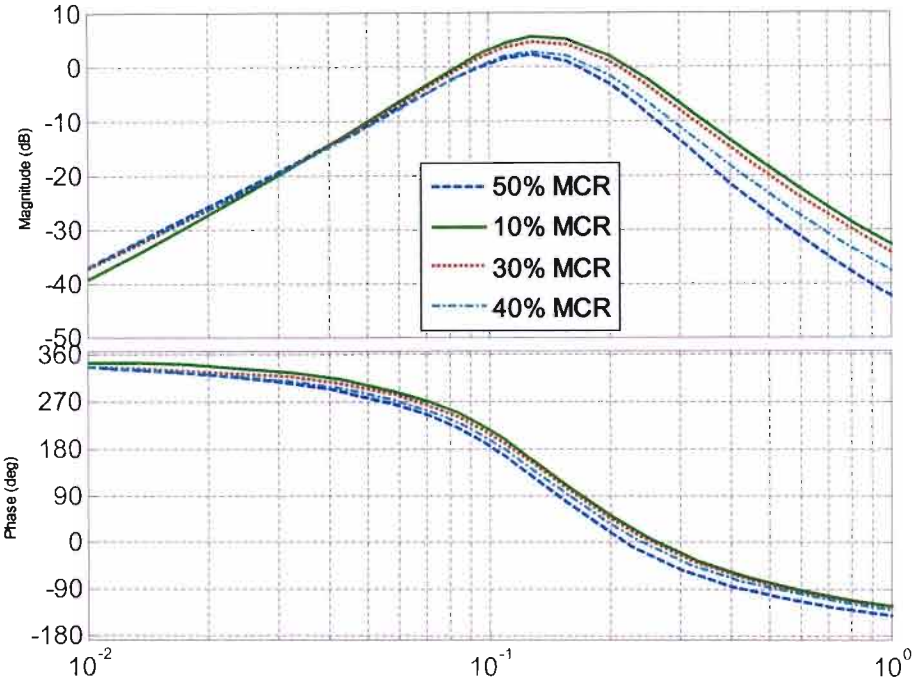

Figure 6.7: Bode plot of L_{evap} at 10%, 30%, 40% and 50% MCR

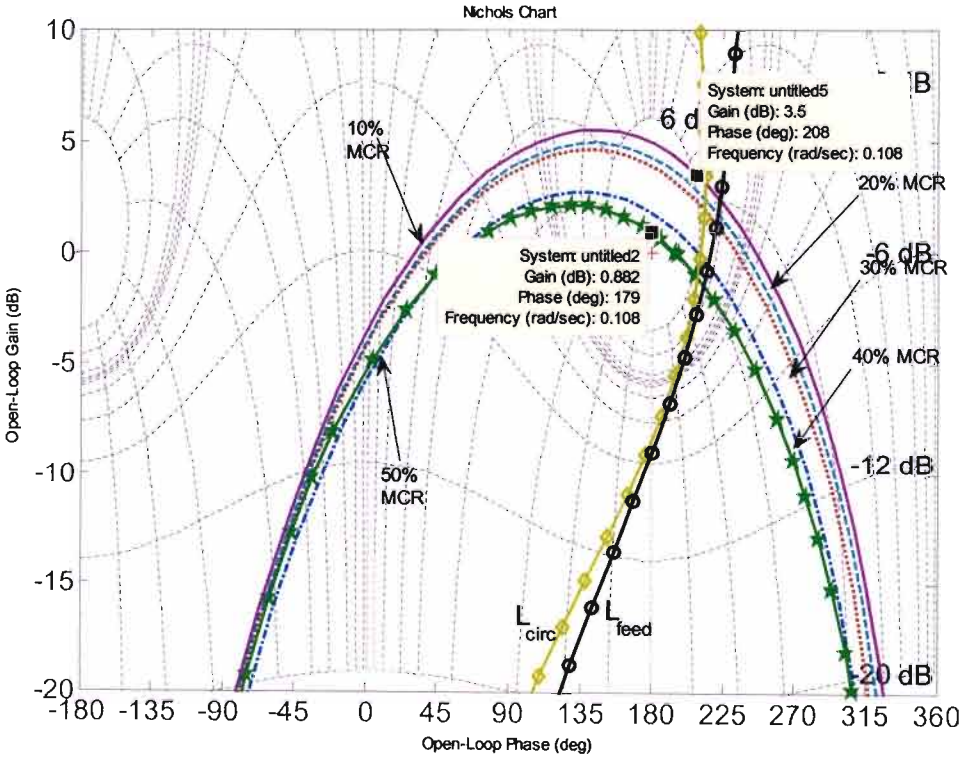

Figure 6.8: Nichols chat plot of L_{evap} at 10% to 50% MCR, L_{circ} and L_{feed}

Figure 6.7, shows a reduction in the magnitude of L_{evap} at the corner frequency as the firing rate increases from 10% MCR to 50% MCR, this agrees with Eitelberg and Boje (2004), that the system becomes stable as the firing rates increase. At 50% MCR, the frequency at the Nyquist points is about 0.1 rad/s.

Taking a look at figure 6.9, which is the warm start up used in the simulation, the measured economiser mass flow rate is compared to the blow down mass flow and the firing rate.

For the hot start up in figure 6.9, three patterns of the boiler operation can be observed. Once the boiler is started up, the boiler goes into a limit cycle of about 10 – 15 minute cycles. In the first sector of start up, the flow pattern is affected by water plug, consisting of water filling the upstream part of the circulation, while steam begins to expand at an intermediate point in the evaporator as described by Maffezzoni and Ferrarini (1989). This water plug is a very difficult thermal process to control. The oscillation can be seen to be caused by the blow down interlock. This happens when the water pumped into the economiser comes out of the evaporator with little steam being generated into the evaporator. This causes more water to enter the collecting vessel and the safety interlock opens the blow down valves to drain. The level of the collecting vessel will collapse, leading to more cold water being feed into the economiser.

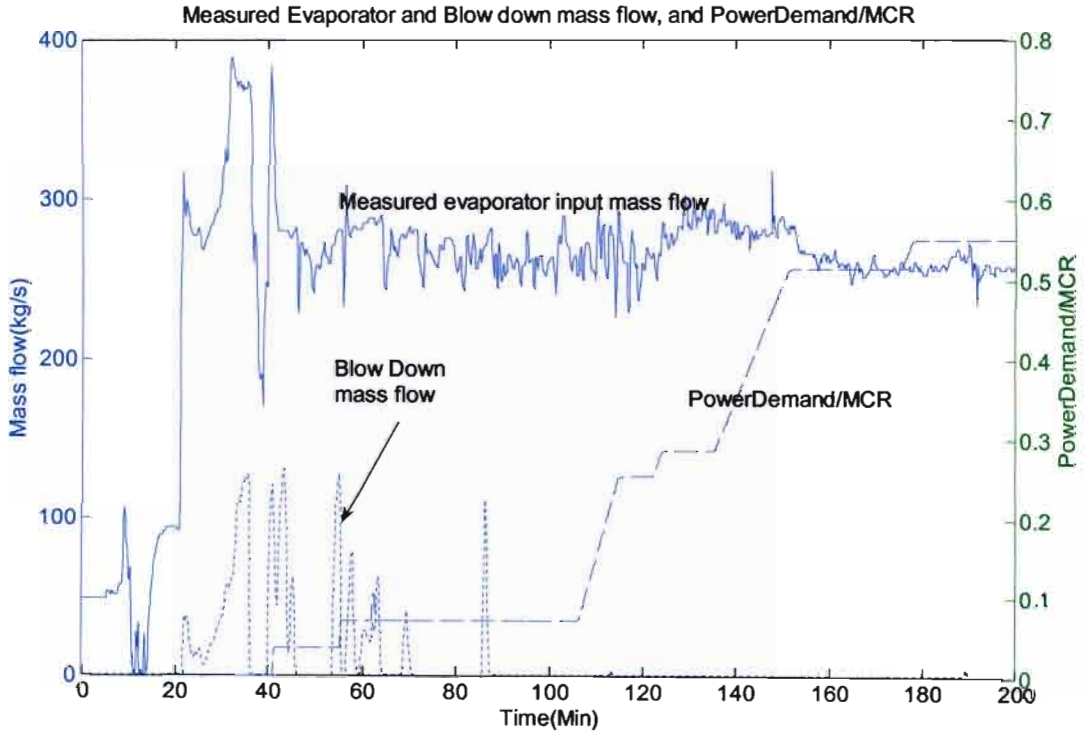

Figure 6.9: Hot start up measured evaporator and blow down mass flow rate Majuba Unit 6. The measured power demand is also plotted.

The second pattern occurs from about 100 minutes to 150 minutes, where the oscillation with periods of about 1.5 minutes is seen (see figure 6.10). This occurs when the boiler is operating between 10 % MCR - 50 % MCR. The oscillation is normally caused by limit cycling control loop around some gain changing nonlinear system components, which may be caused by something that saturates temporarily (see Eitelberg and Boje, 2004). The oscillation seems to be persistent between 110 minutes - 120 minutes, and seems to diminish as the firing rate increases. This agrees with the previous observation of the stability increasing with increase in firing order. The small oscillation occurring after the firing rate increases above 50% and constitutes the third pattern observed in the boiler operation. During this period, steam comes out of the evaporator and the boiler is operating in Benson mode. At this point there is no recirculation, which would suggest that most of the limit cycle oscillation observed between 110 minutes - 120 minutes is affected by the circulation control loop, since the oscillation diminishes when recirculation ends.

The fast Fourier transform analysis of the signal between 100 and 140 minutes is shown in figure 6.10. The peak of the energy spectrum seems to occur at approximately 17 mHz The width of the peak around 17 mHz are due to the erratic nature of the oscillation. The Nichols chat plot of L_{evap} (see Fig 6.8) shows the frequency at the Nyquist point is about 0.10 rad/s.

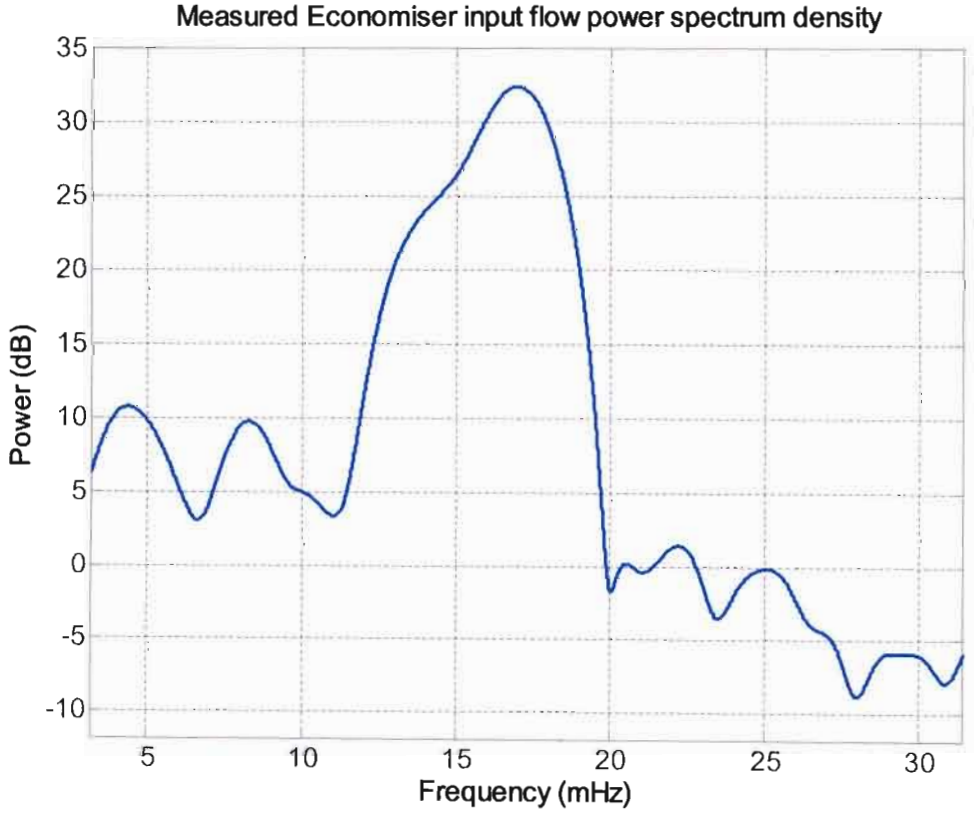

Figure 6.10: Energy spectrum (FFT) of economiser flow rate between 110 – 150 minutes, sampling time of 10 seconds. Peak occurs between 16 mHz and 17 mHz.

This gives a frequency of:

$$\text{Frequency of oscillation} = \frac{0.10}{2\pi} = 0.16 \text{ mHz} \qquad (6.15)$$

The calculated frequency is 16 mHz and the energy spectrum analysis also shows a peak at about 17mHz. It can be concluded that erratic oscillation occurring between 110 and 150 minutes is caused by limit cycling control loops around some gain changing non-linear system components. The validity of the model is shown as the linearised model limit cycle frequency is similar to the measured results.

From figure 6.6, it is seen that either reducing the circulation loop bandwidth or increasing the feed loop bandwidth would reduce the problem of excess gain at the gain cross over frequency of $L_{circ}/(1 + L_{circ})$ and $1/(1+ L_{feed})$. Since the feed water may already be tuned to its maximum bandwidth as observed by Eitelberg and Boje (2004), the only reliable and sensible thing to do is to tune the level controller. This is done by either reducing the circulation control gain (see Eitelberg and Boje, 2004) or implementing a PI control with gain scheduling and collecting level set point.

This thesis focuses on the design of a gain scheduled and set point PI controller. A PI controller will allow automatic control of boiler start up. Another advantage of using a PI controller is that it improves the steady state performance of the level control, while allowing stability at any loads, giving a robust water circulation control.

6.5 Robust Controller Design of Level Control Loop

The first step in the control design is deriving the actual loop transfer of the circulation loop. From figure 6.1, the control loop diagram simplifies to the figure 6.12

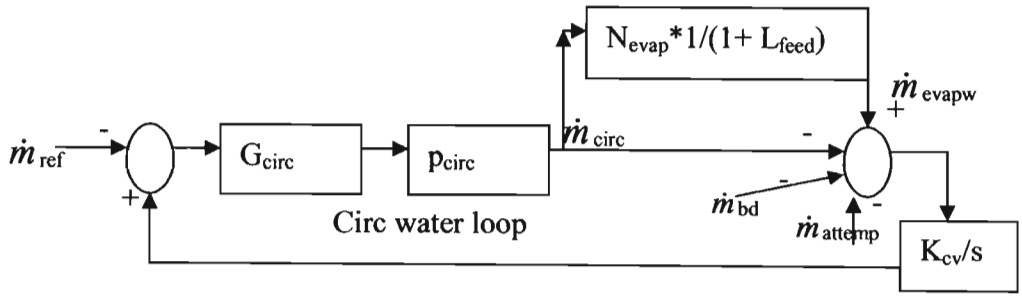

Figure 6.11: simplified control loop of figure 5.1, reducing the feed control loop

From figure 6.11 we get

$$L_{levelcontrol} = L_{circ} \times \left(\frac{N_{evap}}{1 + L_{feed}} - 1 \right) \qquad (6.16)$$

Since N_{evap} varies continuously during start up, for a specific N_{evap} at a specific MCR rating, the corresponding L_{feed} is chosen for that MCR rating. The first step in the controller design requires the frequency specification of the plant operation, which includes:

1) Maximum bandwidth. Due to small volume of the collecting vessel, the circulation loop has to be fast to prevent the collecting vessel from filling up.

2) $T_{Y/Do} = 1/ (1+ Lcirc) < 3db$ (for allω), the disturbance rejection at the output and the differential sensitivity must be minimised, making the system robust.

3) Zero steady state error, (not necessarily important, but emphasize the controller being designed is a PI controller)

Since the plant varies during start up, a frequency analysis is done at different MCR's and the worst case plant is used to design the controller. The Nichols chart of the $L_{levelcontrol}$ at different MCR's is shown in figure 6.12. The figure shows that at 180° phase lag (marked points are at frequency of about 0.35 rads/s), the plant only differs in magnitude at different loads. From figure 6.12, it is seen that at 50% MCR the plant has minimum bandwidth and maximum bandwidth at 10% MCR. Since the design specifications require maximum bandwidth, the plant requires different proportional gain values at different load values during start up. This means the designed controller will have a proportional gain which varies with load.

The controller is designed using the quantitative feedback control toolbox in the Matlab/Simulink environment.

The Nichols chart and the templates in figure 6.12 and 6.13 respectively show that the frequency response is similar at different MCR values. The templates show the locus of the plant at different frequencies as the plant varies. From the templates it is seen that at about 0.35 Hz, the frequency response of $L_{levelcontrol}$, at different MCR values, only differs in magnitude. This means that the designed PI controller can have a variable gain to accommodate the different load demands during start up. Once the PI controller is designed, gain scheduling is implemented to shrink the high frequency response to avoid over design. This results in increased bandwidth at high MCR values.

The controller is designed from low to high frequencies. The integrator is added first and the gain adjusted. Then the lead term is added to meet sensitivity specs (see also Maciejowski, 1989) .

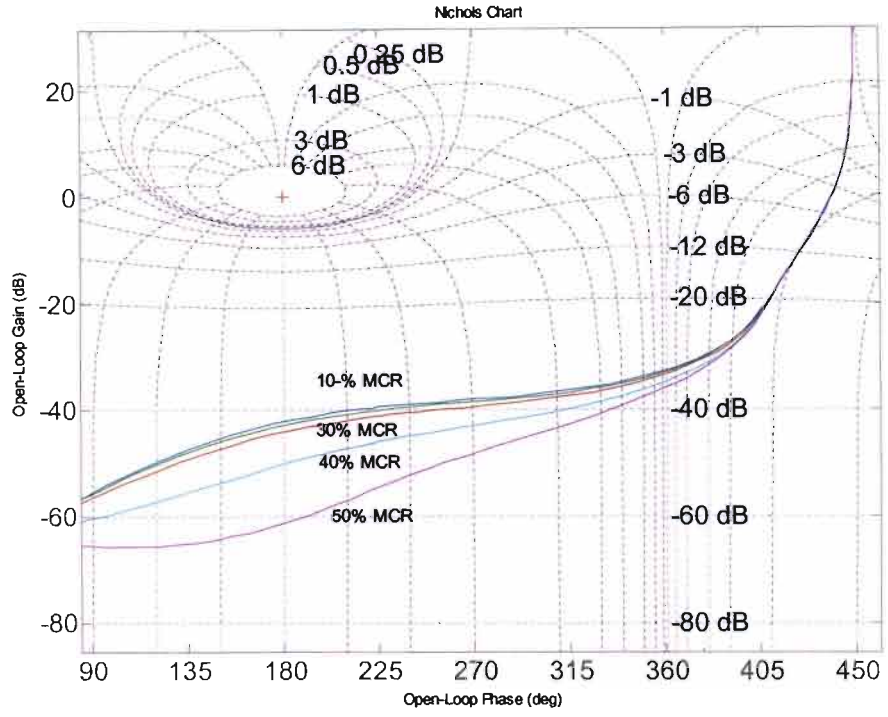

Figure 6.12: Nichols chart plot of $L_{levelcontrol}$ at different MCR values

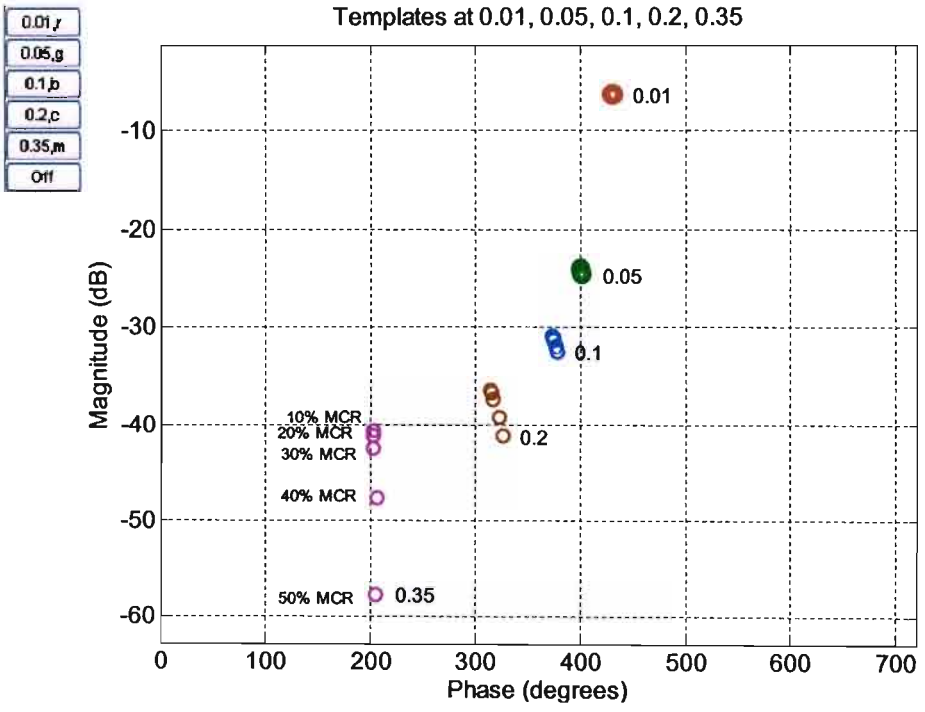

Figure 6.13: Nichols chart templates of $L_{levelcontrol}$ at different MCR values, at different frequencies

The $L_{levelcontrol}$ at 50% MCR was chosen as the nominal plant, and locus of the specification are drawn on a log-polar plane (Nichols chart).

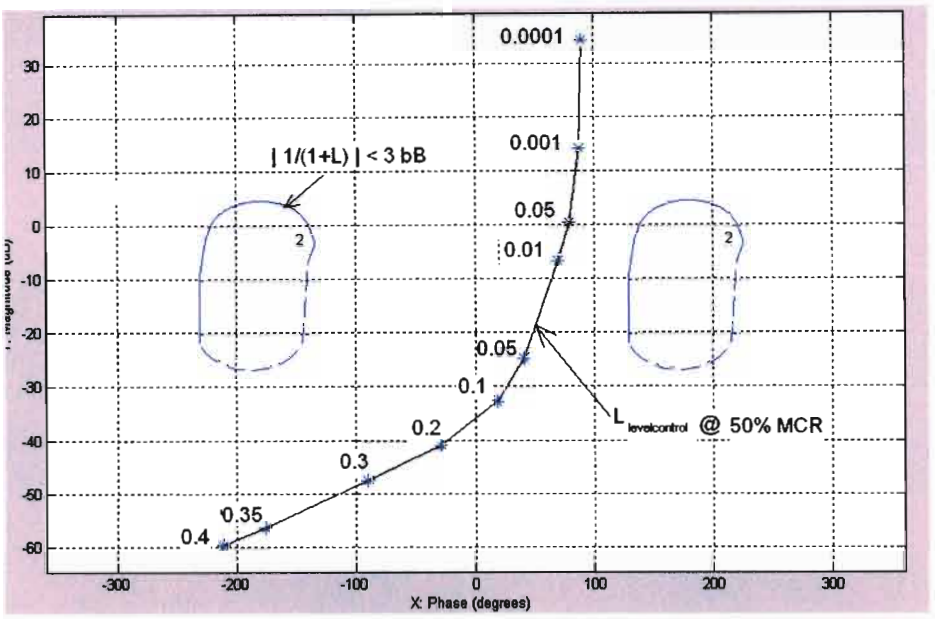

Figure 6.14: Nichols chart showing specification boundary and $L_{levelcontrol}$ at 50% MCR without PI controller

Since the controller is designed from low to high frequency, the first step in controller design is the addition of an integrator. Since a PI controller is being designed, 1 integrator is added.

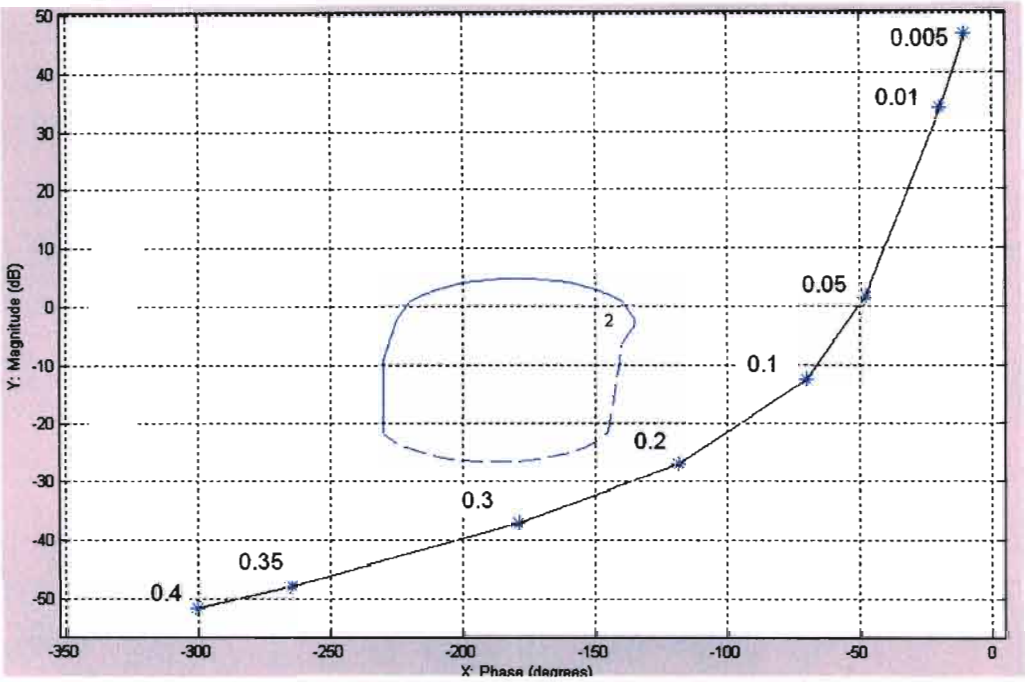

Figure 6.15: $L_{levelcontrol}$ with an integrator

The Nichols chart shows the first step in the controller design, which is the addition of the integrator to $L_{levelcontrol}$. From the figure it can be seen that adding the integrator increases the gain and adds a phase lag of 90 degrees.

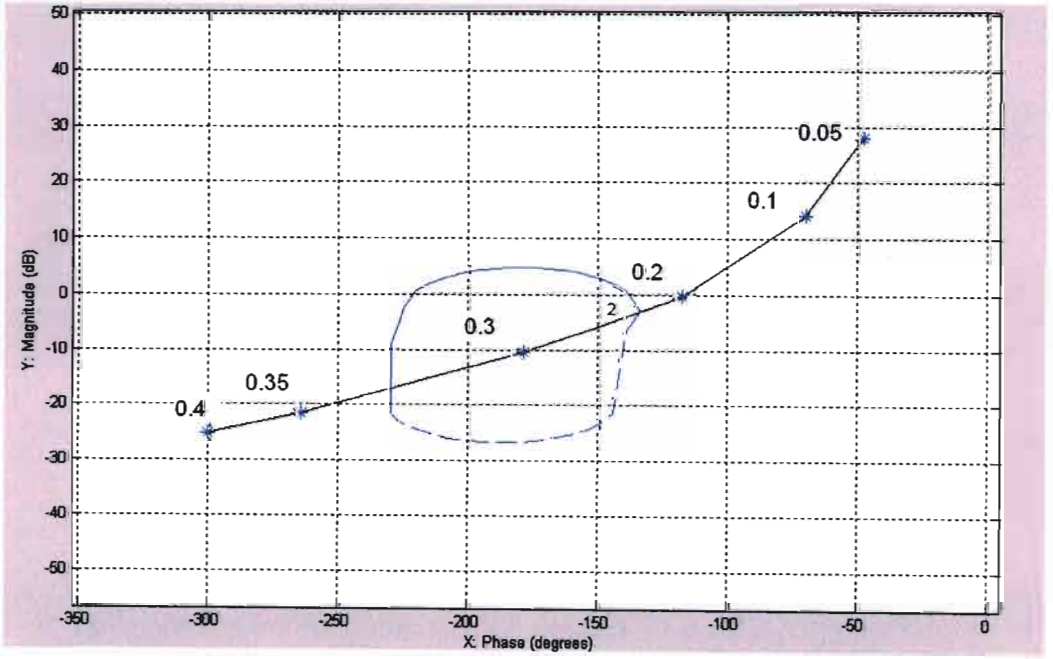

Figure 6.16: Gain of 22 is added to the system in figure 6.15

Adding a PI controller numerator term (zero)to get a phase lead of 60 degrees at 0.3 rads/s gives ,
Zero = 0.3/tan(60) = 0.17 rad/s
Reducing the gain gives the frequency response in figure 6.17

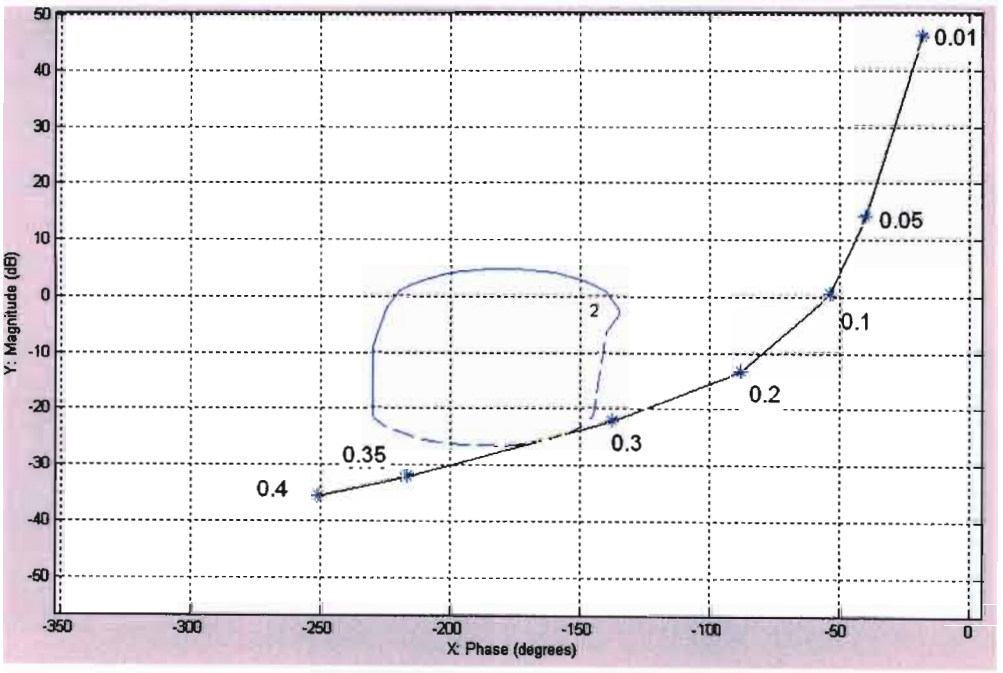

Figure 6.17: Frequency response of $L_{levelcontrol}$ with An integrator, a gain (5.6) and a lead term (zero = 0.17).

The designed controller $G_{circ} = 5.6\frac{(s+1/6)}{s}$, which is similar to the one given by Eitelberg and Boje (2004). The bode plot of the new $\frac{L_{circ}}{1+L_{circ}}$ with the controller and $\frac{1}{1+L_{feed}}$ is shown if figure 6.18.

Figure 6.18 shows that the combined magnitude of $\left|\frac{1}{1+L_{feed}}\frac{L_{circ}}{1+L_{circ}}\right| < 1$ at all frequencies. This implies that the system is less likely to be unstable since N_{evap} varies from [-3, 3] dB at 0.1 rads/s, figure 6.7.

From Figure 6.18, it's seen that L_{evap} reduces in magnitude at 0.1 rads/s, compared to L_{evap} in figure 6.6.

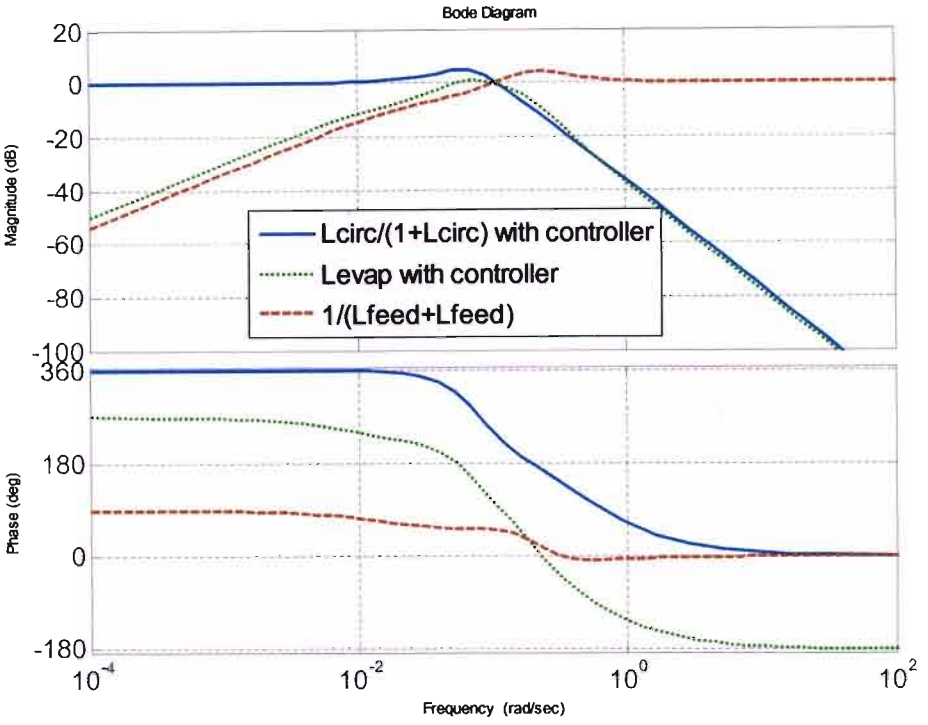

Figure 6.18: Frequency response of the 1/ (1 + L_{feed}), L_{evap} and L_{circ}/ (1 + L_{circ}), with the new controller in L_{circ}. N_{evap} is at 30 MCR

At different MCR values the controller requires different gains to meet the second specification, $T_{Y/Do}$ = 1/ (1+ Lcirc) < 3db. Since maximum bandwidth is required, a gain scheduling system is implemented to give the plant maximum performance at different MCR values. To get the gains required at each MCR value below 55% MCR, a quantitative feedback design is done on each plant separately. The controller in each case has the same lead term, and only the proportional gain value is different. The controller structure is the same since the frequency response at different MCR values only differs in magnitude as seen in figure 6.13 (Template at $\omega = 0.35$). The gains obtained are given in table 6.1.

% MCR	Proportional gain (Kp)
10	5.6
20	5.8
30	6
40	9
50	20

Table 6.1: Shows Proportional Controller gains required at each MCR

Any gain schedule is clearly non linear, but since the power added to the boiler changes very slowly, the scheduled gains are assumed to be time invariant.

Using Parseval's theorem (see McGillem and Cooper, 1991), it can be shown that increasing the bandwidth improves the performance of the system, as most of the oscillation generated in the circulation loop is filtered out.
Assuming a linear system H(s), which alters the energy spectrum of a signal transmitted through it, the output and input will be related by:

$$Y(s) = H(s)\, X(s) \tag{6.17}$$

Using Parseval's theorem, the energy spectrum of the output is then found to be

$$|Y(s)|^2 = Y(s)Y^*(s) \Rightarrow [H(s)X(s)]\cdot[H^*(s)X^*(s)] \tag{6.18}$$

$$= |H(s)|^2 |X(s)|^2 \tag{6.19}$$

Equation 6.19 (see McGillem and Cooper, 1991), shows that the energy spectrum of the output is related to the input energy spectrum by the quantity $|H(s)|^2$. $|H(s)|^2$ is sometimes called the energy transfer function of the system. This means that if a signal with an arbitrary energy spectrum is passed through a band pass filter with a narrow pass band at a frequency f, the energy spectrum of the output will be the portion of the energy spectrum of the input corresponding to the frequency of the filter pass band. In the collecting vessel loop, letting H(s) equal,

$$H(s) = \frac{K_{cv}/s}{1 + K_{cvs} \times G_{circ} \times P_{circ}} \tag{6.20}$$

were P_{circ} is the valve dynamics of the circulation flow and G_{circ} is the control designed.

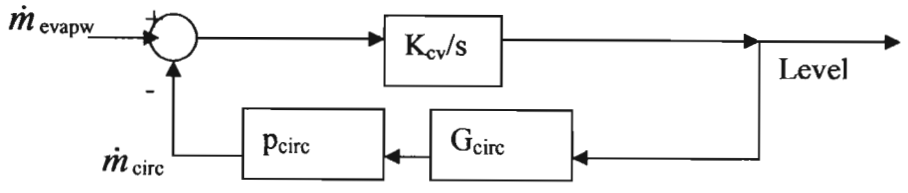

Figure 6.19: Control loop of collecting vessel.

Following the explanation, the narrower the frequency response graph of H(s) or the lower the gain, the smaller the energy spectrum at the output. This occurs because H(s) only allows the portion of the energy spectrum of the input corresponding to the frequencies in the H(s) pass band. Figure 6.20 shows the bode plot of H(s) with PI proportional gain (KP) of 5.6 and 20, which meet the required specs for 10 % MCR and 50 % MCR respectively.

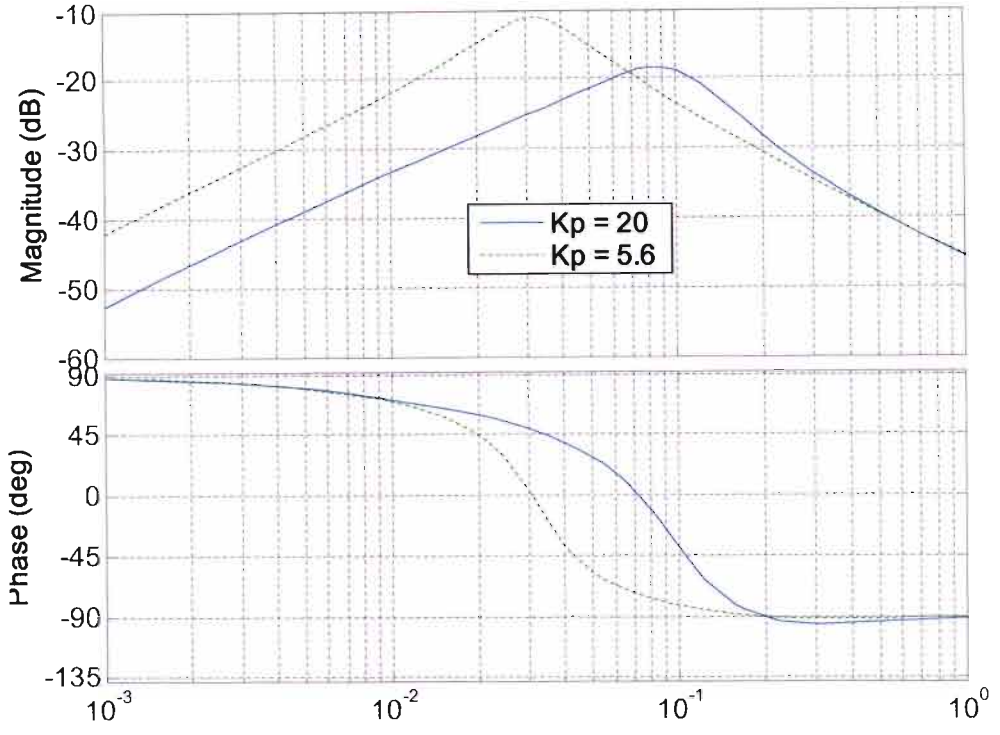

Figure 6.20: Bode plot of H(s) = $\frac{K_{cv}/s}{1+\frac{K_{cvs}\times G_{circ}\times P_{circ}}{s}}$ with Kp =5.6 and Kp = 20

The frequency response shows that the energy spectrum at the output would be smaller with a large Kp because of lower gain. Hence bandwidth is required to filter out most of the oscillation from the evaporator.

6.6 Simulated Boiler Operation with PI Level Controller.

The designed controller is implemented in the circulation loop, and is run with the collecting vessel level set point set at 2, 4 and 6 metres. The circulation loop block diagram in figure 3.8 has the proportional gain replaced with the designed PI controller. The same inputs used in the simulation in chapter 5 are used in simulation in chapter 7.

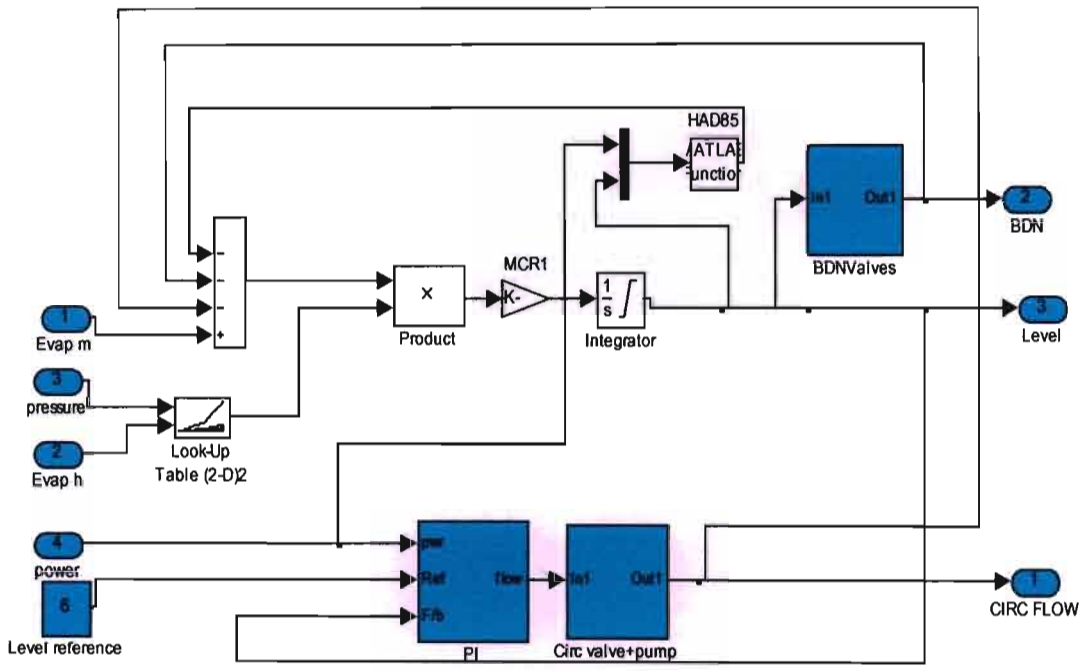

Figure 6.21: Collecting Vessel simulation block diagram, with circulation controller.

BOILER OPERABILITY ISSUES

Chapter 7

7.1 Finite Collecting Vessel Level Set Point Values

Figure 7.1 shows the boiler operating with a level set point of 6 metres. Initially as the boiler starts up, the collecting vessel fills up, while the circulation valve opens. Since the collecting vessel has a capacity of about 7.5 seconds (at minimum evaporator flow) and the circulation controller has a reset time of 7 seconds, the collecting vessel fills up to almost 8 metres at about 20 minutes when cold water is suddenly pumped into the evaporator (see also figure 5.10). The blow down valves then open to their maximum, as the circulation flow increases. A high set point level means that there is more blow down interlock action in the circulation loop, as the blowdown prevents the collecting vessel from filling up. This results in increased oscillation, observed in both the blow down flow and collecting vessel level in figure 7.1. The oscillations are not that pronounced in the circulation flow, implying that the oscillation is generated by blow down interlock action. The oscillations observed have the same frequency as the frequency of closing and opening the blow down valves.

When the boiler is in pre-Benson mode, a constant blowdown flow would reduce the oscillation caused by the blow down interlock. The simulation shows that the magnitude of the 10-15 minutes oscillation observed in figure 5.10 have been reduced in magnitude by the PI controller. Since there is more blow down, there is less water recirculation. This means that more cold water is being fed into the economiser, resulting in less chances of boiling occurring in the evaporator. This will reduce the 10-15 minute thermal oscillation caused by evaporation of water in the wrong place. The oscillations reduce in intensity as load demand increases, as less water is re-circulated. The increase in blow down flow means an increase in operation costs when the boiler is operating pre-Benson mode (more de-ionised water being blown down to drain).

Figure 7.2 below shows the simulation of the boiler with a collecting vessel level set point at 4 metres. As seen in the figure, below 5 metres the blow down action is very little. The oscillation caused by blow down interlock observed in figure 7.1, are not observed in the circulation flow. The PI controller regulates the circulation flow and prevents blow down interlock action.

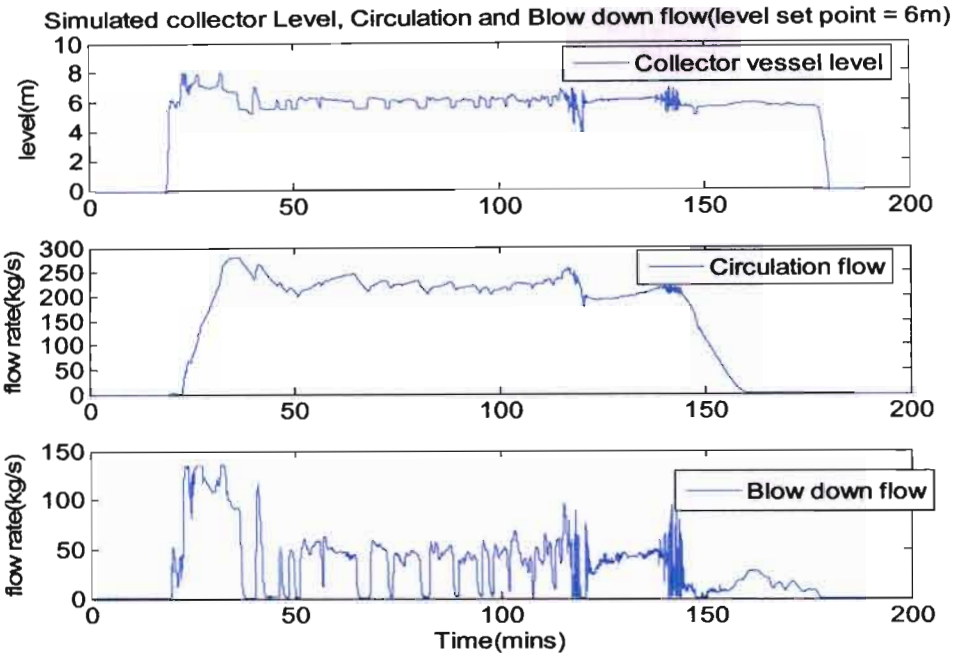

Figure 7.1: Simulated Collecting Vessel level, Circulation and Blow down flow. The oscillation observed is caused by continuous blow down interlock at a level set point of 6 m

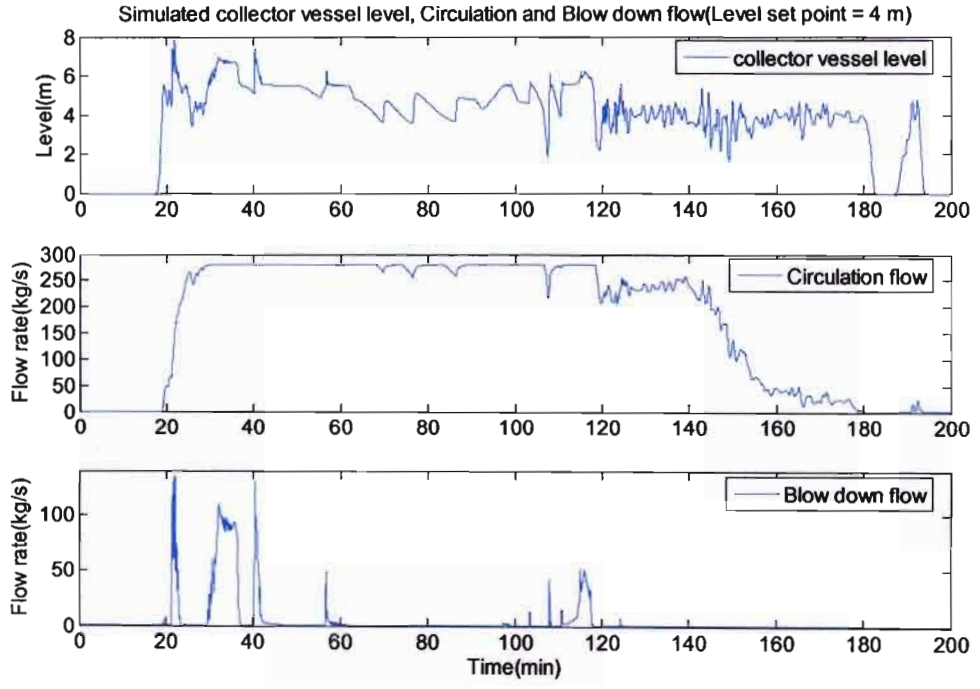

Figure 7.2: Simulated collecting vessel level, circulation flow and Blow down flow. Blow down valves are closed for most of the start up at collecting vessel set point of 4m

Figure 7.3 shows the boiler operation with a collecting vessel level set at 2 metres. Since the set point level is very low, the controller's response to the sudden increase in water level is very fast and with the help of the blow down flow the level reduces much faster than when the set point is set to 4 and 6 metres. The blow down interlock action is kept to a minimum with a set point of 2 metres, since the level is low. This means that the 15 minute oscillations are observed, but are not as intense as in figure 5.10. Since the level is very low, the controller has time to respond to sudden changes in mass flow rate and hence reduce the level without the blow down interlock action.

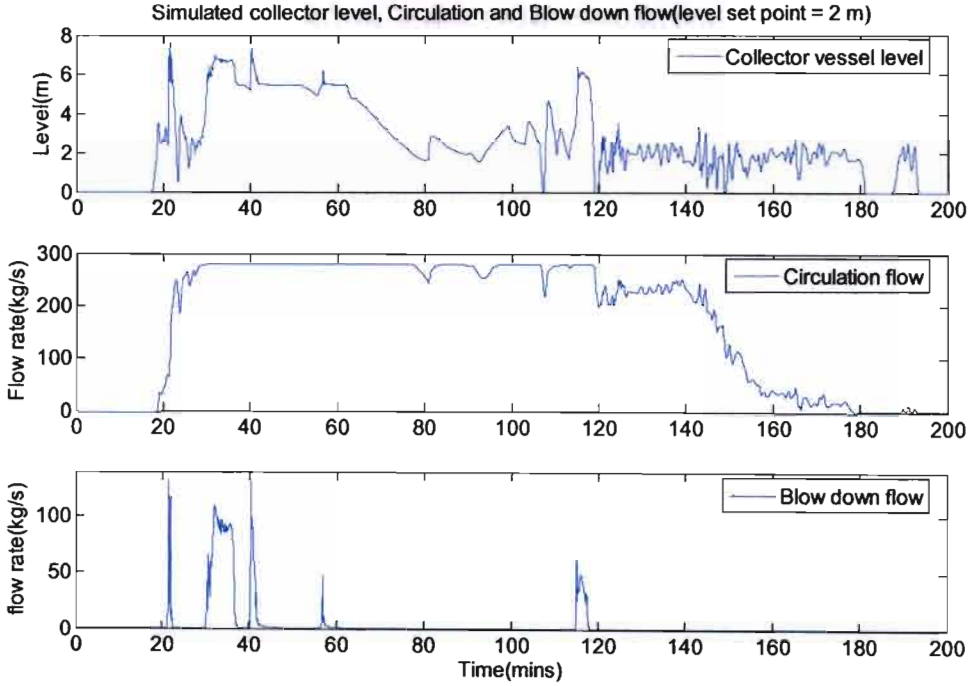

Figure 7.3: Simulated Collecting Vessel level, Circulation flow and Blow down flow. Set point level of 2 m looks like a much better operation set point.

7.2 Constant Blow down Valve Gain

The problem of thermal limit cycle caused by the incipient boiling in the top part of boilers, resulting in amplified water plug flow is a very difficult control problem as explained by Eitelberg and Boje (2004). During hot start up procedure of the boiler, the operational pressure drops to about 3.5MPa, while the temperature of the water in the economiser and evaporators remains at about 280° as is the case in the hot start up investigated in this thesis. This will result in boiling in the economiser, creating water plug which results in much larger water mass flow.

Figure 7.1 shows that thermal oscillation reduces with continuous blow down, while there is less circulation flow from the circulation pump. This could be due to the fact that less circulation flow means more cold feed flow, and hence reduction in the input specific enthalpy at the economiser input. The problem with his method is that most of the

circulation water will be blown down during start. If the collecting vessel level is set to a low level and the blow down valves given a constant gain, it appears that the system would work well. The controller action in the circulation loop would prevent the level from increasing too high or reducing too low, therefore prevent the feed of circulation pumps from tripping and improving start up reliability.

More feed water during hot start up would mean more energy and time required to bring the plant online, but would prevent the possibility of a pump trip. A constant blow down flow would also mean less oscillation caused by the valves opening and shutting down.

In order to observe the effect of continuous, constant blow down flow, the model is run at a constant blow down, allowing a flow rate of about 110 kg/s (when collecting vessel inflow is more than 120kg/s), while the collecting vessel level is set to 2 metres. When the collecting vessel level increases above 6 metres the blow down valves are completely opened. When the collecting vessel level reduces, the blow down valves close and allow a constant flow rate of about 110 kg/s. Figure 7.4 and 7.5 below shows the circulation, blow down and feed flow, when the level set point is set to 2 meters.

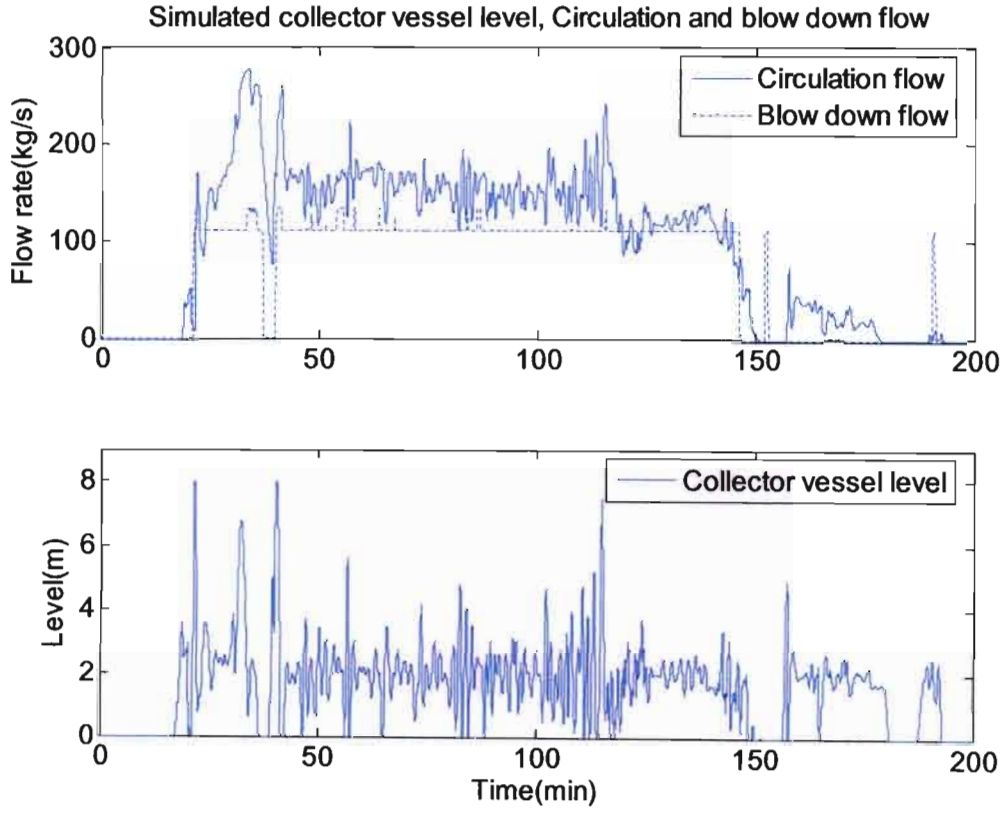

Figure 7.4: Model run with a collecting level set point of 2 metres and the blow down valve opened continuous when the inflow flow from the evaporator is more than 120 kg/s

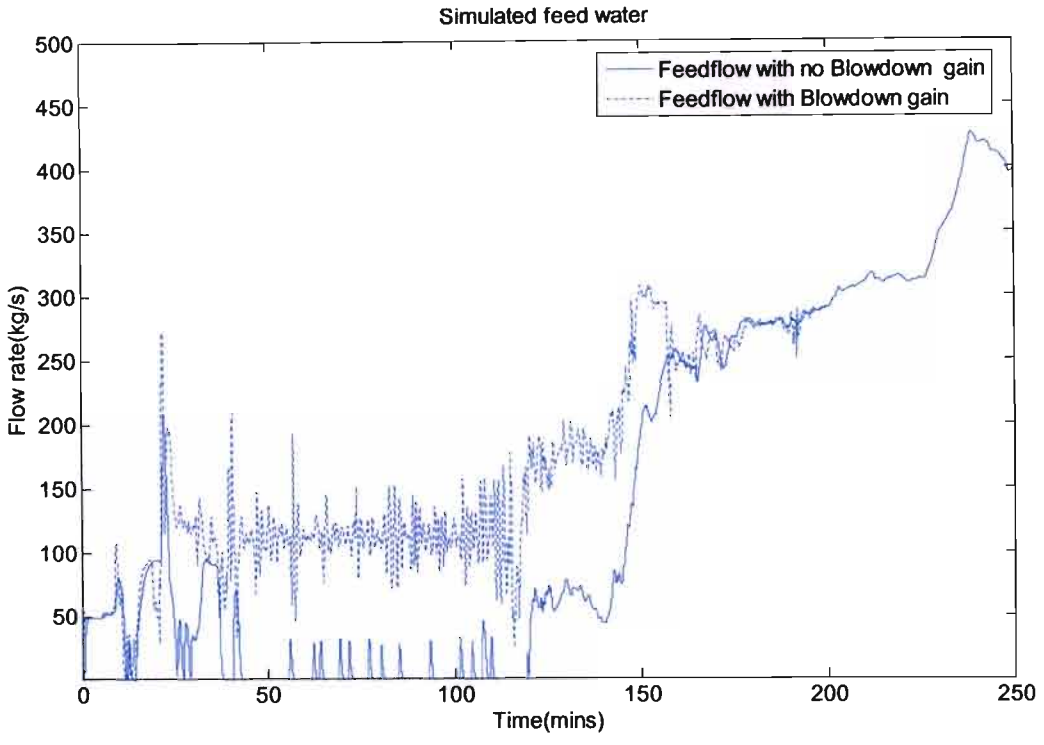

Figure 7.5: Comparison the feed flow when the level set point is set at 2 metres, but in one case the blow down valves operate in their normal way and the other case the valves are opened to allow a constant flow of 110kg/s

Figure 7.4 shows that blowdown flow remains constant, but increases when the collecting level increases above 6 metres. Figure 7.5 shows the feed water flow is much higher when the blowdown valves have a constant gain. This would lower the input specific enthalpy and temperatures, thereby reducing the thermal oscillation. The cold water would reduce the water temperature in the economiser and prevent water plug from forming during start up at low pressure.

Constant blowdown has the disadvantage of continuously less of de-ionised water, which might be costly. The performance improvement of the designed controller could not be measured or calculated due to unavailability of operation costs.

From figure 7.5, it can be concluded that constant blow down would result in more feed flow, meaning the feed pump could be used to pump minimum evaporator flow.

7.3 Simulation with no Gain Scheduling

The model is run with the collecting vessel level set at 2 metres. The controller designed in section 6.5 is used, but this time only one gain value is used. The gain which satisfies, $T_{Y/Do} = 1/ (1+ Lcirc) < 3db$ (for allω), is used. The results of the simulation are compared to the results obtained when simulation is run with a gain scheduled controller.

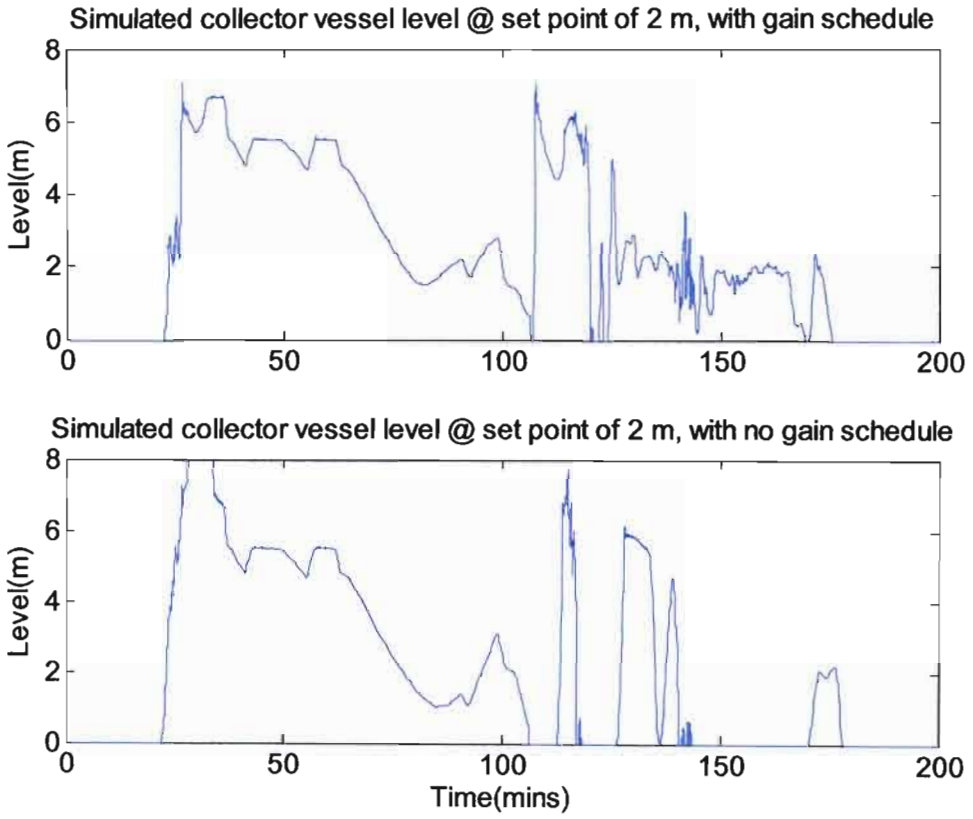

Figure 7.6: Collecting level, when the simulation is run with and without gain scheduling. The collecting level set point is set to 2 m. The controller with no gain scheduling has a controller gain, Kp = 5.6.

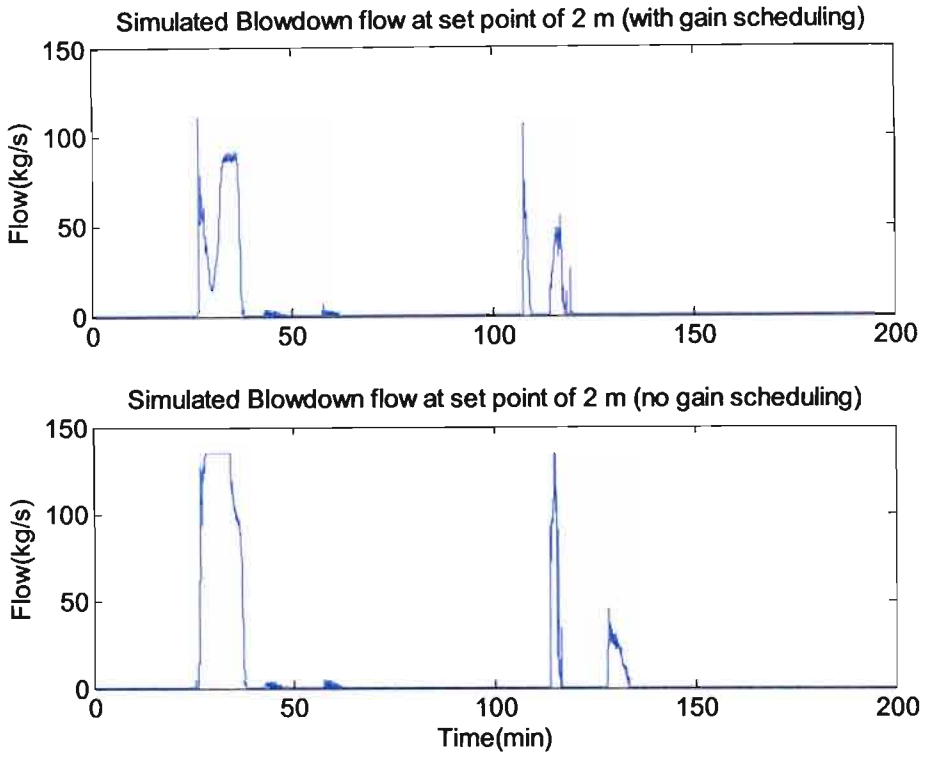

Figure 7.7: Blow down flow, when the simulation is run with and without gain scheduling. The collecting level set point is set to 2 m. The controller with no gain scheduling has a controller gain, kp = 5.6.

Figure 7.6 shows how the collecting vessel level fills up easily with no gain scheduling (low bandwidth). This is because the response of a low bandwidth controller is slower than a controller with high bandwidth. With low bandwidth, the controller can not maintain a level of about 2 metres at high MCR values. From figure 7.7, it is seen that for low bandwidth, the blow down flow tends to be greater than the blow down flow of high bandwidth. This is because at low bandwidth, the circulation is slow and the collecting vessel tends to fill up much faster than when the bandwidth is high.

Chapter 8

CONCLUSION

This thesis shows the development of a simple non linear model of a Benson boiler from first principles. Assuming a known pressure and input enthalpy, the boiler is modelled with the energy conservation equation as the state differential equation. The heat transfers in the boiler were defined using empirical heat flux correlations for both single and two phase flow. The validity of the developed model is shown in chapter 5. The hot start up of the boiler was modelled accurately enough to show the dynamics required for control analysis.

The nonlinear model was linearised, at different MCR values below 50 % MCR. A frequency domain analysis was done on the linearised boiler. It was found that at about 0.1 rad/s the system would be unstable due to excess gain in the feed and circulation control loops. The measured results from the boilers were observed to oscillate persistently in a regular fashion at a frequency of about 0.1 rad/s, when the collecting vessel level was about 4 metres. From the control analysis it was observed that the oscillation was often caused by limit cycling control loop around some gain changing non-linear components. The boiler control problem and specification were defined. The thesis presents a loop by loop approach to multivariable feedback control design. The choice of the design method was preferred by the author because it represented the physical equipment and processes.

The thesis proposes a gain scheduled PI controller for the collecting vessel level rather than the traditional proportional gain controller. The controller was designed using the quantitative feedback theory, which makes the system more robust and reliable. The results of the control analysis and simulation show that gain scheduling was required for maximum bandwidth at different loads during start up. The PI controller allows automatic control and improves the steady state performance of the collecting vessel level. The PI controller also prevents the circulation pump from tripping, since the water level does not get too low. The thesis also proposes a start up procedure, with a constant blow down flow and level set point. The start up procedure analysed has a disadvantage of more blow down flow, but is more reliable and robust. The procedure would also help reduce the 10-15 minute thermal oscillation, as more cold water is fed into the economiser during hot start up, preventing evaporation from taking place at wrong places in the boiler.
There are unanswered questions in the level control and start up procedure, which would provide scope for further research. These would include:

1) The start-up procedure of the hot start-up. One of the key issues in the hot start up is the low pressure, which allows boiling to occur in wrong places in the boiler. The start–up procedure requires pressure regulation in the economiser and

evaporator. The pressure needs to be controlled to allow steam development in the upper section of the evaporator. This would eliminate the thermal oscillation and hence prevent blow down. The reduction in blow down interlock would reduce the chances of the pump tripping.

2) Since the ability to bring the plant online takes 5 hours, and a two shift a day is required. Further work could be done in analysing the cost of starting up the boiler using the controller designed in this project. The cost of start up and shutting down the plant using the designed controller could be compared to the cost of letting the plant run at low load (40% MCR $\approx$ 280 MW) during off peak hours. The boiler could generate electricity which is not being used, but might be cheaper than a two shift scheme. Once the costs are known, a better decision could be made on the implementation of a fast start controller.

In summary, the thesis has studied the important problem of boiler units under the new electrical market context. A model was developed, which was accurate enough to show the boiler start-up and shut down dynamics. The project presents a dynamic non-linear model of thermal behaviour of the boiler and validates the results with experimental data from an actual power station. Based on the new model, the project investigates gain scheduled PI and robust QFT control approaches to design a controller for the collecting vessel level and evaporator flow rate. The thesis then designs a compensator to control significant variables of the system.

APPENDIX A

Boiler parameter

The tubes were assumed to be made from steel, hence the density was 7850 kg/s and heat capacity was 755 kJ/kg

Name	Outside diameter (mm)	Inside Diameter (mm)	Approx Length (m)	No of parallel tubes
Economiser	51	42	80	320
Evaporator (helical)	44.5	35	190	320
Evaporator (vertical)	31	20	30	1284
Collecting vessel	-	585	8	-

APPENDIX B

Boiler steady state values

p = 19.8

$\dot{m}$ = 570 kg/s

h = 2700 kJ/kg

Φ = 1851 kg/m^{2}s

$\dot{q} \approx 0.178$ MW/m^2

ξ=0.0131

$\rho_{S/H}$ = 46kg/m^3

$\rho_{Evaporator}$ = 215kg/m^3,

$\frac{\partial p}{\partial z}_{S/H}$ = 14899 /m,

$\frac{\partial p}{\partial z}_{Evaporator}$ = 2365 /m

τ_0 = 284 N/m^2

1) from Eq.18,

$$Re = \frac{4 \times 570}{0.114 \times \Pi \times 0.035} = 1.8 \times 10^5$$

2) Steam content X_{do} at dryout, Lausterer, Franke and Eitelberg (1980,EQ. A8)

$x_{do} = 46*0.035^{-0.7}\ \dot{q}^{-0.125}\Phi^{-0.333}e^{-0.0025p}$, p(), $\dot{q}(W/m^2)$,Φ(kg/m^{2}s)

= 0.9734

3) Capacity of collecting vessel at minimum evaporator flow rate (260 kg/s)
density $\approx$ 900 kg/s

Capacity = 900*8*0.2688 / 260 = 7.44 sec

4) Typical linearised plant at 50% MCR

$$N_{evap} = \frac{0.2628\ s\text{^}15 + 9.946\ s\text{^}14 + \ldots\ldots\ldots + 1.54e\text{-}005\ s + + 1.028e\text{-}007}{s\text{^}15 + 37.24\ s\text{^}14 + \ldots\ldots\ldots\ldots + 1.194e\text{-}005\ s + + 6.659e\text{-}008}$$

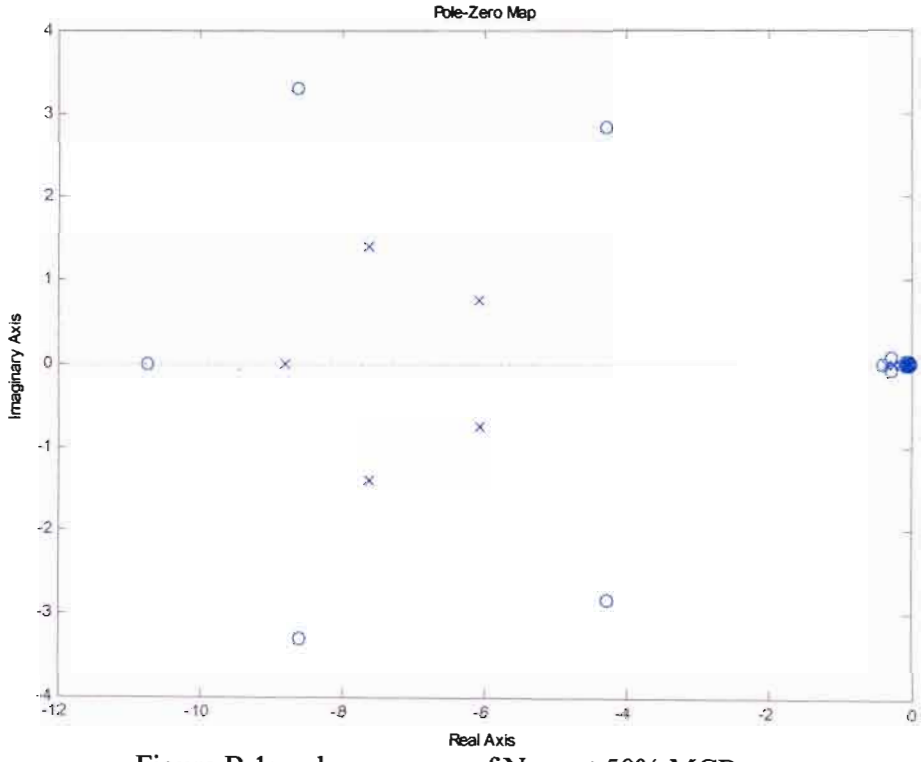

Figure B.1: pole zero map of N_{evap} at 50% MCR

APPENDIX C

Matlab program

Start up M –file

The m- file reads measured data from an excel document. The m-file defines variables of the measured data in the Matlab command window.

The m-file defines the steam tables and the required thermodynamics gradients. The important sections of the Matlab code are shown below.

% steam tables: fluid temperature, specific volume, specific heat capacity of water..
%.. thermal conductivity of water and viscosity of water.

```
for iP=1:27
        T_matrix(1:50,iP)=interp1(enthalpy(:,iP),temperature,h_col);

        v_matrix(1:50,iP)=interp1(enthalpy(:,iP),specific_vol(:,iP)/1000,h_col);

        cp_h_matrix(1:50,iP)=interp1(enthalpy(:,iP),cp(:,iP),h_col);

        lambda_h_matrix(1:50,iP)=interp1(enthalpy(:,iP),lambda(:,iP),h_col);

        neta_h_matrix(1:50,iP)=interp1(enthalpy(:,iP),neta(:,iP),h_col);
end

Rho_matrix=1./v_matrix;                    % Density steam table
```

% Gradients of temperature and density with respect to pressure and
% temperature

```
[dTdP,dTdh]=gradient(T_matrix,pressure*1000000,h_col*1000);
[drdP,drdh]=gradient(Rho_matrix,pressure*1000000,h_col*1000);

drdP=min(drdP,5.2e-4);
drdh=max(drdh,-2.5e-3);
```

The m-file finally defines the look up table for the gain scheduling.

% look up table for proportional gain

```
pwr  = [0 70e6 140e6 210e6 280e6 350e6 750e6];    % power
progain = [5.6 5.6 5.7 6 9 21 22];                % kp
```

Benson _model m-file

```
% They function is used to model a Benson boiler. The boiler  initial
%  and boundary condition are determined first. Valid values of
% pressure, enthalpy and mass flow rate are then determined. The
% function then calls the different sections of the boilers, starting
% with the economiser, then evaporator. The functions outputs a
% vector Xdot and accepts a vector W from the simulink model

function xdot = Benson_model(W)
i = 15;                          % number of divisions of the boiler section being modelled
                                 % function which initiates the program
Tm = W(1:i);                     % reads wall temperature from simulink
h(2:(i+1)) = W((i + 1): (2*i));  % reads enthalpy j/kg from simulink
pressure_initial = W(i*2 +1);    % initial pressure in

p(1) = pressure_initial;         % Boundary conditions
heatadded = W(i*2 +2)*1.044;     % heated added to the system in w
temperature_initial=W (i*2 +3);  % initial temperature in degrees Celsius
Mdot(1)=W(i*2 +4);               % Boundary condition mass flow rate in Kg/
pdot=W(i*2 +5);                  % initial conditions

%  Boundary conditions enthalpy of fluid J/Kg

h(1)=interp2(pressure,temperature,enthalpy,p(1),temperature_initial)*1000 ;

% h is within range of steam table, and also makes sure initial conditions are met

]h=min(max(h,h_col(1)*1000),h_col(length(h_col)-1)*1000) ;

% P is within range of steam table, and also makes sure initial conditions are met
p=min(max(p,1),21) ;

Mdot=max(Mdot,1) ;               % makes sure initial conditions are met
economiser                       % The Economiser M-file  called
eva_helical                      % The Helical tube M-file called
eva_vertical                     % The vertical tube M-file called

xdot=[h_dt,dT_dt,Mdot(:,2:16),X,q ]; % output vector
```

Economiser and Evaporator

The Matlab codes containing the state equation representing dynamics in the economiser, evaporator helical and vertical section are similar. Only the number of tubes and tube sizes are the biggest difference in the different boiler sections. The Matlab code used to calculate the heat flux for lumped elements with transition from 1 phase to the other is shown below.

```
gap=10000;
```

```
if abs(h(n+1)-Hl(n))<gap        % transition from single to 2 phase

   % 2 phase: Jens and Lottes

   q_gap1 =sign(Tm(n)-T(n))*((1/0.79) * exp(p(n)/6.2) .* (Tm(n)' - Ts)).^4;

   % 1 phase

   % Thermal conductivity W/(K m)
Lambda= INTERP2(pressure,h_col,lambda_h_matrix,p((n)),(Hl(n)-gap)/1000)*1e-3;

%specific heat capacity of steam/water j/(kgK)
Cp = INTERP2(pressure,h_col,cp_h_matrix,p((n)),(Hl(n)-gap)/1000)*1000;

 % dynamic viscosity Pas
Neta = INTERP2(pressure,h_col,neta_h_matrix,p((n)),(Hl(n)-gap)/1000)*1e-6 ;

% general equations
Re  = (Mdot((n))/No_pipes).* di ./(Area .* Neta);          % calculate Reynold number
zeta=1/(1.14+2*log10(di/k))^2;
Zeta=1./(2.*log10(k./3.71./di+2.51./Re./sqrt(zeta))).^2;  % friction coefficient
pr = Cp.*Neta./Lambda ;                                   % prandtl number
Nu=Zeta./8.*(Re-1000).*pr./(1+12.7.*sqrt(Zeta./8).*(pr.^(2/3)-1)); % Nusselt Num
q_gap2= Lambda.*(Nu.*(Tm(n)'-T(n)))./di;

selection =(Hl(n)+gap-h(n+1))./2./gap;                    % 1 at h=hl-gap, 0 at h=hsat+gap
q(n)=q_gap1.*(1-selection)+q_gap2.*selection;
end

gap=10000;          % transition from two phase to single phase
 if abs(h(n+1)-Hg(n))<gap
   q_gap1 =sign(Tm(n)-T(n))*((1/0.79) * exp(p(n)/6.2) .* (Tm(n)' - T(n))).^4;

   % 1 phase

Lambda = INTERP2(pressure,h_col,lambda_h_matrix,p((n)),(Hg(n)-gap)/1000)*1e-3
Cp = INTERP2(pressure,h_col,cp_h_matrix,p((n)),(Hg(n)-gap)/1000)*1000;
Neta = INTERP2(pressure,h_col,neta_h_matrix,p((n)),(Hg(n)-gap)/1000)*1e-6

% general equations

Re  = (Mdot((n))/No_pipes).* di ./(Area .* Neta);
zeta=1/(1.14+2*log10(di/k))^2;
Zeta=1./(2.*log10(k./3.71./di+2.51./Re./sqrt(zeta))).^2;
pr = Cp.*Neta./Lambda ;
Nu=Zeta./8.*(Re-1000).*pr./(1+12.7.*sqrt(Zeta./8).*(pr.^(2/3)-1));
q_gap2= Lambda.*(Nu.*(Tm(n)'-T(n)))./di;

selection =(Hg(n)+gap-h(n+1))./2./gap;                    % 1 at h=hg-gap, 0 at h=hsat+gap
q(n)=q_gap2.*(1-selection)+q_gap1.*selection;
```

```
end

% ODE
%  steel temperature dT/dt

dT_dt(n) = (heat - q(n) .* As)./ (cm * RhoSteel * Vs);

% water enthalpy calculation
h_dt(n)=(q(n)*As + Mdot(n).*(-dh_dz(n))+Vi*pdot)./(Rho(n)*Vi);

% Mass calculation
Mdot(n+1)=Mdot(n)-Vi.*(dr_dh(n).*h_dt(n)+dr_dP(n)*pdot);

Mdot(n+1)=(max(Mdot(n+1),0.1))
```

The compact disc included in the thesis contains the software used and developed during the course of this work. There are 5 the main section, namely

1) Boiler programs, (includes economiser, evaporator, circulation and blowdown)
2) Linearization program and simulink model
3) Boiler simulink model
4) Qualitative feed back control programme for $L_{levelcontrol}$
5) Measured data

REFERENCE

L and C Steinmüller,1999,"Descriptive of steam generator plant at Majuba Powers Station", *volume 1 Rev. 0*

Lausterer, G.K., Franke, J., Eitelberg,E.1980. "Mathematical modelling of a steam generator", *The IFAC/IFIP conference on digital computer application to process control* ,(pp 411-417)

Eduard Eitelberg & Edward Boje, 2004. "Water circulation control during one through boiler start-up", *Control engineering practice 12*,(pp 677-685)

Edward Boje, 2003,"Further study of Circulation Control", *private correspondence*, (pp 9,12-13)

Eduard Eitelberg & Edward Boje, 2001, " Water Circulation Control during Start up", *private correspondence*, (pp 31 -32)

D. Butterworth and G.F Hewitt,1977. "Two Phase Flow and ", *Oxford University Press*, (pp 159-160)

R.Bulirsch and J.Stoer, 1980 "Introduction to Numerical Analysis", *Pergamon press,(pp 462-463)*

Futoshi Takana, Takashi Hibiki,Yasushi, Kaichiro Mushima 2001. " study for thermal hydraulic design of solid state of spallation neuron state", *Journal of nuclear science and technology, vol 38, No. 10,(* pp 842-843).

Clare D. McGillem and George R. Cooper, 1991"Continous and Discrete signal and system analysis (Third edition)",*Saunders college publishing*,(pp 136-139)

Katsuhiko Ogata,1997, " Modern control Engineering, Third Edition", *Prentice-Hall International INC*,(pp 100 - 120)

Frank P. Incropera and David P. Dewitt, 2001, " Introduction to , Third Edition", *John Wiley and Sons inc*,(chapter 8)

John G Collier,1981, " Convection boiling and condensation, third edition", Mcgraw – Hill internation Book company,(pp 163-166)

Maffezzoni C., G. Magnani and L. Marcocci, 1983, "Computer Aided Modelling of Large Power Plants", *IFAC Workshop on Modelling and Control of Electric Power Plants,* Como, Sept.(pp 2-4).

Marie-Noelle Dumont and Georges heyen,2001, " Mathematical modelling and Design of an advanced Once-through Heat recovery steam generator",*LASSC,Univerity of Liege,*,(pp2-3)

C. Maffezzoni and L. Ferrarini, 1989, "Dynamic design of tha fast start-up of a Benson boiler", *Journal A,30(4)*,(pp 7-16)

J.M. Maciejowski,1989, " Multivariable Feedback Design", *Addison-Wesley Publishing company*,(pp203 -210)

J.Adams, D.R Clark, J.R Louis, And J.P Spanbauer, " Mathematical modelling of once Trough Boiler Dynamics", *IEEE Trans. App. And System, vol. 84,2*,pp(146-156)

L. Borsi, 1974, "Extended linear Mathematical model for a power station unit with a once Through Boiler" , *Siemens forchungs- und Entwicklungsbericht, Bb.3,5*, pp(273 - 290)

N.A Afgan Nad J.M Beer,1974, " Heat transfer in flames", *Scripta Book Company*, Chapter 3